

SEP 25 1958 Copy 242

14318

RM A58F02

14125

NACA RM A58F02



TECH LIBRARY KAFB, NM

0143472



# RESEARCH MEMORANDUM

0659

APPROXIMATE SOLUTIONS FOR THE FLOW ABOUT FLAT-TOP  
WING-BODY CONFIGURATIONS AT HIGH  
SUPERSONIC AIRSPEEDS

By Raymond C. Savin

Ames Aeronautical Laboratory  
Moffett Field, Calif.

Classification controlled *Unclassified*  
By authority of CEN # 1 (NASA) (1-17)

By NCS-1

C-5-11

18 Jan 1963

This material contains information affecting the National Defense of the United States within the meaning of the espionage laws, Title 18, U.S.C., Secs. 793 and 794, the transmission or revelation of which in any manner to unauthorized person is prohibited by law.

NATIONAL ADVISORY COMMITTEE  
FOR AERONAUTICS

WASHINGTON

September 15, 1958



0143472

## NATIONAL ADVISORY COMMITTEE FOR AERONAUTICS

RESEARCH MEMORANDUM

## APPROXIMATE SOLUTIONS FOR THE FLOW ABOUT FLAT-TOP

## WING-BODY CONFIGURATIONS AT HIGH

## SUPERSONIC AIRSPEEDS\*

By Raymond C. Savin

## SUMMARY

The flow about slender flat-top wing-body configurations traveling at high supersonic speeds and small angles of attack is investigated analytically. In the case of conical configurations, approximate algebraic solutions to the flow field are obtained. In the case of configurations which are conical at the vertex but curved in the stream direction, these solutions are combined with a slender-body approximation to the generalized shock-expansion method to obtain the flow downstream of the vertex.

Surface pressures were obtained experimentally at Mach numbers from 3.0 to 6.0 and angles of attack up to  $6^\circ$  for several flat-top wing-body configurations. These configurations consisted of half-bodies of revolution mounted beneath thin highly swept wings. Three different bodies were employed. The two conical bodies consisted of one-half of a fineness-ratio-5 cone and one-half of a fineness-ratio-2-1/2 cone. The body of the third configuration consisted of one-half of a fineness-ratio-5 ogive. For the ogive configuration, the leading edges of the wing were curved and designed to just maintain the theoretically determined bow shock along the leading edge at a Mach number of 5.0 and an angle of attack of  $3^\circ$ . The predictions of the conical flow theory of this paper for the surface pressures are found to be in good agreement with experiment at Mach numbers of 5.0 and 6.0 up to angles of attack of approximately  $3^\circ$ . Estimated lift, drag, and pitching-moment coefficients, as well as maximum lift-drag ratio, are also in good agreement with existing experimental data at a Mach number of 5.0 for a conical configuration having an arrow plan-form wing. It is also found that the generalized shock-expansion method yields reasonably good agreement with experiment for the surface pressures on the half-ogive configuration at a Mach number of 5.0 and an angle of attack of  $3^\circ$ .

---

\*Title, Unclassified.

---

## INTRODUCTION

A class of flat-top wing-body combinations was proposed in reference 1 as being capable of developing high lift-drag ratios at high supersonic speeds. The type of configuration suggested consists of a thin highly swept wing of essentially arrow plan form beneath which is mounted a half-body of revolution with its vertex common to the vertex of the wing. Theoretical and experimental results presented in references 1 and 2 indicated that these configurations have a high aerodynamic efficiency at high supersonic speeds. It is of interest, therefore, to consider more refined theoretical methods for treating the flow about flat-top wing-body combinations. Such methods are necessary if accurate estimates of pressure forces and moments as well as detailed local flow properties are to be obtained. Local flow conditions are required, of course, in order to determine skin-friction and heat-transfer characteristics which are so important at hypersonic speeds.

A method for estimating the aerodynamic forces on flat-top wing-body configurations has been presented in reference 3. This method was obtained with the aid of linear theory. In fact, in the past, virtually all treatments of the flow about wing-body combinations have employed linear theory (see, e.g., refs. 3 through 7). Although these methods have been shown to be adequate for low supersonic speeds, their application to hypersonic speeds is questionable due to the restrictions of linear theory. Thus, at the present time, there is no well-established theory applicable to the accurate prediction of the aerodynamic characteristics of wing-body combinations traveling at high supersonic speeds. The objective of the present paper, therefore, is to obtain an improved theoretical method for predicting the flow about flat-top wing-body configurations having supersonic leading edges. In this connection, a hypersonic theory applicable to conical configurations is obtained. This result is then combined with a slender-body approximation to the generalized shock-expansion method to obtain the flow about configurations which are curved in the stream direction.

## NOTATION

- a local speed of sound, ft/sec
- $C_A$  axial-force coefficient,  $\frac{\text{axial force}}{q_\infty S}$
- $C_D$  drag coefficient,  $\frac{\text{drag}}{q_\infty S}$
- $C_L$  lift coefficient,  $\frac{\text{lift}}{q_\infty S}$

$C_m$	pitching-moment coefficient, $\frac{\text{moment about vertex}}{q_\infty S l}$
$C_N$	normal-force coefficient, $\frac{\text{normal force}}{q_\infty S}$
$C_p$	pressure coefficient, $\frac{p - p_\infty}{q_\infty}$
$c_p$	specific heat at constant pressure, ft-lb slug $^{\circ}\text{R}$
$c_v$	specific heat at constant volume, ft-lb slug $^{\circ}\text{R}$
$E$	entropy, ft-lb slug $^{\circ}\text{R}$
$l$	characteristic reference length, ft
$M$	Mach number (ratio of local airspeed to local speed of sound)
$p$	static pressure, lb/sq ft
$p_t$	total pressure, lb/sq ft
$q$	dynamic pressure, lb/sq ft
$R$	gas constant, ft-lb slug $^{\circ}\text{R}$
$r$	distance along conical ray measured from vertex, ft
$S$	total plan area, sq ft
$u$	velocity component parallel to $r$ , ft/sec
$v$	velocity component normal to $u$ in a meridian plane, ft/sec
$V$	resultant velocity, $\sqrt{u^2 + v^2 + w^2}$ , ft/sec
$\hat{V}$	maximum velocity obtainable by expanding to zero temperature, ft/sec
$w$	velocity component normal to a meridian plane, ft/sec
$\alpha$	angle of attack, radians unless otherwise specified
$\gamma$	ratio of specific heats, $\frac{c_p}{c_v}$
$\delta$	angle of flow inclination in meridian plane measured from configuration axis, radians unless otherwise specified
$\delta_W$	wedge angle of wing in streamwise direction

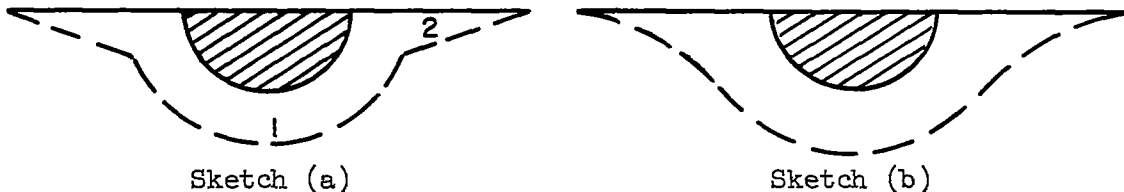
- △ angle of flow inclination in meridian plane measured from free-stream direction, radians unless otherwise specified
- ε angular difference between free-stream direction and locus of points representing center of curvature of shock in plane of symmetry, radians unless otherwise specified
- λ semivertex angle of wing (i.e., complement of leading-edge sweep angle; see fig. 1), radians unless otherwise specified
- μ Mach angle, radians unless otherwise specified
- ρ mass density, slugs/cu ft
- φ angle of meridian plane with respect to plane of symmetry, radians unless otherwise specified (see fig. 1)
- ψ dihedral angle at shock between streamwise plane normal to shock and plane containing axis of configuration, radians unless otherwise specified
- Ψ dihedral angle at shock between streamwise plane normal to shock and plane containing free-stream velocity vector, radians unless otherwise specified
- ω angle between axis of cone and ray passing through vertex of cone, radians unless otherwise specified
- Ω angle of ray on conical shock measured with respect to free-stream direction, radians unless otherwise specified

#### Subscripts

- B body
- c evaluated at cone surface
- e evaluated at external surface of vortical layer
- S evaluated at shock wave
- W wing
- ∞ free-stream conditions
- o conditions at  $\phi = 0$
- $\frac{\pi}{2}$  conditions at  $\phi = \frac{\pi}{2}$

## THEORY

The purpose of this analysis is to obtain a simplified theory for predicting flow fields about a class of flat-top wing-body configurations traveling at hypersonic speeds and at small angles of attack. The configuration to be treated is assumed to consist of a half-body of revolution mounted beneath a thin wing, the vertex of which is common to the vertex of the body and whose leading edges are sharp and always supersonic. Furthermore, the configuration is assumed slender and the surface slopes are everywhere small compared to 1. In addition, the free-stream Mach number is assumed large compared to 1 and the angle of attack small compared to 1. Thus, the local Mach number will be large compared to 1 and the inclination of the nose shock wave will be small. Only flow fields which are either wholly conical or conical at the vertex are studied. Consider now the flow field as it would appear in cross-section view normal to the configuration axis. A conical flow field of the double shock type is shown in sketch (a), where region 1 is three-dimensional in type and is generated by the body, and region 2 is a two-dimensional flow field generated by the wing (the configuration is presumed to be at angle of attack). Another conical flow field is a single-shock type as represented in sketch (b). Experimental observations of the shock-wave patterns to



date indicate that the flow field is of the single-shock type, at least for configurations having highly swept wings. It was also found that the pressures on the wing were not only continuous across the entire wing but were also higher in region 2 than the pressures which would be expected if the flow were two-dimensional in this region. In the following analysis, approximate solutions to the flow field satisfying the boundary conditions corresponding to the single-shock type will be obtained.

## Flow About Conical Flat-Top Wing-Body Configurations

For conical flow fields, all derivatives with respect to radial distance vanish and the equations of motion and continuity in spherical polar coordinates become (a schematic diagram of the polar coordinate system is shown in fig. 1)

$$v \frac{\partial u}{\partial \omega} + \frac{w}{\sin \omega} \frac{\partial u}{\partial \phi} - v^2 - w^2 = 0 \quad (1a)$$

$$v \frac{\partial v}{\partial \omega} + \frac{w}{\sin \omega} \frac{\partial v}{\partial \phi} + \frac{1}{\rho} \frac{\partial p}{\partial \omega} + uv - w^2 \cot \omega = 0 \quad (1b)$$

$$v \frac{\partial w}{\partial \omega} + \frac{w}{\sin \omega} \frac{\partial w}{\partial \phi} + \frac{1}{\rho \sin \omega} \frac{\partial p}{\partial \phi} + uw + vw \cot \omega = 0 \quad (1c)$$

and

$$2\rho u \sin \omega + v \sin \omega \frac{\partial p}{\partial \omega} + \rho \sin \omega \frac{\partial v}{\partial \omega} + vp \cos \omega + w \frac{\partial p}{\partial \phi} + \rho \frac{\partial w}{\partial \phi} = 0 \quad (2)$$

respectively. Now the law of conservation of energy requires the following relations to be satisfied:

$$\left. \begin{aligned} \frac{\gamma}{\gamma - 1} \left( \frac{1}{\rho} \frac{\partial p}{\partial \phi} - \frac{p}{\rho^2} \frac{\partial \rho}{\partial \phi} \right) &= - \left( u \frac{\partial u}{\partial \phi} + v \frac{\partial v}{\partial \phi} + w \frac{\partial w}{\partial \phi} \right) \\ \frac{\gamma}{\gamma - 1} \left( \frac{1}{\rho} \frac{\partial p}{\partial \omega} - \frac{p}{\rho^2} \frac{\partial \rho}{\partial \omega} \right) &= - \left( u \frac{\partial u}{\partial \omega} + v \frac{\partial v}{\partial \omega} + w \frac{\partial w}{\partial \omega} \right) \end{aligned} \right\} \quad (3)$$

The entropy at any point in the flow field may be expressed in the form

$$E - E_\infty = \frac{R}{\gamma - 1} \ln \left[ \frac{p}{p_\infty} \left( \frac{p_\infty}{\rho} \right)^{\gamma} \right] \quad (4)$$

Equations (1), (2), and (3) together with the relation

$$a^2 = \frac{\gamma - 1}{2} (\hat{v}^2 - v^2)$$

may be combined (by eliminating the pressure and density terms) to obtain the equation of motion

$$\begin{aligned} \frac{\gamma - 1}{2} (\hat{v}^2 - v^2) \left( 2u + v \cot \omega + \frac{\partial v}{\partial \omega} + \frac{1}{\sin \omega} \frac{\partial w}{\partial \phi} \right) - uv^2 - uw^2 - \\ v^2 \frac{\partial v}{\partial \omega} - \frac{w^2}{\sin \omega} \frac{\partial w}{\partial \phi} - \frac{vw}{\sin \omega} \frac{\partial v}{\partial \phi} - vw \frac{\partial w}{\partial \omega} = 0 \quad (5) \end{aligned}$$

which is general for all steady-state conical flows.

It is convenient first to define the flow conditions on the leeward or expansion side of the wing.<sup>1</sup> For flows of the type under consideration, the expressions defining the Mach number and pressure are simply those applicable to a flat plate and may be written (see ref. 8)

---

<sup>1</sup>Since the shock wave is assumed to be always attached to the leading edge of the wing, the flow fields on the windward and leeward sides may be treated independently.

$$\frac{M_\infty}{M} = 1 - \frac{\gamma - 1}{2} M_\infty (\alpha - \delta_w) \quad (6)$$

and

$$\frac{p}{p_\infty} = \left[ 1 - \frac{\gamma - 1}{2} M_\infty (\alpha - \delta_w) \right]^{\frac{2\gamma}{\gamma-1}} \quad (7)$$

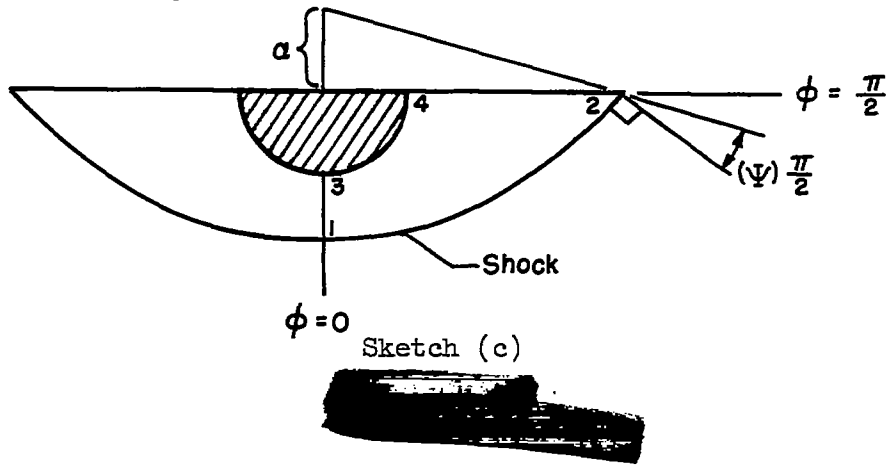
respectively, where  $\alpha$  is the angle of attack and  $\delta_w$  is the streamwise wedge angle of the wing.

The remaining part of this analysis will be concerned with the study of the interference flow field on the high-pressure side of flat-top wing-body configurations. Before proceeding with the actual solution for the flow field, it is convenient first to consider the basic assumptions underlying the solution and to outline briefly the method of attack in obtaining this solution. As mentioned earlier, only hypersonic flows and slender configurations at small angles of attack are considered in this paper. Thus, the following simplifications are employed throughout this analysis:

$$\begin{array}{ll} M \gg 1 & \omega \ll 1 \\ \delta \ll 1 & \alpha \ll 1 \end{array}$$

It is further assumed that the present flow fields represent only a small departure from flow fields generated by circular cones. The subsequent analysis, then, will be similar in many respects to that presented in reference 9 for the flow about circular cones at small angles of attack. In particular, the flow in the region of the plane of symmetry (i.e., at  $\phi = 0$ ) is assumed to be identical to that generated by a circular cone in this region. The general form of the expression for the  $w$  component of velocity employed in reference 9 is also assumed to be applicable for the present flow fields.

The following procedure is employed with the above assumptions to obtain a solution for the interference flow field. An expression defining the  $w$  component of velocity throughout the flow field (see fig. 1) is first obtained. The flow is then treated in four parts as shown in sketch (c), which represents the boundaries of the flow field in a plane normal to the configuration axis.



Expressions which define flow conditions along the shock (1-2), in the plane of symmetry (1-3), in the plane of the wing (2-4), and around the surface of the body (3-4) will be obtained in terms of flow conditions at  $\phi = 0$  and  $\phi = \pi/2$ . Solution of the flow in the plane of symmetry determines all conditions at  $\phi = 0$ . All the expressions obtained, then, may be written in terms of known quantities and/or  $(\Psi)_{\pi/2}$ . The parameter  $(\Psi)_{\pi/2}$  is obtained by an iteration process which involves matching at point 4 the pressure calculated by proceeding along 1-3-4 to the pressure calculated by proceeding along 2-4. A discussion of the evaluation of  $(\Psi)_{\pi/2}$  is presented. An analysis of the flow off the surface, that is, between the body surface and the shock, is discussed and expressions defining this part of the flow field will be obtained. Finally, analytic expressions in closed form are obtained for the lift, drag, and pitching-moment coefficients for conical flat-top wing-body combinations. With these points in mind, the analysis for the  $w$  component of velocity will now be considered.

Determination of  $w$  component of velocity. - It was found in reference 9 that the  $w$  and  $\phi$  dependence of  $w$  could be separated into a product for the case of circular cones. Since the present flow fields represent a small departure from that of the circular cone, the same dependence is assumed here; namely,

$$\frac{w}{V_\infty} = w_1(\omega)w_2(\phi) \quad (8)$$

Furthermore, the variation of  $w$  with  $\omega$  is assumed to be the same as in the case of the circular cone so that this variation between the surface and the shock may be written (see ref. 9)

$$w_1(\omega) = \frac{\omega_S}{\omega}$$

Now it is obvious that the variation of  $w$  with  $\phi$  will differ from that for a circular cone since the presence of the wing will alter the boundary conditions. The term  $w_2(\phi)$ , then, will be defined by the polynomial (noting that  $w$  must be an odd function)

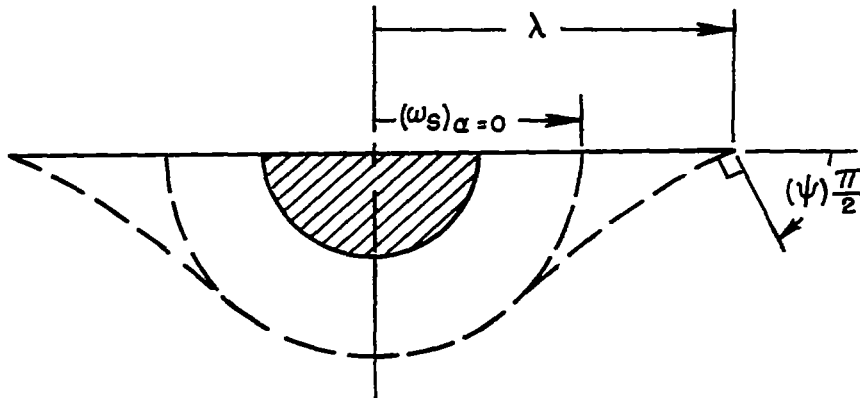
$$w_2(\phi) = c_1\phi + c_2\phi^3 + c_3\phi^5$$

Since  $w = 0$  at  $\phi = 0$  because of the symmetry of the flow and also at  $\phi = \pi/2$  because of the presence of the wing, the coefficients in the above expression are easily evaluated in terms of  $\partial w_2 / \partial \phi$  at  $\phi = 0$  and  $\phi = \pi/2$  to yield (when combined with eq. (8))

$$\begin{aligned} \frac{w}{V_\infty} = & \left( \frac{\omega_S}{\omega} \right) \phi \left\{ \left( \frac{\partial w_2}{\partial \phi} \right)_0 - \frac{2}{\pi^2} \left[ \left( \frac{\partial w_2}{\partial \phi} \right)_{\pi/2} + 4 \left( \frac{\partial w_2}{\partial \phi} \right)_0 \right] \phi^2 + \right. \\ & \left. \frac{8}{\pi^4} \left[ \left( \frac{\partial w_2}{\partial \phi} \right)_{\pi/2} + 2 \left( \frac{\partial w_2}{\partial \phi} \right)_0 \right] \phi^4 \right\} \end{aligned} \quad (9)$$

Expression (9) defines the  $w$  component of the velocity throughout the flow field on the windward side of the configuration. There remains, however, the determination of the shock-wave angle,  $\omega_S$ , and the quantities  $(\partial w_2 / \partial \phi)_0$  and  $(\partial w_2 / \partial \phi)_{\pi/2}$ . An expression for  $\omega_S$  will now be obtained by considering the flow conditions at the conical shock.

Flow conditions at the shock. - The shape of the shock wave will be influenced by the shape of the body, the angle of attack, and the leading-edge sweep of the wing. For example, at  $\alpha = 0^\circ$  the conical shock will be circular between the planes  $\phi = 0$  and  $\phi = \pi/2$  provided the leading-edge angle of the wing,  $\lambda$ , is equal to the axially symmetric shock angle for the complete circular cone. If  $\lambda > (\omega_S)_{\alpha=0}$ , then the shock will impinge on the wing leading edge at an acute angle similar to that shown in sketch (d). The angle  $(\psi)_{\pi/2}$  shown in this sketch (see also fig. 1)



Sketch (d)

is the angle of the dihedral between a plane normal to the shock and the plane of the wing and

$$\tan \psi = \frac{1}{\omega_S} \frac{\partial \omega_S}{\partial \phi} \quad (10)$$

which holds for any meridian plane. Consider now the case where  $\alpha > 0$ . As the angle of attack increases, the pressures on the body, and therefore throughout the flow field, increase causing the shock in the plane of the wing to "spread" beyond that for  $\alpha = 0^\circ$ . Now if the shock is to remain attached to the leading edge, the leading-edge sweep must be decreased. Thus, in the present analysis, there is a minimum  $\lambda$  (maximum sweep) which can be treated for each angle of attack. It is clear from the foregoing discussion that if a reasonably accurate prediction of the flow field is to be obtained, particular attention must be paid to the shape of the shock wave. The conical shock will then be defined by a power series in  $\phi$  where the coefficients are determined from the following conditions:

at  $\phi = 0$ ,

$$\omega_S = (\omega_S)_0 \quad \frac{\partial \omega_S}{\partial \phi} = 0$$

at  $\phi = \frac{\pi}{2}$ ,

$$\omega_S = \lambda \quad \frac{\partial \omega_S}{\partial \phi} = \lambda \tan(\psi)_{\pi/2}$$

Thus, the expression

$$\begin{aligned} \frac{\omega_S}{\delta_c} &= \left( \frac{\omega_S}{\delta_c} \right)_0 + \left( \frac{2}{\pi} \right)^2 \left( \frac{\lambda}{\delta_c} \right) \left\{ 2 \left[ 1 - \frac{(\omega_S)_0}{\lambda} \right] - \frac{\pi}{4} \tan(\psi)_{\pi/2} \right\} \phi^2 - \\ &\quad \left( \frac{2}{\pi} \right)^4 \left( \frac{\lambda}{\delta_c} \right) \left[ 1 - \frac{(\omega_S)_0}{\lambda} - \frac{\pi}{4} \tan(\psi)_{\pi/2} \right] \phi^4 \end{aligned} \quad (11)$$

defines the conical shock with respect to the configuration axis. The tangent operator on  $\psi$  is retained in the above expression since at  $\phi = \pi/2$  this angle represents the attenuation of the shock due to leading-edge sweep and there is no way of determining a priori its order of magnitude. Now for small angles of attack, the shock-wave angle,  $\Omega$ , and flow-deflection angle,  $\Delta$ , measured from the wind axis may be related to the shock angle,  $\omega_S$  and flow-deflection angle,  $\delta_S$ , measured from the configuration axis by

$$\Omega = \omega_S + \alpha \cos \phi \quad (12)$$

and

$$\Delta = \delta_S + \alpha \cos \phi \quad (13)$$

respectively. It can also be shown that, consistent with the above approximations,

$$\Psi = \psi - \frac{\alpha \sin \phi}{\omega_S + \alpha \cos \phi} \quad (14)$$

where  $\Psi$  is the angle of the dihedral at a point on the shock between a streamwise plane normal to the shock and the plane containing the wind axis. Thus, the oblique-shock-wave relations may be written

$$\left( \frac{M_S}{M_\infty} \right)^2 = \frac{(\gamma + 1)^2 M_\infty^2 \Omega^2 \cos^2 \Psi}{[2\gamma M_\infty^2 \Omega^2 \cos^2 \Psi - (\gamma - 1)][(\gamma - 1) M_\infty^2 \Omega^2 \cos^2 \Psi + 2]} \quad (15)$$

$$\frac{\Delta}{\delta_c} = \frac{M_\infty^2 \Omega^2 \cos^2 \Psi - 1}{\frac{\gamma + 1}{2} M_\infty \delta_c M_\infty \Omega \cos \Psi} \quad (16)$$

$$\frac{p_S}{p_\infty} = \frac{2\gamma M_\infty^2 \Omega^2 \cos^2 \Psi - (\gamma - 1)}{\gamma + 1} \quad (17)$$

Equations (11) through (17) completely define conditions immediately downstream of the shock wave in terms of flow parameters referred to the configuration axis. It is clear, of course, that  $(\omega_S)_0$  and  $(\Psi)_{\pi/2}$  are yet to be determined.

Flow conditions in the plane  $\phi = 0$ . - As a by-product of the solution of the flow in this plane, the two quantities  $(\omega_S)_0$  and  $(\partial w_2/\partial\phi)_0$  will be determined. Because of the symmetry of the flow in this plane,  $w = 0$  and the equation of motion (eq. (5)) reduces to

$$\frac{\gamma - 1}{2} (\hat{V}^2 - V^2) \left( 2u + v \cot \omega + \frac{\partial v}{\partial \omega} + \frac{1}{\sin \omega} \frac{\partial w}{\partial \phi} \right) - v^2 \left( u + \frac{\partial v}{\partial \omega} \right) = 0 \quad (18)$$

Now from the flow pattern, the velocity components may be written

$$u = V \cos(\omega - \delta)$$

$$v = -V \sin(\omega - \delta)$$

and from equation (1a)

$$v = \frac{\partial u}{\partial \omega}$$

It can also be shown that

$$\frac{dV}{V} = -\tan(\omega - \delta) d\delta \quad (19)$$

Substitution of the above expressions into equation (18) results in

$$\frac{\gamma - 1}{2} \left[ \left( \frac{\hat{V}}{V} \right)^2 - 1 \right] \left[ \cot(\omega - \delta) \left( 1 + \frac{\partial \delta}{\partial \omega} \right) - \cot \omega + \tan(\omega - \delta) \frac{\partial \delta}{\partial \omega} + \frac{\csc(\omega - \delta)}{V \sin \omega} \frac{\partial w}{\partial \phi} \right] - \tan(\omega - \delta) \frac{\partial \delta}{\partial \omega} = 0$$

Consistent now with the assumption of  $\delta \ll 1$  and  $\omega \ll 1$ , the above expression may be written

$$\frac{\delta}{\omega} + \frac{\partial \delta}{\partial \omega} \left[ 1 - (M\omega)^2 \left( 1 - \frac{\delta}{\omega} \right)^2 \right] + \frac{1}{V\omega} \frac{\partial w}{\partial \phi} = 0$$

Furthermore, since  $M\omega$  and  $\delta/\omega$  are both of the order of 1, there is finally obtained (by virtue of eq. (8))

$$\frac{\partial \delta}{\partial \omega} + \frac{\delta}{\omega} + \frac{V_\infty}{V} \frac{\omega_S}{\omega^2} \left( \frac{\partial w_2}{\partial \varphi} \right)_o = 0 \quad (20)$$

Consider now the term  $(\partial w_2 / \partial \varphi)_o$ . If the angle of attack is small and the leading-edge angle of the wing does not differ too greatly from the angle of the shock wave generated by the equivalent circular cone, then one might expect the flow in the plane of symmetry to differ but little from that of the circular cone.<sup>2</sup> It is assumed, therefore, that, as a first approximation, the flow in this plane will be the same as that for the circular cone. Then (see ref. 9)

$$\left( \frac{\partial w}{\partial \varphi} \right)_o = V_\infty \epsilon \frac{\omega_S}{\omega}$$

where  $\epsilon$  is the angle between the axis of the conical shock and the free-stream-velocity vector. It follows, then, from equation (8) that

$$\left( \frac{\partial w_2}{\partial \varphi} \right)_o = \epsilon$$

and, therefore, equation (20) yields upon integration (noting that  $V_\infty/V \approx 1$ )

$$\frac{\delta}{\delta_c} = \frac{\delta_c}{\omega} - \left( \frac{\epsilon}{\delta_c} \right) \left( \frac{\omega_S}{\omega} \right) \ln \frac{\omega}{\delta_c} \quad (21)$$

which defines the flow-deflection angle. The expression for the flow velocity is obtained by integration of the resulting combination of equations (19) and (21) and may be written

$$\frac{v}{V_S} = \left( \frac{\omega}{\omega_S} \right)^{\left( \delta_c^2 + \epsilon \omega_S \right) \frac{1}{2} (\delta^2 - \delta_S^2)} - \frac{\epsilon \omega_S}{2} \left[ \left( \ln \frac{\omega}{\delta_c} \right)^2 - \left( \ln \frac{\omega_S}{\delta_c} \right)^2 \right] \quad (22)$$

Now the Mach number may be expressed in terms of the above velocity ratio by

$$M^2 = \frac{\left( \frac{v}{V_S} \right)^2 M_S^2}{1 - \frac{\gamma - 1}{2} M_S^2 \left[ \left( \frac{v}{V_S} \right)^2 - 1 \right]}$$

---

<sup>2</sup>Experimental results indicate (as will be shown later) that, at small angles of attack, the shock-wave angles and pressure coefficients in the plane  $\varphi = 0$  are approximately the same as those for the circular cone.

which, after substitution of equation (22) and neglecting second-order terms, becomes

$$\left(\frac{M_S}{M}\right)^2 = 1 - \frac{\gamma - 1}{2} \left(M_S \delta_c\right)^2 \left\{ \left(\frac{\delta}{\delta_c}\right)^2 - \left(\frac{\omega_S}{\delta_c}\right)^2 - 2 \left(1 + \frac{\epsilon \omega_S}{\delta_c^2}\right) \ln \frac{\omega_S}{\omega} - \frac{\epsilon \omega_S}{\delta_c^2} \left[ \left(\ln \frac{\omega}{\delta_c}\right)^2 - \left(\ln \frac{\omega_S}{\delta_c}\right)^2 \right] \right\} \quad (23)$$

Finally, flow conditions at the shock are obtained from the oblique-shock relations given by equations (15), (16), and (17) reduced to the form

$$\left(\frac{M_S}{M_\infty}\right)^2 = \frac{(\gamma + 1)^2 M_\infty^2 (\omega_S + \alpha)^2}{[2\gamma M_\infty^2 (\omega_S + \alpha)^2 - (\gamma - 1)][(\gamma - 1)M_\infty^2 (\omega_S + \alpha)^2 + 2]} \quad (24)$$

$$M_\infty(\delta_S + \alpha) = \frac{M_\infty^2 (\omega_S + \alpha)^2 - 1}{\frac{\gamma + 1}{2} M_\infty (\omega_S + \alpha)} \quad (25)$$

and

$$\frac{p_S}{p_\infty} = \frac{2\gamma M_\infty^2 (\omega_S + \alpha)^2 - (\gamma - 1)}{\gamma + 1} \quad (26)$$

respectively.

There remains the determination of  $\epsilon$  in order to obtain the shock-wave angle,  $\omega_S$ , from equations (21) and (25). It can be shown by an analysis identical to that presented in reference 9 that<sup>3</sup>

$$\frac{\epsilon}{\alpha} = \frac{\gamma + 1}{4} \frac{1 + \frac{\gamma + 3}{2} (M_\infty \delta_c)^2}{\left[1 + \frac{\gamma + 1}{2} (M_\infty \delta_c)^2\right] \left\{1 - \frac{\gamma + 1}{8} \ln \left[ \frac{(M_\infty \delta_c)^2}{1 + \frac{\gamma + 1}{2} (M_\infty \delta_c)^2} \right]\right\}} \quad (27)$$

The shock angle can now be evaluated by the simultaneous solution of equations (21), (25), and (27). This has been done with the aid of the

---

<sup>3</sup>An expression for  $1 - \epsilon/\alpha$  was developed in reference 9 and differs from the present relation in the logarithm term since only the first term of a logarithm series was retained in that development.

IBM 650 electronic computing machine, and results in the form  $(\omega_S/\delta_c)_0$  for values of  $M_\infty \delta_c$  from 0.1 to 3.0 and  $\alpha/\delta_c$  from 0 to 1 are presented in table I. Once the shock-wave angle has been obtained from the table, it is a simple matter to determine all the other flow quantities in the plane  $\phi = 0$  from equations (21) through (27).

Flow conditions in the plane of the wing ( $\phi = \pi/2$ ). - Because of the presence of the wing in this plane,  $w = 0$  and the conical-flow equations obtained for the plane  $\phi = 0$  hold identically in the plane of the wing. Thus, the flow-deflection angle is defined by (noting that  $(\omega_S)_{\pi/2} = \lambda$ )

$$\frac{\delta}{\delta_c} = \frac{\delta_c}{\omega} - \frac{1}{\delta_c} \left( \frac{\partial w_2}{\partial \phi} \right)_{\pi/2} \left( \frac{\lambda}{\omega} \right) \ln \frac{\omega}{\delta_c} \quad (28)$$

Similarly, the expressions for the velocity and Mach number become

$$\frac{V}{V_S} = \left( \frac{\omega}{\lambda} \right)^{\delta_c^2 + \lambda} \left( \frac{\partial w_2}{\partial \phi} \right)_{\pi/2} e^{\frac{1}{2}(\delta^2 - \delta_S^2)} - \frac{\lambda}{2} \left( \frac{\partial w_2}{\partial \phi} \right)_{\pi/2} \left[ \left( \ln \frac{\omega}{\delta_c} \right)^2 - \left( \ln \frac{\lambda}{\delta_c} \right)^2 \right] \quad (29)$$

and

$$\begin{aligned} \left( \frac{M_S}{M} \right)^2 &= 1 - \frac{\gamma - 1}{2} (M_S \delta_c)^2 \left\{ \left( \frac{\delta}{\delta_c} \right)^2 - \left( \frac{\delta_S}{\delta_c} \right)^2 - 2 \left[ 1 + \frac{\lambda}{\delta_c^2} \left( \frac{\partial w_2}{\partial \phi} \right)_{\pi/2} \right] \ln \frac{\lambda}{\omega} - \right. \\ &\quad \left. \frac{\lambda}{\delta_c^2} \left( \frac{\partial w_2}{\partial \phi} \right)_{\pi/2} \left[ \left( \ln \frac{\omega}{\delta_c} \right)^2 - \left( \ln \frac{\lambda}{\delta_c} \right)^2 \right] \right\} \end{aligned} \quad (30)$$

respectively. The ratio of the local static pressure to the static pressure at the shock for hypersonic flow is given by

$$\frac{p}{p_S} = \left( \frac{M_S}{M} \right)^{\frac{2\gamma}{\gamma-1}} \quad (31)$$

The Mach number, flow deflection, and static pressure at the shock are, of course, obtained from the oblique-shock relations (15), (16), and (17) which now become

$$\left( \frac{M_S}{M_\infty} \right)^2 = \frac{(\gamma + 1)^2 (M_\infty \lambda)^2 \cos^2(\Psi)_{\pi/2}}{\left[ 2\gamma (M_\infty \lambda)^2 \cos^2(\Psi)_{\pi/2} - (\gamma - 1) \right] \left[ (\gamma - 1) (M_\infty \lambda)^2 \cos^2(\Psi)_{\pi/2} + 2 \right]} \quad (32)$$

$$\frac{\delta_S}{\delta_c} = \frac{(M_\infty \lambda)^2 \cos^2(\Psi)_{\pi/2} - 1}{\frac{\gamma + 1}{2} M_\infty \delta_c M_\infty \lambda \cos(\Psi)_{\pi/2}} \quad (33)$$

and

$$\frac{P_S}{P_\infty} = \frac{2\gamma(M_\infty \lambda)^2 \cos^2(\Psi)_{\pi/2} - (\gamma - 1)}{\gamma + 1} \quad (34)$$

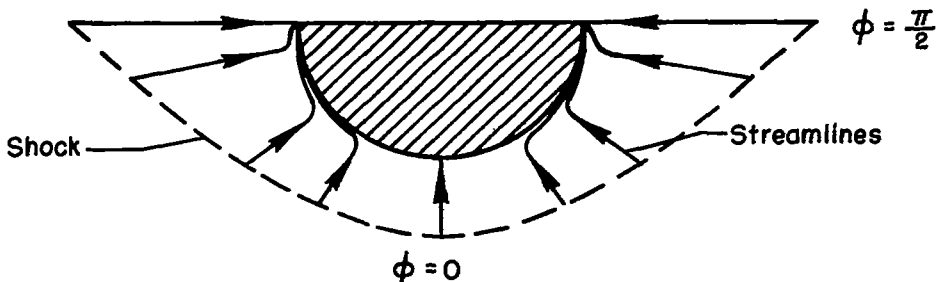
respectively. Consider now equation (28) in combination with equation (33). Then,

$$\frac{1}{\delta_c} \left( \frac{\partial w_2}{\partial \phi} \right)_{\pi/2} = \frac{1 + \frac{\gamma + 1}{2} (M_\infty \delta_c)^2 \cos(\Psi)_{\pi/2} - (M_\infty \lambda)^2 \cos^2(\Psi)_{\pi/2}}{\frac{\gamma + 1}{2} M_\infty \delta_c M_\infty \lambda \cos(\Psi)_{\pi/2} \ln \frac{\lambda}{\delta_c}} \quad (35)$$

The only remaining unknown in the foregoing expressions is  $(\Psi)_{\pi/2}$ . If this angle were known, flow conditions on the wing, as well as those around the shock and in the plane  $\phi = 0$ , could be calculated by means of the expressions so far obtained. As mentioned earlier in the discussion of the flow pattern shown in sketch (c),  $(\Psi)_{\pi/2}$  can be evaluated by matching at the wing-body juncture the pressure calculated in the plane of the wing to the pressure calculated on the surface of the body. Now the static pressure in the plane of the wing can be calculated by means of equations (31) and (34). However, in order to calculate the static pressure on the body surface, expressions defining the flow on this surface must be obtained. Attention is therefore turned to this matter.

Flow conditions on the body surface. - The concept of a vortical singularity in supersonic flow around a cone was introduced by Ferri in reference 10 where it was shown that all constant entropy surfaces must intersect along the generator lying in the meridian plane on the leeward side. It was also demonstrated that for small angles of attack the singularity lies on the surface itself. Holt, in reference 11, demonstrated that such a singularity can arise only at points where the resultant velocity is directed along the radial line (i.e.,  $w = v = 0$ ), and that at the singularity the velocity is many-valued and the vorticity is infinite, but the pressure is single-valued. For configurations of the type under

consideration, then, the lines of constant entropy in a plane normal to the configuration axis will appear something like those shown in sketch (e).



Sketch (e)

The singularities will occur at the wing-body junctures since  $w = v = 0$  and  $\partial w / \partial \phi < 0$  at these points. Thus, the angle of attack is assumed sufficiently small that the singularity will remain on the surface of the cone. The thickness of the vortical layer around the cone surface can be neglected then, since it was shown in reference 10 to be the order of  $\alpha^2$ . Since the entropy on the surface is constant it must have the value that exists in the plane  $\phi = 0$ . Thus,

$$p_c = p_e$$

$$v_c = v_e = 0$$

and

$$E_c = (E)_o$$

where the subscripts c and e refer to conditions inside and outside the vortical layer, respectively. It follows then from equation (la) that

$$\frac{\partial u}{\partial \phi} = \delta_c w$$

or

$$\frac{u}{(v_c)_o} = 1 + \delta_c \int_0^\phi \frac{w}{(v_c)_o} d\phi \quad (36)$$

which holds on either side of the vortical layer, even though w is discontinuous across the layer. Consider now the w component of velocity on the surface externally adjacent to the vortical layer expressed in the form

$$\frac{w_e}{(v_c)_o} = F' \quad (37)$$

where the prime in the above expression refers to the derivative with respect to  $\phi$ . Then, upon integration, equation (36) becomes

$$\frac{u_e}{(v_c)_o} = 1 + \delta_c F \quad (38)$$

and the resultant surface velocity may be written

$$\left[ \frac{v_e}{(v_c)_o} \right]^2 = 1 + 2\delta_c F + (F')^2 \quad (39)$$

since, as will be shown subsequently,  $F$  and  $F'$  are first-order quantities. The corresponding Mach number ratio may be expressed as

$$\left[ \frac{(M_c)_o}{M_e} \right]^2 = \frac{1 - \frac{\gamma - 1}{2} (M_c)_o^2 \left\{ \left[ \frac{v_e}{(v_c)_o} \right]^2 - 1 \right\}}{\left[ \frac{v_e}{(v_c)_o} \right]^2} \quad (40)$$

which, by virtue of equation (39), reduces to

$$\left[ \frac{(M_c)_o}{M_e} \right]^2 = 1 - \frac{\gamma - 1}{2} (M_c \delta_c)_o^2 \left[ 2 \frac{F}{\delta_c} + \left( \frac{F'}{\delta_c} \right)^2 \right] \quad (41)$$

where (from eqs. (9), (11), and (37))

$$\begin{aligned} \frac{F'}{\delta_c} &= \frac{\lambda}{\delta_c} \phi \left\{ \frac{(\omega_s)_o}{\lambda} + \left( \frac{2}{\pi} \right)^2 \phi^2 \left[ 2 \left( 1 - \frac{(\omega_s)_o}{\lambda} \right) - \frac{\pi}{4} \tan(\psi)_{\pi/2} \right] - \right. \\ &\quad \left. \left( \frac{2}{\pi} \right)^4 \phi^4 \left[ 1 - \frac{\pi}{4} \tan(\psi)_{\pi/2} - \frac{(\omega_s)_o}{\lambda} \right] \right\} \left\{ \frac{1}{\delta_c} \left( \frac{\partial w_2}{\partial \phi} \right)_o - \right. \\ &\quad \left. \frac{2}{\pi^2} \left[ \frac{1}{\delta_c} \left( \frac{\partial w_2}{\partial \phi} \right)_{\pi/2} + \frac{1}{\delta_c} \left( \frac{\partial w_2}{\partial \phi} \right)_o \right] \phi^2 + \frac{8}{\pi^4} \left[ \frac{1}{\delta_c} \left( \frac{\partial w_2}{\partial \phi} \right)_{\pi/2} + \frac{2}{\delta_c} \left( \frac{\partial w_2}{\partial \phi} \right)_o \right] \phi^4 \right\} \end{aligned} \quad (42)$$

and (upon integration of eq. (42))

$$\begin{aligned}
 \frac{F}{\delta_c} = & \frac{(\omega_S)_o}{\delta_c} \varphi^2 \left\{ \frac{1}{2\delta_c} \left( \frac{\partial w_2}{\partial \varphi} \right)_o - \frac{1}{2\pi^2} \left[ \frac{1}{\delta_c} \left( \frac{\partial w_2}{\partial \varphi} \right)_{\pi/2} + \frac{1}{\delta_c} \left( \frac{\partial w_2}{\partial \varphi} \right)_o \right] \varphi^2 + \frac{1}{3\pi^4} \left[ \frac{1}{\delta_c} \left( \frac{\partial w_2}{\partial \varphi} \right)_{\pi/2} + \frac{2}{\delta_c} \left( \frac{\partial w_2}{\partial \varphi} \right)_o \right] \varphi^4 \right\} + \\
 & \left( \frac{2}{\pi} \right)^2 \left( \frac{\lambda}{\delta_c} \right) \varphi^4 \left[ 2 \left( 1 - \frac{(\omega_S)_o}{\lambda} \right) - \frac{1}{4} \tan(\psi)_{\pi/2} \right] \left\{ \frac{1}{4\delta_c} \left( \frac{\partial w_2}{\partial \varphi} \right)_o - \frac{1}{3\pi^2} \left[ \frac{1}{\delta_c} \left( \frac{\partial w_2}{\partial \varphi} \right)_{\pi/2} + \frac{1}{\delta_c} \left( \frac{\partial w_2}{\partial \varphi} \right)_o \right] \varphi^2 + \frac{1}{\pi^4} \left[ \frac{1}{\delta_c} \left( \frac{\partial w_2}{\partial \varphi} \right)_{\pi/2} + \frac{2}{\delta_c} \left( \frac{\partial w_2}{\partial \varphi} \right)_o \right] \varphi^4 \right\} - \\
 & \left( \frac{2}{\pi} \right)^4 \left( \frac{\lambda}{\delta_c} \right) \varphi^6 \left[ 1 - \frac{1}{4} \tan(\psi)_{\pi/2} - \frac{(\omega_S)_o}{\lambda} \right] \left\{ \frac{1}{6\delta_c} \left( \frac{\partial w_2}{\partial \varphi} \right)_o - \frac{1}{4\pi^2} \left[ \frac{1}{\delta_c} \left( \frac{\partial w_2}{\partial \varphi} \right)_{\pi/2} + \frac{1}{\delta_c} \left( \frac{\partial w_2}{\partial \varphi} \right)_o \right] \varphi^2 + \frac{1}{5\pi^4} \left[ \frac{1}{\delta_c} \left( \frac{\partial w_2}{\partial \varphi} \right)_{\pi/2} + \frac{2}{\delta_c} \left( \frac{\partial w_2}{\partial \varphi} \right)_o \right] \varphi^4 \right\}
 \end{aligned} \tag{43}$$

It can be seen from equations (42) and (43) that  $F'$  and  $F$  are of the order of  $\delta_c$ . Thus, the two right-hand terms in equation (39) are second-order terms. The Mach number directly on the body surface,  $M_c$ , may be related to the Mach number at the vortical layer,  $M_e$ , by (see ref. 9)

$$\left( \frac{M_e}{M_c} \right)^2 = e^{\frac{E_c - E_e}{\gamma c_v}}$$

where (by virtue of eq. (4))

$$\frac{E_c - E_e}{\gamma c_v} = \left[ \frac{2\gamma M_\infty^2 (\omega_S + \alpha)_o^2 - (\gamma - 1)}{2\gamma (M_\infty \Omega)^2 \cos^2 \Psi - (\gamma - 1)} \right]^{\frac{1}{\gamma}} \left\{ \frac{(M_\infty \Omega)^2 \cos^2 \Psi [(\gamma - 1) M_\infty^2 (\omega_S + \alpha)_o^2 + 2]}{M_\infty^2 (\omega_S + \alpha)_o^2 [(\gamma - 1) (M_\infty \Omega)^2 \cos^2 \Psi + 2]} \right\} \tag{44}$$

and  $\Omega$  and  $\Psi$  are defined by equations (12) and (14), respectively. Then,

$$\left[ \frac{(\omega_S)_o}{M_c} \right]^2 = e^{\frac{E_c - E_e}{\gamma c_v}} \left[ \frac{(\omega_S)_o}{M_e} \right]^2 \left( \frac{M_S}{M_c} \right)_o^2 \tag{45}$$

and the ratio of the static pressure anywhere on the body surface to the static pressure at the shock at  $\varphi = 0$  is given by

$$\frac{p_c}{(p_s)_o} = \left[ \frac{(\omega_S)_o}{M_c} \right]^{\frac{2\gamma}{\gamma-1}} \tag{46}$$

Finally, the ratio of the surface pressure to the free-stream static pressure may be obtained by the combination of equations (26) and (46) which yields

$$\frac{p_c}{p_\infty} = \left[ \frac{2\gamma M_\infty^2 (\omega_S + \alpha)_o^2 - (\gamma - 1)}{\gamma + 1} \right] \left[ \frac{(M_S)_o}{M_c} \right]^{\frac{2\gamma}{\gamma-1}} \quad (47)$$

The pressure coefficient is, of course, given by the relation

$$C_p = \frac{2}{\gamma M_\infty^2} \left( \frac{p_c}{p_\infty} - 1 \right) \quad (48)$$

It will be noted that the foregoing equations predict the ratios of local to free-stream Mach number and local to free-stream static pressures to be the same at corresponding points on related configurations, provided the flow fields about these configurations are defined by the same respective values of the hypersonic similarity parameters,  $M_\infty \delta_c$ ,  $M_\infty \alpha$  (or  $\alpha/\delta_c$ ), and  $M_\infty \lambda$  (or  $\lambda/\delta_c$ ). These predictions are in agreement with those of reference 12 for inviscid flow about slender three-dimensional shapes.

Evaluation of  $(\Psi)_{\pi/2}$ . - We are now in a position to calculate  $(\Psi)_{\pi/2}$  and, therefore, all flow properties on the surface of the complete configuration. This may be accomplished in the following manner. If the Mach number, angle of attack, and the conical configuration are given, then  $M_\infty \delta_c$ ,  $\alpha/\delta_c$ , and  $\lambda/\delta_c$  are known and a value for  $(\Psi)_{\pi/2}$  is assumed. Then  $(\Psi)_{\pi/2}$  is known from equation (14) and the pressure under the vortical layer at  $\phi = \pi/2$  can be calculated by means of equation (47). The pressure externally adjacent to the vortical layer in the plane of the wing can be calculated by means of equations (31) and (34). Since there is no pressure change across the vortical layer, an iteration on  $(\Psi)_{\pi/2}$  can be performed until the pressures on both sides of the layer are equal. This iteration has been performed on the IBM 650 electronic computing machine and the resulting values of  $(\Psi)_{\pi/2}$  for  $M_\infty \delta_c$  from 0.1 to 3.0 and  $\alpha/\delta_c$  from 0 to 1 are given in table I for various values of  $\lambda/\delta_c$ . The values of the ratio of the static pressure to the free-stream static pressure at the bottom of the body,  $(p_c/p_\infty)_o$ , at the wing-body juncture,  $(p_c/p_\infty)_{\pi/2}$ , and at the leading-edge of the wing,  $(p/p_\infty)_\lambda$ , are also given in table I.

It should be noted in table I that the range of  $\alpha/\delta_c$  is restricted for certain values of  $\lambda/\delta_c$ . As was mentioned previously in the analysis for conditions at the shock, this results from the fact that there is a maximum angle of attack for a given configuration and Mach number at which the shock wave can no longer remain attached to the leading edge of the wing. This occurs at  $(\Psi)_{\pi/2} = 0$ , since it represents zero attenuation of the strength of the shock. Thus, the values of  $\lambda/\delta_c$  given in table I for  $(\Psi)_{\pi/2} = 0$  represent minimum values (maximum leading-edge sweeps) for which the present theory will apply for a particular  $\alpha/\delta_c$  and, of

course,  $M_\infty \delta_c$ . This is perhaps more clearly demonstrated in figure 2 where  $(\lambda/\delta_c)_{\min}$  is shown plotted as a function of  $(\alpha/\delta_c)_{\max}$  for various  $M_\infty \delta_c$ . Thus, for example, each line of constant  $M_\infty \delta_c$  represents an upper limit of  $\alpha/\delta_c$  and a lower limit of  $\lambda/\delta_c$  on the applicability of the theory for a given free-stream Mach number.

Flow conditions off the surface. - Since only flows at high Mach number are considered in this analysis, the variation of the magnitude of the resultant velocity in a meridian plane will be small. Hence, the variation of  $u$  and  $v$  will be small and may be represented by a power series in  $(\omega - \delta_c)$  where the coefficients are evaluated in terms of the velocity component at the surface and at the shock and its derivative at the surface. Thus,

$$u = u_e + \left( \frac{\partial u}{\partial \omega} \right)_e (\omega - \delta_c) \left( \frac{\omega_s - \omega}{\omega_s - \delta_c} \right) + (u_s - u_e) \left( \frac{\omega - \delta_c}{\omega_s - \delta_c} \right)^2 \quad (49)$$

$$v = \left( \frac{\partial v}{\partial \omega} \right)_e (\omega - \delta_c) \left( \frac{\omega_s - \omega}{\omega_s - \delta_c} \right) + v_s \left( \frac{\omega - \delta_c}{\omega_s - \delta_c} \right)^2 \quad (50)$$

where it can be shown that (see ref. 9)

$$\left( \frac{\partial u}{\partial \omega} \right)_e = \left( \frac{w}{u} \right)_e \left[ \left( \frac{\partial w}{\partial \omega} \right)_e + \frac{w_e}{\delta_c} \right]$$

and (setting  $v = 0$  in eq. (5))

$$\left( \frac{\partial v}{\partial \omega} \right)_e = \left[ u_e + \frac{1}{\delta_c} \left( \frac{\partial w}{\partial \varphi} \right)_e \right] \left[ M_e^2 \left( \frac{w}{v} \right)_e^2 - 1 \right] - u_e$$

In the above expressions,  $\omega_s$ ,  $w_e$ ,  $u_e$ , and  $M_e$  are given by equations (9), (11), (38), and (41), respectively, and  $(\partial w/\partial \omega)_e$  and  $(\partial w/\partial \varphi)_e$  may be obtained by the proper differentiation of equation (9). Finally, the radial component of velocity at the shock may be determined from the relation

$$u_s = v_\infty \cos(\omega_s + \alpha \cos \varphi)$$

and the normal component of velocity may be written

$$v_s = - \sqrt{v_s^2 - u_s^2 - w_s^2}$$

where

$$\left(\frac{V_S}{\hat{V}}\right)^2 = \frac{\frac{\gamma - 1}{2} M_S^2}{1 + \frac{\gamma - 1}{2} M_S^2}$$

The Mach number at the shock,  $M_S$ , is defined by equation (15). The components of the local velocity anywhere in the flow field external to the vortical layer and between the planes  $\phi = 0$  and  $\phi = \pi/2$  are now known from equations (9), (49), and (50). Hence, the magnitude and direction of the resultant velocity and, consequently, the Mach number may be easily determined. The local pressure coefficient, then, may be obtained from the relation

$$C_p = \frac{2}{\gamma M_\infty^2} \left( \frac{p_S}{p_\infty} \frac{p}{p_S} - 1 \right)$$

where  $p_S/p_\infty$  is given by equation (17) and

$$\frac{p}{p_S} = \left( \frac{M_S}{M} \right)^{\frac{2\gamma}{\gamma-1}}$$

The flow field about slender, conical, flat-top wing-body configurations traveling at high supersonic speeds and at small angles of attack can be calculated by means of the foregoing expressions. Explicit expressions defining the lift, drag, and pitching-moment coefficients will now be obtained.

Lift, drag, and pitching-moment coefficients. - Because of the rather complicated nature of the expressions previously developed, resort must be made to graphical or numerical integration of the pressures acting on the surface in order to calculate the integrated aerodynamic forces. It is first undertaken, therefore, to obtain algebraic expressions, yielding the surface pressures, which are amenable to simple analytic integration. In this regard, the tabulated pressure ratios in table I may be used to good advantage. For example, it will be noted from equation (1c) that  $\partial p/\partial \phi = 0$  when  $w = v = 0$ . On the surface of the body, then,  $\partial p/\partial \phi = 0$  at  $\phi = 0$  and  $\phi = \pi/2$ , since  $w = v = 0$  at these two points. Therefore, to a good approximation, the variation of static pressure around the body surface may be expressed in the form

$$\frac{p_c}{p_\infty} = \left( \frac{p_c}{p_\infty} \right)_0 \cos^2 \phi + \left( \frac{p_c}{p_\infty} \right)_{\pi/2} \sin^2 \phi \quad (51)$$

Similarly, the pressure at any axial station on the wing may be expressed in terms of the pressure at the wing-body juncture, the derivative at

this point, and the pressure at the leading edge. Thus<sup>4</sup>

$$\frac{p}{p_{\infty}} = \left( \frac{p_c}{p_{\infty}} \right)_{\pi/2} - \left[ \left( \frac{p_c}{p_{\infty}} \right)_{\pi/2} - \left( \frac{p}{p_{\infty}} \right)_{\lambda} \right] \left( \frac{\tan \omega - \tan \delta_c}{\tan \lambda - \tan \delta_c} \right)^2 \quad (52)$$

since, from equation (1b),  $\partial p / \partial \omega = 0$  when  $w = v = 0$ . The surface pressures can be easily calculated by means of equations (51) and (52) and with the aid of table I. These equations are also easily integrated to obtain the lift, drag, and pitching-moment coefficients. Thus, for example, the normal-force coefficient for the body may be written

$$C_{N_B} = \frac{2l_B^2 \tan \delta_c}{\gamma M_{\infty}^2 S} \int_0^{\pi/2} \left( \frac{p_c}{p_{\infty}} - 1 \right) \cos \varphi d\varphi \quad (53)$$

whereas that due to the wing may be expressed in the form

$$C_{N_W} = \frac{2}{\gamma M_{\infty}^2 S} \int_{\delta_c}^{\lambda} \left( \frac{p}{p_{\infty}} - 1 \right) r_{te}^2 d\omega - \frac{2}{\gamma M_{\infty}^2} \left\{ \left[ 1 - \frac{\gamma - 1}{2} M_{\infty}(\alpha - \delta_W) \right]^{\frac{2\gamma}{\gamma-1}} - 1 \right\} \quad (54)$$

where  $S$  is the total plan area and  $r_{te}$  is the radial distance from the vertex of the wing to the trailing edge. The integral term in equation (54) represents the normal force due to the pressures acting on the exposed area of the windward side of the wing whereas the last term is the contribution due to the leeward side of the wing. The axial-force coefficient for the body and the wing may be written (neglecting base drag)

$$C_{A_B} = \frac{2l_B^2 \tan^2 \delta_c}{\gamma M_{\infty}^2 S} \int_0^{\pi/2} \left( \frac{p_c}{p_{\infty}} - 1 \right) d\varphi \quad (55)$$

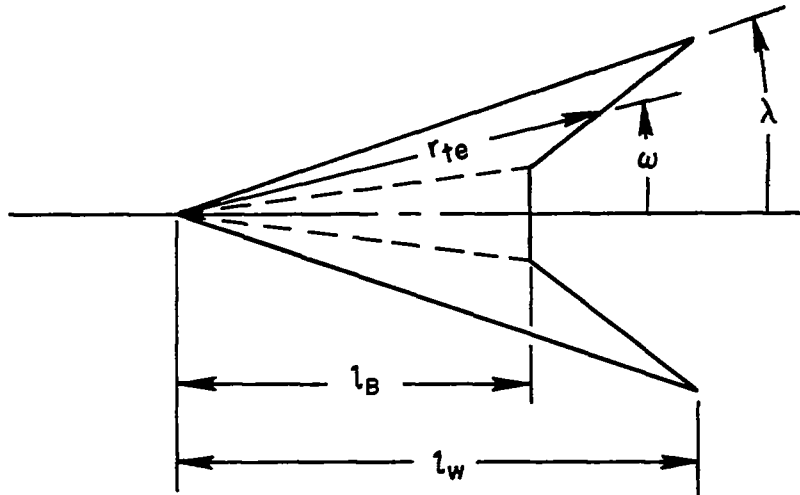
and

$$C_{A_W} = \frac{2 \tan \delta_W}{\gamma M_{\infty}^2} \left\{ \left[ 1 - \frac{\gamma - 1}{2} M_{\infty}(\alpha - \delta_W) \right]^{\frac{2\gamma}{\gamma-1}} - 1 \right\} \quad (56)$$

---

<sup>4</sup>The tangents are retained rather than the angles in the following expression to facilitate a subsequent analytic integration to obtain the aerodynamic forces acting on the wing.

respectively. Consider now a configuration having an arrow plan-form wing as shown in sketch (f). Then



Sketch (f)

$$r_{te} = \frac{l_B l_W (\tan \lambda - \tan \delta_c) \sec \omega}{l_W \tan \lambda - l_B \tan \delta_c - (l_W - l_B) \tan \omega} \quad (57)$$

and

$$S = l_B l_W (\tan \lambda - \tan \delta_c) + l_B^2 \tan \delta_c \quad (58)$$

Thus, upon substitution of equations (51) and (58) into (53) and equations (52), (57), and (58) into (54) there is obtained, upon integration,

$$C_{NB} = \frac{2 \left[ \frac{2}{3} \left( \frac{p_c}{p_\infty} \right)_0 + \frac{1}{3} \left( \frac{p_c}{p_\infty} \right)_{\pi/2} - 1 \right]}{\gamma M_\infty^2 \left[ \left( \frac{l_w}{l_B} \right) \left( \frac{\tan \lambda}{\tan \delta_c} - 1 \right) + 1 \right]} \quad (59)$$

$$C_{NW} = \frac{2 \left( \frac{l_W}{l_B} \right) \left( \frac{\tan \lambda}{\tan \delta_c} - 1 \right)}{\gamma M_\infty^2 \left[ \left( \frac{l_W}{l_B} \right) \left( \frac{\tan \lambda}{\tan \delta_c} - 1 \right) + 1 \right]} \left\{ \begin{aligned} & \left( \frac{p_c}{p_\infty} \right)_{\pi/2} - 1 - \\ & \left[ \left( \frac{p_c}{p_\infty} \right)_{\pi/2} - \left( \frac{p}{p_\infty} \right)_\lambda \right] \left( \frac{l_W}{l_B} \right) \left[ \left( \frac{l_W}{l_B} \right)^2 - 2 \left( \frac{l_W}{l_B} \right) \ln \frac{l_W}{l_B} - 1 \right] \\ & \left( \frac{l_W}{l_B} - 1 \right)^3 \end{aligned} \right\} - \\ \frac{2}{\gamma M_\infty^2} & \left\{ \left[ 1 - \frac{\gamma - 1}{2} M_\infty (\alpha - \delta_W) \right]^{\frac{2\gamma}{\gamma-1}} - 1 \right\} \quad (60) \end{math>$$

In the case of a delta wing (i.e.,  $l_W = l_B$ ), equation (60) is indeterminate in its present form. However, it can be shown that when  $l_W = l_B$

$$C_{NW} = \frac{2 \left( 1 - \frac{\tan \delta_c}{\tan \lambda} \right)}{\gamma M_\infty^2} \left[ \frac{2}{3} \left( \frac{p_c}{p_\infty} \right)_{\pi/2} + \frac{1}{3} \left( \frac{p}{p_\infty} \right)_\lambda - 1 \right] - \\ \frac{2}{\gamma M_\infty^2} \left\{ \left[ 1 - \frac{\gamma - 1}{2} M_\infty (\alpha - \delta_W) \right]^{\frac{2\gamma}{\gamma-1}} - 1 \right\} \quad (61)$$

The axial-force coefficient due to the body is obtained by the integration of equation (55) which yields

$$C_{AB} = \frac{\pi \tan \delta_c \left[ \frac{1}{2} \left( \frac{p_c}{p_\infty} \right)_0 + \frac{1}{2} \left( \frac{p_c}{p_\infty} \right)_{\pi/2} - 1 \right]}{\gamma M_\infty^2 \left[ \left( \frac{l_W}{l_B} \right) \left( \frac{\tan \lambda}{\tan \delta_c} - 1 \right) + 1 \right]} \quad (62)$$

The axial-force coefficient contributed by the wing is given by equation (56). Finally, the lift and pressure-drag coefficients may be calculated from the expressions

$$C_L = C_N \cos \alpha - C_A \sin \alpha \quad (63)$$

$$C_D = C_A \cos \alpha + C_N \sin \alpha \quad (64)$$

where, of course,

$$C_N = C_{N_B} + C_{N_W}$$

$$C_A = C_{A_B} + C_{A_W}$$

Now the expression for the pitching-moment coefficient due to the pressure forces acting on the fuselage side of an arrow plan-form wing may be written (see sketch (f))

$$(C_m)_W^L \text{ lower} = - \frac{4}{3\gamma M_\infty^2 l_B S} \int_{\delta_c}^\lambda \left( \frac{p}{p_\infty} - 1 \right) r_{te}^3 \cos \omega d\omega \quad (65)$$

which, upon substitution of equations (52), (57), and (58), may be integrated to yield

$$(C_m)_W^L \text{ lower} = - \frac{2 \left( \frac{l_W}{l_B} \right) \left( \frac{\tan \lambda}{\tan \delta_c} - 1 \right)}{3\gamma M_\infty^2 \left[ \left( \frac{l_W}{l_B} \right) \left( \frac{\tan \lambda}{\tan \delta_c} - 1 \right) + 1 \right]} \left\{ \begin{aligned} & \left( \frac{l_W}{l_B} + 1 \right) \left[ \left( \frac{p_c}{p_\infty} \right)_{\pi/2} - 1 \right] - \\ & \left( \frac{l_W}{l_B} \right)^2 \left[ \left( \frac{p_c}{p_\infty} \right)_{\pi/2} - \left( \frac{p}{p_\infty} \right)_\lambda \right] \left[ \left( \frac{l_W}{l_B} - 3 \right) \left( \frac{l_W}{l_B} - 1 \right) + 2 \ln \frac{l_W}{l_B} \right] \\ & \left( \frac{l_W}{l_B} - 1 \right)^3 \end{aligned} \right\} \quad (66)$$

Since the pressure on the leeward side of the wing is assumed constant, this contribution to the pitching-moment coefficient can be shown to be (by virtue of eq. (7))

$$(C_{mW})_{\text{upper}} = \frac{2}{\gamma M_\infty^2} \left\{ \left[ 1 - \frac{\gamma - 1}{2} M_\infty (\alpha - \delta_W) \right]^{\frac{2\gamma}{\gamma-1}} - 1 \right\}$$

$$\left\{ \frac{2 \left( \frac{l_W}{l_B} \right)^3 \frac{\tan \lambda}{\tan \delta_c} - \left( \frac{l_W}{l_B} - 1 \right) \left[ \left( \frac{l_W}{l_B} \right) \left( \frac{\tan \lambda}{\tan \delta_c} + 1 \right) + 2 \left( \frac{l_W}{l_B} \right)^2 \frac{\tan \lambda}{\tan \delta_c} + 2 \right]}{3 \left[ \left( \frac{l_W}{l_B} \right) \left( \frac{\tan \lambda}{\tan \delta_c} - 1 \right) + 1 \right]} \right\} \quad (67)$$

The pitching-moment coefficient for slender conical bodies of revolution is defined by

$$C_{mB} = - \frac{2}{3} C_{NB}$$

Thus, the total pitching-moment coefficient may be written

$$C_m = - \frac{2}{3} C_{NB} + (C_{mW})_{\text{lower}} + (C_{mW})_{\text{upper}} \quad (68)$$

In the case of a delta wing configuration (i.e.,  $l_W = l_B$ ), the total pitching-moment coefficient is, of course,

$$C_m = - \frac{2}{3} C_N$$

The lift and major portion of the pressure drag, as well as the pitching moment, may be calculated by means of the foregoing expressions<sup>5</sup> since the pressure ratios in these expressions are tabulated in table I. It is clear, of course, that the leading-edge drag, base-pressure drag, and skin-friction drag must also be considered in a complete evaluation of the lift and drag characteristics of the configuration.

---

<sup>5</sup>The retention of the trigonometric functions is optional in these expressions. They have been retained since they result from purely geometrical considerations.

Flow About Pointed Flat-Top Wing-Body Configurations  
Which are Curved in the Stream Direction

It was demonstrated in reference 13 that many three-dimensional hypersonic flows may be treated by a generalized shock-expansion method which is analogous to that employed in reference 8 for two-dimensional flows. Application of the method in meridian planes about curved bodies of revolution (see ref. 13) indicated that these flow fields could be calculated with good accuracy provided the hypersonic similarity parameter,  $M_\infty \delta_c$ , is about 1 or greater and the angle of attack is small. Since the present configurations are assumed to have half-bodies of revolution, the generalized shock-expansion method is also applicable to these configurations when  $M_\infty \delta_c \geq 1$  and  $\alpha \ll 1$ . In fact, the general procedure of calculating the flow is identical to that employed in reference 9. It is clear, of course, that the initial conical flow conditions at the vertex are determined from the expressions previously developed in the present paper. In this connection, expressions defining the flow downstream of the vertex are obtained which are applicable to hypersonic flow about slender configurations and, thus, are compatible with those defining the flow at the vertex. The following expressions, then, can be deduced directly from those presented in reference 9 by applying the condition of hypersonic flow and slender bodies. With these points in mind, attention is first turned to the calculation of the flow on the surface of the body.

Flow conditions on the body surface. - The differential equation for Prandtl-Meyer flow relating the change in Mach number with flow inclination angle along a streamline<sup>6</sup> reduces to (see ref. 14)

$$d\mu = \frac{\gamma - 1}{2} d\delta$$

for hypersonic flows. This expression is easily integrated to yield

$$\frac{M_c}{M} = 1 - \frac{\gamma - 1}{2} (M_c \delta_c) \left( 1 - \frac{\delta}{\delta_c} \right)$$

where  $M_c$  is the Mach number under the vortical layer at the vertex and is defined by equation (45). Now the pressure rise across the shock is given by equation (26) and the ratio of the pressure anywhere on the body surface to the pressure at the shock in the plane  $\phi = 0$  may be determined from the relation

---

<sup>6</sup>It should be noted that since  $w = 0$  at  $\phi = 0$  and  $\phi = \pi/2$ , the meridian lines in these two planes are exactly streamlines.

$$\frac{p}{(p_S)_o} = \left[ \frac{(M_S)_o}{M} \right]^{\frac{2\gamma}{\gamma-1}}$$

Thus, the expression defining the pressure coefficient anywhere on the surface of the body may be written in the form

$$C_p = \frac{2}{\gamma M_\infty^2} \left\{ \frac{2\gamma M_\infty^2 (\omega_S + \alpha)_o^2 - (\gamma - 1)}{\gamma + 1} \left[ \frac{(M_S)_o}{M_c} - \frac{\gamma - 1}{2} (M_S \delta_c)_o \left( 1 - \frac{\delta}{\delta_c} \right) \right]^{\frac{2\gamma}{\gamma-1}} - 1 \right\}$$

Flow conditions in the plane of the wing. - Flow properties on the wing surface are dictated by the flow field generated by the body in the plane  $\phi = \pi/2$ , subject, of course, to the boundary conditions imposed by the wing. Thus, the calculation of the flow in this plane is similar to the calculation of the flow field between the body surface and the shock in a meridian plane for a body of revolution. Consistent, then, with the hypersonic approximations of the present paper, expressions presented in reference 9 for calculating the flow inclination, the static pressure, and the total pressure along a line normal to the body axis a short distance downstream of the vertex reduce to

$$\delta = \delta_B \left[ 1 - \zeta \left( \frac{y}{y_B} - 1 \right) \right] + \left\{ \delta_S - \delta_B \left[ 1 - \zeta \left( \frac{y_S}{y_B} - 1 \right) \right] \right\} \left( \frac{y - y_B}{y_S - y_B} \right)^2$$

$$p = p_B \left[ 1 - \gamma K_B M_B^2 (y - y_B) \right] + \left\{ p_S - p_B \left[ 1 - \gamma K_B M_B^2 (y_S - y_B) \right] \right\} \left( \frac{y - y_B}{y_S - y_B} \right)^2$$

and

$$p_t = (p_t)_B + \left[ \frac{(dp_t/d\theta)(d\theta/dS)}{\theta - \delta} \right]_S (y - y_S) + \\ \left\{ (p_t)_B - (p_t)_S - \left[ \frac{(dp_t/d\theta)(d\theta/dS)}{\theta - \delta} \right]_S (y_B - y_S) \right\} \left( \frac{y - y_S}{y_B - y_S} \right)^2$$

respectively, where B and S are points on the line corresponding to the body surface (wing-body juncture) and the shock (wing leading edge), respectively. The derivatives in the above expressions reduce to

$$\frac{dp_t}{d\theta} = - \frac{4\gamma}{(\gamma + 1)\theta} \left[ \frac{(\gamma + 1)^2 (M_\infty \theta)^2}{2\gamma (M_\infty \theta)^2 - (\gamma - 1)} \right]^{\frac{\gamma}{\gamma-1}} \left\{ \frac{[(M_\infty \theta)^2 - 1]^2}{[(\gamma - 1)(M_\infty \theta)^2 + 2]^{\frac{2\gamma-1}{\gamma-1}}} \right\}$$

and

$$\left( \frac{d\theta}{ds} \right)_{\text{vertex}} = K_B \left[ \frac{2\gamma (M_\infty \theta)^2 - (\gamma - 1)}{4M_\infty \theta} \right] \left( \frac{M_c}{M_\infty} \right) \left[ 1 - M_c(\lambda - \delta_c) \right]^{\frac{1}{2\zeta}} \quad (69)$$

where  $K_B$  is the curvature of the body at the vertex;

$$\theta = \lambda \cos \Psi \quad (70)$$

$$\zeta = 1 + \frac{\lambda}{\delta_c^2} \left( \frac{\partial w_2}{\partial \phi} \right)_{\pi/2}$$

and  $(1/\delta_c)(\partial w_2/\partial \phi)_{\pi/2}$  is given by equation (35). The derivative given by equation (69) is evaluated at the vertex and therefore can be determined from the previous solution of the flow about flat-top conical configurations. The shock-wave parameter,  $\theta$ , in the above expressions is defined by equation (70) and represents the shock angle associated with the component of free-stream Mach number normal to the shock at the leading edge. Flow conditions on the surface of the wing in the region of the vertex can be completely determined by means of the foregoing expressions. The remainder of the flow field in the plane of the wing can be calculated by employing the procedure discussed in reference 9 pertaining to bodies of revolution. The pressure on the leeward side of the wing may be calculated from equation (7).

It is interesting to note that the flow about flat-top configurations having wings with straight leading edges, as well as those which are curved in the stream direction, can be calculated by means of the generalized shock-expansion method. To illustrate, consider the following three cases: (1) a wing with leading edges which are curved but with the shock always normal to the leading edge; (2) a wing with constant leading-edge sweep; and (3) a wing with curved leading edges but with local sweeps always less than case (1). All these wings, of course, have supersonic leading edges. Now if the shock is normal to the leading edge, then  $\Psi = 0$  (see sketch (c)) and the variation of  $\lambda$  can be determined from equation (70). This is tantamount to replacing  $\theta$  by  $\lambda$  in the Rankine-Hugoniot shock relations. Thus, case (1) corresponds to the calculation of the flow on a wing which is designed to just contain the flow field bounded by the body surface and the bow shock and the "design" plan form will vary with angle of attack. The flow on the wings corresponding to cases (2) and (3) can also be calculated since  $\lambda$  is known and, therefore,  $\Psi$  can be calculated from equation (70) once  $\theta$  has been determined.

~~CONFIDENTIAL~~  
EXPERIMENT

In order to obtain a check on the predictions of the preceding theoretical analysis, the pressures acting on the surfaces of several wing-body configurations were determined experimentally at Mach numbers from 3.0 to 6.0 and at angles of attack up to  $6^\circ$ . A brief description of these tests follows.

## Test Apparatus

Tests were conducted in the Ames 10- by 14-inch supersonic wind tunnel. A detailed description of the wind tunnel and auxiliary equipment may be found in reference 15. The pressures acting on the model surfaces were measured with a mercury U-tube manometer or by means of a dibutyl-phthalate U-tube manometer when the pressures were low enough to be recorded on the latter.

Pressure-distribution models were mounted on a  $3^\circ$  bent support which could be pitched through an angle-of-attack range of  $-3^\circ$  to  $+3^\circ$ . The test models consisted of three basic configurations - two conical models and one ogive model. The conical models consisted of thin triangular wings beneath which were mounted fuselages composed of, in one case, one-half of a fineness-ratio-5 cone and, in the other, one-half of a fineness-ratio-2-1/2 cone. Two wings of different leading-edge sweep were tested on each body. In the case of the ogive model, the fuselage consisted of one-half of a fineness-ratio-5 ogive mounted beneath a thin wing, the leading edges of which were coincident with the theoretically determined shock wave for  $(\Psi)_{\pi/2} = 0$  (case (1) in the analysis section) at a Mach number of 5.0 and an angle of attack of  $3^\circ$ . The dimensions of these models and the location of the pressure orifices are shown in figure 3.

Pressures on the model surfaces were measured at  $0^\circ$ ,  $3^\circ$ , and  $6^\circ$  angles of attack at test Mach numbers of 3.0, 4.0, 5.0, and 6.0. The Reynolds number per foot varied from 8.6 million at Mach number 3.0 to 1.4 million at Mach number 6.0. The pressures around the body surface and on the high-pressure side of the wing were recorded simultaneously at each Mach number and angle of attack at stations symmetrically disposed with respect to the plane of symmetry (i.e.,  $\pm\phi$ ; see fig. 3). These pressures were reduced to coefficient form and the average pressure coefficient was assumed to represent the pressure coefficient at each meridian angle,  $\phi$ , and ray angle,  $w$ .

~~CONFIDENTIAL~~

### Accuracy of Test Results

The variation in Mach number from the nominal value did not exceed  $\pm 0.05$  in the region of the test section where the models were located. The precision of the computed pressure coefficients was affected by inaccuracies in the pressure measurements, as well as uncertainties in the stream angle and the free-stream dynamic pressure. The resulting errors in pressure coefficients were generally less than  $\pm 0.005$  throughout the Mach number range for all angles of attack. The meridian angles and angular wing stations at which the pressure coefficients are plotted are considered accurate to within  $\pm 1^\circ$ .

### RESULTS AND DISCUSSION

It will be recalled in the development of the theory that the flow field in the plane of symmetry ( $\phi = 0$ ) was assumed to be the same as that for the circular cone. It is appropriate, therefore, to examine the validity of this assumption before proceeding with a comparison of the theoretical and experimental surface pressures. To this end, the shock-wave angle at  $\phi = 0$  was measured from shadowgraph pictures for each test Mach number at  $\alpha = 3^\circ$ . The results of these measurements are compared in figure 4 with the shock angles for the complete cones which were also obtained from shadowgraph pictures. Only one set of data is shown for each fuselage since the effect of leading-edge sweep was not discernible from the shadowgraph pictures. Also shown for comparative purposes are the predictions of Stone's first-order theory for inclined circular cones (ref. 16), as presented in reference 17, along with the predictions of the theory of the present paper. It is evident that the wing has little effect on the shock-wave angle of the cone at  $\phi = 0$ , at least for angles of attack up to  $3^\circ$ . It will be noted that the present theory yields shock-wave angles which are slightly too large. The variation of pressure coefficient at  $\phi = 0$  with angle of attack for the two test configurations is shown in figure 5 for the test Mach numbers 3.0 and 5.0. Experimental results taken from reference 9 are also shown for the fineness-ratio-2-1/2 cone ( $\delta_c = 11.42^\circ$ ). As in the case of the shock-wave angles, only one set of pressure data for each configuration is shown since the pressures were essentially unaffected by the small changes in leading-edge sweep of the test models. (Experimental data for a fineness-ratio-5 cone were not available.) Stone's second-order theory for inclined cones (ref. 18) applied in the manner described in reference 19 is also presented except for the case where  $\delta_c = 11.42^\circ$  and  $M_\infty = 5.0$  which is beyond the range of the M.I.T. tables (ref. 20). For this case, the predictions of the theory for inclined cones presented in reference 9 are shown. It appears in figure 5 that the presence of the wing increases the pressures slightly in the plane  $\phi = 0$ , particularly in the case of the more slender of the two configurations. However, this effect is sufficiently small

(approximately within the range of experimental scatter) so that it can, for all practical purposes, be neglected. It should be noted that agreement between the present theory and experiment improves with increasing slenderness and increasing Mach number. On the basis of the comparisons shown in figures 4 and 5 it is indicated that, at least for cases where the leading edges of the wing are subsonic ( $M < 5$ ) or moderately supersonic, flow conditions in the plane  $\phi = 0$  can be considered to be the same as those associated with the corresponding circular cone with only a slight loss in accuracy.

The experimental pressure distributions obtained on the four conical flat-top wing-body combinations (see fig. 3) are shown in figures 6, 7, 8, and 9. The data are plotted in the form of surface pressure coefficients as a function of the meridian angle,  $\phi$ , for the body and as a function of the difference between the ray angle,  $\omega$ , and the body vertex angle,  $\delta_c$ , for the wing. Also shown in these figures are the predictions of the present conical-flow theory, where applicable, as well as results obtained from reference 21 for noninclined cones. Although the latter results are strictly applicable only for the cases where the wing leading-edge angle is equal to the axially symmetric shock angle produced by the body (i.e.,  $M_\infty = 5.0$ ,  $\lambda = 13^\circ$  and  $\lambda = 16.9^\circ$ ; see figs. 6(c) and 8(c)), the theoretical pressure coefficients are nevertheless shown for all test Mach numbers at  $\alpha = 0^\circ$ . It is interesting to note that the results of reference 21 are in good agreement with experiment even for the subsonic leading-edge cases ( $M_\infty < 5$ ). It also appears from the magnitude and continuous distribution of pressures on the wing at  $M_\infty = 6.0$  that the bow shock remains attached to the leading edge and the cone pressure field is distributed over the entire surface of the wing. It should also be noted that the pressures on the body are negligibly affected by the wing at all test Mach numbers at  $\alpha = 0^\circ$ . Consider now the predictions of the conical flow theory of the present paper. Although the theory is not strictly applicable below a Mach number of 5.0 for the test configurations (see fig. 2), theoretical results obtained for  $(Y)_{\pi/2} = 0$  are nevertheless shown for the lower test Mach numbers at  $\alpha = 0^\circ$ . As in the case of the predictions of reference 21, the present theory may, from a practical standpoint, also be considered applicable to wings whose leading edges lay inboard of the bow shock wave at  $\alpha = 0^\circ$ . It should be recalled, however, that the theory is applicable to hypersonic flow fields and, therefore, would be expected to yield good results only at relatively high Mach numbers. It can be seen from figure 2 that for  $\lambda = 13^\circ$  ( $\lambda/\delta_c = 2.28$ ) the theory is applicable only for  $\alpha = 0^\circ$  at  $M_\infty = 5.0$  and for angles of attack up to  $3^\circ$  ( $\alpha/\delta_c = 0.525$ ) at  $M_\infty = 6.0$  (fig. 6). Similarly, when  $\lambda = 14.6^\circ$  ( $\lambda/\delta_c = 2.55$ ), the theory is applicable for angles of attack up to  $3^\circ$  at  $M_\infty = 5.0$  and for angles of attack up to  $5.7^\circ$  ( $\alpha/\delta_c = 1$ ) at  $M_\infty = 6.0$  (fig. 7). The same general remarks concerning the applicability of theory also apply to the less slender configurations. The predictions of theory where applicable are compared with experiment for these configurations in figures 8 and 9. It will be recalled that the development of the theory proceeded from the basic assumptions

that  $\delta \ll 1$ ,  $\omega \ll 1$ , and  $M \gg 1$ . It would be expected, then, that theory should yield more reliable results for slender configurations at high Mach numbers. It is indicated by the results shown in figures 6 through 9 that agreement between theory and experiment improves with increasing Mach number and, in general, agreement is better for the more slender configurations. The pressure distributions calculated by means of equations (51) and (52) are also shown in figures 6, 7, 8, and 9 and, in general, are in reasonably good agreement with experiment, although equation (52) tends to overestimate the pressures slightly on the wing (compared to the more exact equation) at  $\alpha = 0^\circ$ . It should be noted in table I that  $(\Psi)_{\pi/2}$  attains its maximum value at  $\alpha = 0^\circ$  when  $\lambda > (\omega_S)_{\alpha=0}$  and increases quite rapidly with increasing  $\lambda$ . Thus, for example, for the case where  $\lambda = 14.6^\circ$  at  $M_\infty = 6.0$  and  $\alpha = 0^\circ$  (fig. 7(d)),  $(\Psi)_{\pi/2}$  is  $41^\circ$ . From the definition of  $\Psi$  as shown in figure 1, it can readily be seen that the cross-sectional shape of the conical shock will deviate considerably from a circular arc when  $(\Psi)_{\pi/2} = 41^\circ$ .

Since the theory is based on the assumptions  $\delta \ll 1$  and  $\lambda \ll 1$ , it is evident that when the wing semivertex angle is large compared to the axially symmetric shock angle produced by the body or, in effect, large values of  $\lambda/\delta_c$ , the theory will tend to break down. More experimental data are needed to determine the practical range of applicability of the theory with respect to this parameter. It should be noted, however, that considerations of drag and aerodynamic heating will dictate high sweep and, hence, moderate values of  $\lambda/\delta_c$  at hypersonic speeds.

It is of interest now to consider briefly the accuracy of the predictions of theory for the lift, drag, and pitching-moment coefficients. These coefficients have been calculated by means of equations (63), (64), and (68) (and, of course, table I) for a configuration having an arrow plan-form wing ( $\lambda = 15^\circ$ ) beneath which is mounted one-half of a fineness-ratio-5 cone. The results of these calculations for a Mach number of 5.0 along with experimental results taken from reference 2 (model 6 in that reference) are shown in figure 10. The drag polar was obtained by calculating the variation of drag with angle of attack by means of equation (64). The drag coefficient was then matched with the experimentally measured drag coefficient at  $\alpha = 0^\circ$ . The difference in drag coefficient thus obtained was assumed constant over the angle-of-attack range. In effect, then, the skin-friction drag, leading-edge drag, and base-pressure drag were assumed to be independent of angle of attack. In general, agreement between theory and experiment is good.

As a final point, consideration is now given to the accuracy with which the solutions for flow about conical configurations in combination with the generalized shock-expansion method predict the flow about wing-body combinations which are curved in the stream direction. The pressure distributions on the surface of a configuration having a fuselage consisting of one-half of a fineness-ratio-5 ogive mounted beneath a thin wing whose leading edges were theoretically determined so that they coincided

with the shock wave for  $(\Psi)_{\pi/2} = 0$  at  $M_\infty = 5.0$  and  $\alpha = 3^\circ$  were calculated using the methods of this paper. These distributions along with the results of pressure-distribution tests are presented in figure 11. The trend of the pressure distribution on the wing is in good agreement with experiment. Although the absolute magnitude of the pressure is low, it should be noted that the similarity parameter,  $M_\infty \delta_c$ , is 1 in this case and, thus, represents the minimum condition for applicability of the shock-expansion method.

#### CONCLUDING REMARKS

The flow about conical flat-top wing-body configurations at high supersonic speeds was investigated analytically. With the assumptions of high supersonic Mach numbers, slender configurations, supersonic leading edges, and small angles of attack, an approximate theory was developed yielding the Mach number and pressure distributions on the surface. Simple, explicit, algebraic expressions for calculating the lift, pressure-drag, and pitching-moment coefficients were also presented. A solution to the flow about pointed flat-top wing-body configurations which are curved in the stream direction was obtained by combining the conical flow solution with a slender-body approximation to the generalized shock-expansion method.

Surface pressures were obtained experimentally at Mach numbers from 3.0 to 6.0 and angles of attack up to  $6^\circ$  for several flat-top wing-body configurations. These configurations consisted of half-bodies of revolution mounted beneath thin highly swept triangular wings. The bodies of the conical configurations consisted of one-half of a fineness-ratio-5 cone in one case and one-half of a fineness-ratio-2-1/2 cone in the other. The body of the third configuration consisted of one-half of a fineness-ratio-5 ogive. For this configuration, the leading edges of the wing were curved and designed to just maintain the theoretically determined bow shock along the leading edge at a Mach number of 5.0 and an angle of attack of  $3^\circ$ . The predictions of the conical-flow theory of this paper for the surface pressures were in good agreement with experiment at Mach numbers of 5.0 and 6.0 up to angles of attack of approximately  $3^\circ$ . Estimated lift, drag due to lift, and pitching-moment coefficients were in good agreement with existing experiment for a conical configuration at a Mach number of 5.0. The generalized shock-expansion method yielded reasonably good agreement with experiment for the half-ogive configuration at a Mach number of 5.0 and angle of attack of  $3^\circ$ .

Ames Aeronautical Laboratory  
National Advisory Committee for Aeronautics  
Moffett Field, Calif., June 2, 1958

CONFIDENTIAL

## REFERENCES

1. Eggers, A. J., Jr., and Syvertson, Clarence A.: Aircraft Configurations Developing High Lift-Drag Ratios at High Supersonic Speeds. NACA RM A55L05, 1956.
2. Syvertson, Clarence A., Wong, Thomas J., and Gloria, Hermilo R.: Additional Experiments With Flat-Top Wing-Body Combinations at High Supersonic Speeds. NACA RM A56I11, 1957.
3. Migotsky, E., and Adams, Gaynor J.: Some Properties of Wing and Half-Body Arrangements at Supersonic Speeds. NACA RM A57E15, 1957.
4. Browne, S. H., Friedman, L., and Hodes, I.: A Wing-Body Problem in a Supersonic Conical Flow. Jour. Aero. Sci., vol. 15, no. 8, Aug. 1948, pp. 443-452.
5. Ferri, Antonio, Clarke, Joseph H., and Casaccio, Anthony: Drag Reduction in Lifting Systems by Advantageous Use of Interference. PIBAL Rep. 272, Polytechnic Institute of Brooklyn, Dept. of Aero. Engr. and Appl. Mech., May 1955.
6. Reyn, John W., and Clarke, Joseph H.: An Assessment of Body Lift Contributions and of Linearized Theory for Some Particular Wing-Body Configurations. PIBAL Rep. 305, Polytechnic Institute of Brooklyn, Dept. of Aero. Engr. and Appl. Mech., June 1956.
7. Rossow, Vernon J.: A Theoretical Study of the Lifting Efficiency at Supersonic Speeds of Wings Utilizing Indirect Lift Induced by Vertical Surfaces. NACA RM A55L08, 1956.
8. Eggers, A. J., Jr., Syvertson, Clarence A., and Kraus, Samuel: A Study of Inviscid Flow About Airfoils at High Supersonic Speeds. NACA Rep. 1123, 1953. (Supersedes NACA TN's 2646 and 2729)
9. Savin, Raymond C.: Application of the Generalized Shock-Expansion Method to Inclined Bodies of Revolution Traveling at High Supersonic Speeds. NACA TN 3349, 1955.
10. Ferri, Antonio: Supersonic Flow Around Circular Cones at Angles of Attack. NACA Rep. 1045, 1951. (Supersedes NACA TN 2236)
11. Holt, M.: A Vortical Singularity in Conical Flow. Quart. Jour. Mech. and Appl. Math., vol. VII, pt. 4, Dec. 1954, pp. 438-445.
12. Hamaker, Frank M., Neice, Stanford E., and Wong, Thomas J.: The Similarity Law for Hypersonic Flow and Requirements for Dynamic Similarity of Related Bodies in Free Flight. NACA Rep. 1147, 1953. (Supersedes NACA TN's 2443 and 2631)

13. Eggers, A. J., Jr., and Savin, Raymond C.: A Unified Two-Dimensional Approach to the Calculation of Three-Dimensional Hypersonic Flows, With Application to Bodies of Revolution. NACA Rep. 1249, 1955.
14. Eggers, A. J., Jr., and Savin, Raymond C.: Approximate Methods for Calculating the Flow About Nonlifting Bodies of Revolution. NACA TN 2579, 1951.
15. Eggers, A. J., Jr., and Nothwang, George J.: The Ames 10- by 14-Inch Supersonic Wind Tunnel. NACA TN 3095, 1954.
16. Stone, A. H.: On Supersonic Flow Past a Slightly Yawing Cone. Jour. Math. and Phys., vol. XXVII, no. 1, April 1948, pp. 67-81.
17. Staff of the Computing Section, under the Direction of Zdeněk Kopal: Tables of Supersonic Flow Around Yawing Cones. MIT, Dept. of Elec. Engr., Center of Analysis. Tech. Rep. No. 3, Cambridge, 1947.
18. Stone, A. H.: On Supersonic Flow Past a Slightly Yawing Cone. II. Jour. Math. and Phys., vol. XXX, no. 4, Jan. 1952, pp. 200-213.
19. Roberts, Richard C., and Riley, James D.: A Guide to the Use of the MIT Cone Tables. NAVORD Rep. 2606, 1953.
20. Staff of the Computing Section, under the Direction of Zdeněk Kopal: Tables of Supersonic Flow Around Cones of Large Yaw. MIT, Dept. of Elec. Engr., Center of Analysis. Tech. Rep. No. 5, Cambridge, 1947.
21. Staff of the Computing Section, under the Direction of Zdeněk Kopal: Tables of Supersonic Flow Around Cones. MIT, Dept. of Elec. Engr., Center of Analysis. Tech. Rep. No. 1, 1947.

TABLE I.- FUNCTIONS FOR CALCULATING THE FLOW ABOUT FLAT-TOP CONFIGURATIONS

$M_\infty \delta_c$	$\frac{\lambda}{\delta_c}$	$\frac{a}{\delta_c}$	$(\frac{w_2}{\delta_c})_o$	$(\frac{p_c}{p_\infty})_o$	$(\frac{v}{v})_{x/2}$	$(\frac{p_c}{p_\infty})_{x/2}$	$(\frac{p}{p_\infty})_\lambda$
0.10	1.01992	0.00	1.00598	0.10399	0.01660	0.10399	0.10138
0.10	1.01992	0.10	0.99854	0.10446	0.01595	0.10429	0.10163
0.10	1.01992	0.20	0.99112	0.10494	0.01522	0.10462	0.10191
0.10	1.01992	0.30	0.98374	0.10546	0.01440	0.10496	0.10220
0.10	1.01992	0.40	0.97638	0.10599	0.01348	0.10533	0.10250
0.10	1.01992	0.50	0.96906	0.10654	0.01243	0.10572	0.10283
0.10	1.01992	0.60	0.96177	0.10711	0.01123	0.10614	0.10317
0.10	1.01992	0.70	0.95451	0.10771	0.00982	0.10657	0.10353
0.10	1.01992	0.80	0.94728	0.10833	0.00809	0.10703	0.10390
0.10	1.01992	0.90	0.94008	0.10896	0.00575	0.10750	0.10429
0.10	1.01992	1.00	0.93292	0.10962	0.00000	0.10799	0.10469
0.10	1.01823	0.00	1.00598	0.10399	0.01557	0.10399	0.10138
0.10	1.01823	0.10	0.99854	0.10446	0.01487	0.10429	0.10164
0.10	1.01823	0.20	0.99112	0.10494	0.01409	0.10462	0.10191
0.10	1.01823	0.30	0.98374	0.10546	0.01320	0.10497	0.10220
0.10	1.01823	0.40	0.97638	0.10599	0.01218	0.10533	0.10251
0.10	1.01823	0.50	0.96906	0.10654	0.01101	0.10573	0.10283
0.10	1.01823	0.60	0.96177	0.10711	0.00964	0.10614	0.10317
0.10	1.01823	0.70	0.95451	0.10771	0.00794	0.10657	0.10353
0.10	1.01823	0.80	0.94728	0.10833	0.00565	0.10703	0.10391
0.10	1.01823	0.90	0.94008	0.10896	0.00000	0.10750	0.10429
0.10	1.01661	0.00	1.00598	0.10399	0.01452	0.10399	0.10139
0.10	1.01661	0.10	0.99854	0.10446	0.01376	0.10429	0.10164
0.10	1.01661	0.20	0.99112	0.10494	0.01290	0.10462	0.10191
0.10	1.01661	0.30	0.98374	0.10546	0.01192	0.10497	0.10220
0.10	1.01661	0.40	0.97638	0.10599	0.01078	0.10534	0.10251
0.10	1.01661	0.50	0.96906	0.10654	0.00944	0.10573	0.10284
0.10	1.01661	0.60	0.96177	0.10711	0.00779	0.10614	0.10318
0.10	1.01661	0.70	0.95451	0.10771	0.00555	0.10657	0.10354
0.10	1.01661	0.80	0.94728	0.10833	0.00000	0.10702	0.10391
0.10	1.01505	0.00	1.00598	0.10399	0.01342	0.10399	0.10139
0.10	1.01505	0.10	0.99854	0.10446	0.01259	0.10429	0.10164
0.10	1.01505	0.20	0.99112	0.10494	0.01164	0.10462	0.10192
0.10	1.01505	0.30	0.98374	0.10546	0.01055	0.10497	0.10221
0.10	1.01505	0.40	0.97638	0.10599	0.00924	0.10534	0.10252
0.10	1.01505	0.50	0.96906	0.10654	0.00763	0.10573	0.10284
0.10	1.01505	0.60	0.96177	0.10711	0.00544	0.10614	0.10318
0.10	1.01505	0.70	0.95451	0.10771	0.00000	0.10657	0.10354
0.10	1.01355	0.00	1.00598	0.10399	0.01227	0.10399	0.10139
0.10	1.01355	0.10	0.99854	0.10446	0.01136	0.10429	0.10165
0.10	1.01355	0.20	0.99112	0.10494	0.01029	0.10462	0.10192
0.10	1.01355	0.30	0.98374	0.10546	0.00903	0.10497	0.10221
0.10	1.01355	0.40	0.97638	0.10599	0.00746	0.10534	0.10252
0.10	1.01355	0.50	0.96906	0.10654	0.00532	0.10573	0.10284
0.10	1.01355	0.60	0.96177	0.10711	0.00000	0.10614	0.10318
0.10	1.01212	0.00	1.00598	0.10399	0.01105	0.10399	0.10139
0.10	1.01212	0.10	0.99854	0.10446	0.01003	0.10429	0.10165
0.10	1.01212	0.20	0.99112	0.10494	0.00881	0.10462	0.10192
0.10	1.01212	0.30	0.98374	0.10546	0.00728	0.10497	0.10221
0.10	1.01212	0.40	0.97638	0.10599	0.00521	0.10534	0.10252
0.10	1.01212	0.50	0.96906	0.10654	0.00000	0.10573	0.10285
0.10	1.01076	0.00	1.00598	0.10399	0.00975	0.10399	0.10139
0.10	1.01076	0.10	0.99854	0.10446	0.00857	0.10429	0.10165
0.10	1.01076	0.20	0.99112	0.10494	0.00710	0.10462	0.10192
0.10	1.01076	0.30	0.98374	0.10546	0.00508	0.10497	0.10222
0.10	1.01076	0.40	0.97638	0.10599	0.00000	0.10534	0.10252
0.10	1.00946	0.00	1.00598	0.10399	0.00833	0.10399	0.10140
0.10	1.00946	0.10	0.99854	0.10446	0.00690	0.10429	0.10165
0.10	1.00946	0.20	0.99112	0.10494	0.00495	0.10462	0.10193
0.10	1.00946	0.30	0.98374	0.10546	0.00000	0.10497	0.10222
0.10	1.00823	0.00	1.00598	0.10399	0.00670	0.10399	0.10140
0.10	1.00823	0.10	0.99854	0.10446	0.00481	0.10429	0.10165
0.10	1.00823	0.20	0.99112	0.10494	0.00000	0.10462	0.10193
0.10	1.00707	0.00	1.00598	0.10399	0.00466	0.10399	0.10140
0.10	1.00707	0.10	0.99854	0.10446	0.00000	0.10429	0.10166
0.10	1.00598	0.00	1.00598	0.10399	0.00000	0.10399	0.10140

TABLE I.- FUNCTIONS FOR CALCULATING THE FLOW ABOUT FLAT-TOP CONFIGURATIONS - Continued

$M_a \delta_c$	$\frac{\lambda}{\delta_c}$	$\frac{\alpha}{\delta_c}$	$(\frac{w_e}{\delta_c})_o$	$(\frac{p_e}{p_m})_o$	$(\gamma)_{\pi/2}$	$(\frac{p_e}{p_m})_{\pi/2}$	$(\frac{p}{p_m})_{\lambda}$
0.20	054437	0.00	051186	011246	003512	011246	010525
0.20	054437	0.10	050504	011422	003356	011372	010662
0.20	054437	0.20	049830	011606	003186	011505	010806
0.20	054437	0.30	049163	011797	002999	011645	010956
0.20	054437	0.40	048504	011996	002792	011793	011112
0.20	054437	0.50	047853	012202	002562	011948	011274
0.20	054437	0.60	047210	012415	002302	012110	011442
0.20	054437	0.70	046574	012637	002001	012280	011616
0.20	054437	0.80	045947	012866	001637	012456	011795
0.20	054437	0.90	045328	013102	001156	012639	011978
0.20	054437	1.00	044718	013347	000000	012824	012162
0.20	054080	0.00	051186	011246	003323	011246	010529
0.20	054080	0.10	050504	011422	003156	011372	010667
0.20	054080	0.20	049830	011606	002973	011505	010811
0.20	054080	0.30	049163	011797	002770	011646	010951
0.20	054080	0.40	048504	011996	002543	011793	011118
0.20	054080	0.50	047853	012202	002286	011948	011281
0.20	054080	0.60	047210	012415	001989	012111	011449
0.20	054080	0.70	046574	012637	001628	012280	011623
0.20	054080	0.80	045947	012866	001150	012456	011802
0.20	054080	0.90	045328	013102	000000	012635	011982
0.20	053730	0.00	051186	011246	003124	011246	010533
0.20	053730	0.10	050504	011422	002944	011372	010671
0.20	053730	0.20	049830	011606	002745	011505	010815
0.20	053730	0.30	049163	011797	002522	011646	010956
0.20	053730	0.40	048504	011996	002369	011794	011124
0.20	053730	0.50	047853	012202	001975	011949	011287
0.20	053730	0.60	047210	012415	001618	012111	011456
0.20	053730	0.70	046574	012637	001144	012280	011630
0.20	053730	0.80	045947	012866	000000	012453	011805
0.20	053385	0.00	051186	011246	002913	011246	010536
0.20	053385	0.10	050504	011422	002718	011372	010675
0.20	053385	0.20	049830	011606	002499	011505	010820
0.20	053385	0.30	049163	011797	002249	011646	010972
0.20	053385	0.40	048504	011996	001959	011794	011129
0.20	053385	0.50	047853	012202	001606	011950	011293
0.20	053385	0.60	047210	012415	001137	012111	011462
0.20	053385	0.70	046574	012637	000000	012277	011633
0.20	053047	0.00	051186	011246	002687	011246	010540
0.20	053047	0.10	050504	011422	002472	011372	010679
0.20	053047	0.20	049830	011606	002227	011505	010825
0.20	053047	0.30	049163	011797	001941	011647	010977
0.20	053047	0.40	048504	011996	001593	011795	011135
0.20	053047	0.50	047853	012202	001129	011950	011299
0.20	053047	0.60	047210	012415	000000	012109	011465
0.20	052716	0.00	051186	011246	002443	011246	010544
0.20	052716	0.10	050504	011422	002202	011373	010683
0.20	052716	0.20	049830	011606	001981	011505	010829
0.20	052716	0.30	049163	011797	001578	011647	010982
0.20	052716	0.40	048504	011996	001120	011795	011140
0.20	052716	0.50	047853	012202	000000	011948	011302
0.20	052393	0.00	051186	011246	002175	011246	010547
0.20	052393	0.10	050504	011422	001899	011373	010687
0.20	052393	0.20	049830	011606	001561	011507	010834
0.20	052393	0.30	049163	011797	001110	011647	010986
0.20	052393	0.40	048504	011996	000000	011794	011144
0.20	052078	0.00	051186	011246	001874	011246	010550
0.20	052078	0.10	050504	011422	001543	011373	010691
0.20	052078	0.20	049830	011606	001098	011507	010838
0.20	052078	0.30	049163	011797	000000	011646	010990
0.20	051771	0.00	051186	011246	001522	011246	010554
0.20	051771	0.10	050504	011422	001085	011373	010695
0.20	051771	0.20	049830	011606	000000	011506	010841
0.20	051474	0.00	051186	011246	001070	011246	010557
0.20	051474	0.10	050504	011422	000000	011373	010698
0.20	051186	0.00	051186	011246	000000	011246	010560

CONFIDENTIAL

TABLE I.- FUNCTIONS FOR CALCULATING THE FLOW ABOUT FLAT-TOP CONFIGURATIONS - Continued

$M_\infty S_c$	$\frac{\lambda}{S_c}$	$\frac{\alpha}{S_c}$	$(\frac{w_0}{S_c})_0$	$(\frac{p_0}{p_{\infty}})_0$	$(\bar{x})_{x/2}$	$(\frac{p_0}{p_{\infty}})_{x/2}$	$(\frac{p}{p_{\infty}})_\lambda$
0.30	039427	0.00	035087	012390	004847	012391	011112
0.30	039427	0.10	034464	012735	004617	012627	011417
0.30	039427	0.20	033853	013097	004368	012878	011735
0.30	039427	0.30	033255	013476	004098	013146	012065
0.30	039427	0.40	032670	013871	003802	013429	012407
0.30	039427	0.50	032099	014284	003477	013728	012751
0.30	039427	0.60	031541	014714	003112	014043	013125
0.30	039427	0.70	030997	015162	002694	014373	013499
0.30	039427	0.80	030466	015628	002194	014719	013882
0.30	039427	0.90	029950	016112	001539	015078	014272
0.30	039427	1.00	029447	016515	000000	015438	014655
0.30	038971	0.00	035087	012390	004608	012390	011127
0.30	038971	0.10	034464	012735	004362	012627	011433
0.30	038971	0.20	033853	013097	004095	012879	011752
0.30	038971	0.30	033255	013476	003802	013147	012084
0.30	038971	0.40	032670	013871	003478	013430	012428
0.30	038971	0.50	032099	014284	003115	013730	012782
0.30	038971	0.60	031541	014714	002699	014044	013147
0.30	038971	0.70	030997	015162	002199	014374	013521
0.30	038971	0.80	030466	015628	001544	014717	013903
0.30	038971	0.90	029950	016112	000000	015064	014280
0.30	038519	0.00	035087	012390	004353	012390	011142
0.30	038519	0.10	034464	012735	004089	012627	011450
0.30	038519	0.20	033853	013097	003799	012879	011770
0.30	038519	0.30	033255	013476	003478	013148	012103
0.30	038519	0.40	032670	013871	003117	013431	012448
0.30	038519	0.50	032099	014284	002701	013731	012803
0.30	038519	0.60	031541	014714	002203	014045	013168
0.30	038519	0.70	030997	015162	001549	014373	013542
0.30	038519	0.80	030466	015628	000000	014706	013913
0.30	038071	0.00	035087	012390	004079	012390	011157
0.30	038071	0.10	034464	012735	003793	012627	011466
0.30	038071	0.20	033853	013097	003474	012880	011788
0.30	038071	0.30	033255	013476	003116	013149	012122
0.30	038071	0.40	032670	013871	002702	013432	012467
0.30	038071	0.50	032099	014284	002206	013731	012823
0.30	038071	0.60	031541	014714	001552	014044	013188
0.30	038071	0.70	030997	015162	000000	014363	013552
0.30	037627	0.00	035087	012390	003782	012390	011172
0.30	037627	0.10	034464	012735	003467	012628	011482
0.30	037627	0.20	033853	013097	003112	012881	011805
0.30	037627	0.30	033255	013476	002701	013149	012141
0.30	037627	0.40	032670	013871	002207	013433	012487
0.30	037627	0.50	032099	014284	001555	013731	012842
0.30	037627	0.60	031541	014714	000000	014037	013199
0.30	037188	0.00	035087	012390	003457	012390	011187
0.30	037188	0.10	034464	012735	003105	012628	011499
0.30	037188	0.20	033853	013097	002698	012881	011823
0.30	037188	0.30	033255	013476	002206	013150	012159
0.30	037188	0.40	032670	013871	001557	013433	012505
0.30	037188	0.50	032099	014284	000000	013725	012854
0.30	036754	0.00	035087	012390	003094	012390	011202
0.30	036754	0.10	034464	012735	002691	012628	011515
0.30	036754	0.20	033853	013097	002203	012882	011840
0.30	036754	0.30	033255	013476	001557	013150	012176
0.30	036754	0.40	032670	013871	000000	013429	012517
0.30	036326	0.00	035087	012390	002681	012390	011217
0.30	036326	0.10	034464	012735	002198	012628	011531
0.30	036326	0.20	033853	013097	001556	012882	011856
0.30	036326	0.30	033255	013476	000000	013147	012189
0.30	035905	0.00	035087	012390	002189	012390	011231
0.30	035905	0.10	034464	012735	001552	012629	011546
0.30	035905	0.20	033853	013097	000000	012880	011870
0.30	035492	0.00	035087	012390	001547	012390	011246
0.30	035492	0.10	034464	012735	000000	012628	011550
0.30	035087	0.00	035087	012390	000000	012390	011260

TABLE I.- FUNCTIONS FOR CALCULATING THE FLOW ABOUT FLAT-TOP CONFIGURATIONS - Continued

$M_\infty \delta_c$	$\frac{\lambda}{\delta_c}$	$\frac{\alpha}{\delta_c}$	$(\frac{w_c}{\delta_c})_o$	$(\frac{p_c}{p_\infty})_o$	$(\gamma)_{x/a}$	$(\frac{p_c}{p_\infty})_{x/a}$	$(\frac{p}{p_\infty})_x$
0.40	0.32269	0.00	0.27295	01.3783	0.05840	01.3788	01.1862
0.40	0.32269	0.10	0.26729	01.4336	0.05546	01.4141	01.2381
0.40	0.32269	0.20	0.25181	01.4921	0.05231	01.4522	01.2920
0.40	0.32269	0.30	0.25652	01.5536	0.04893	01.4931	01.3477
0.40	0.32269	0.40	0.25141	01.6183	0.04527	01.5368	01.4052
0.40	0.32269	0.50	0.24649	01.6863	0.04128	01.5834	01.4643
0.40	0.32269	0.60	0.24176	01.7576	0.03684	01.6328	01.5250
0.40	0.32269	0.70	0.23721	01.8323	0.03180	01.6850	01.5871
0.40	0.32269	0.80	0.23285	01.9104	0.02580	01.7399	01.6506
0.40	0.32269	0.90	0.22867	01.9921	0.01799	01.7973	01.7149
0.40	0.32269	1.00	0.22467	02.0774	0.00000	01.8544	01.7771
0.40	0.31754	0.00	0.27295	01.3783	0.05567	01.3787	01.1901
0.40	0.31754	0.10	0.26729	01.4336	0.05254	01.4140	01.2421
0.40	0.31754	0.20	0.25181	01.4921	0.04916	01.4522	01.2961
0.40	0.31754	0.30	0.25652	01.5536	0.04551	01.4931	01.3519
0.40	0.31754	0.40	0.25141	01.6183	0.04151	01.5369	01.4094
0.40	0.31754	0.50	0.24649	01.6863	0.03706	01.5834	01.4686
0.40	0.31754	0.60	0.24176	01.7576	0.03200	01.6327	01.5293
0.40	0.31754	0.70	0.23721	01.8323	0.02598	01.6848	01.5913
0.40	0.31754	0.80	0.23285	01.9104	0.01814	01.7392	01.6543
0.40	0.31754	0.90	0.22867	01.9921	0.00000	01.7937	01.7155
0.40	0.31242	0.00	0.27295	01.3783	0.05273	01.3786	01.1939
0.40	0.31242	0.10	0.26729	01.4336	0.04938	01.4140	01.2460
0.40	0.31242	0.20	0.25181	01.4921	0.04573	01.4522	01.3001
0.40	0.31242	0.30	0.25652	01.5536	0.04173	01.4932	01.3560
0.40	0.31242	0.40	0.25141	01.6183	0.03728	01.5369	01.4136
0.40	0.31242	0.50	0.24649	01.6863	0.03220	01.5834	01.4728
0.40	0.31242	0.60	0.24176	01.7576	0.02617	01.6326	01.5334
0.40	0.31242	0.70	0.23721	01.8323	0.01829	01.6842	01.5950
0.40	0.31242	0.80	0.23285	01.9104	0.00000	01.7362	01.6553
0.40	0.30732	0.00	0.27295	01.3783	0.04956	01.3785	01.1977
0.40	0.30732	0.10	0.26729	01.4336	0.04592	01.4140	01.2499
0.40	0.30732	0.20	0.25181	01.4921	0.04193	01.4522	01.3041
0.40	0.30732	0.30	0.25652	01.5536	0.03748	01.4932	01.3601
0.40	0.30732	0.40	0.25141	01.6183	0.03239	01.5369	01.4177
0.40	0.30732	0.50	0.24649	01.6863	0.02634	01.5834	01.4768
0.40	0.30732	0.60	0.24176	01.7576	0.01844	01.6322	01.5371
0.40	0.30732	0.70	0.23721	01.8323	0.00000	01.6818	01.5964
0.40	0.30227	0.00	0.27295	01.3783	0.04609	01.3785	01.2015
0.40	0.30227	0.10	0.26729	01.4336	0.04211	01.4140	01.2539
0.40	0.30227	0.20	0.25181	01.4921	0.03766	01.4523	01.3081
0.40	0.30227	0.30	0.25652	01.5536	0.03258	01.4933	01.3642
0.40	0.30227	0.40	0.25141	01.6183	0.02651	01.5369	01.4217
0.40	0.30227	0.50	0.24649	01.6863	0.01858	01.5831	01.4806
0.40	0.30227	0.60	0.24176	01.7576	0.00000	01.6303	01.5388
0.40	0.29725	0.00	0.27295	01.3783	0.04225	01.3784	01.2053
0.40	0.29725	0.10	0.26729	01.4336	0.03782	01.4140	01.2578
0.40	0.29725	0.20	0.25181	01.4921	0.03274	01.4523	01.3121
0.40	0.29725	0.30	0.25652	01.5536	0.02667	01.4933	01.3681
0.40	0.29725	0.40	0.25141	01.6183	0.01872	01.5368	01.4255
0.40	0.29725	0.50	0.24649	01.6863	0.00000	01.5816	01.4827
0.40	0.29227	0.00	0.27295	01.3783	0.03795	01.3783	01.2091
0.40	0.29227	0.10	0.26729	01.4336	0.03288	01.4140	01.2616
0.40	0.29227	0.20	0.25181	01.4921	0.02681	01.4523	01.3160
0.40	0.29227	0.30	0.25652	01.5536	0.01886	01.4932	01.3719
0.40	0.29227	0.40	0.25141	01.6183	0.00000	01.5357	01.4279
0.40	0.28734	0.00	18.3036	11.8904	0.03299	01.3783	01.2129
0.40	0.28734	0.10	0.26729	01.4336	0.02693	01.4140	01.2655
0.40	0.28734	0.20	0.25181	01.4921	0.01898	01.4523	01.3197
0.40	0.28734	0.30	0.25652	01.5536	0.00000	01.4925	01.3746
0.40	0.28247	0.00	0.27295	01.3783	0.02702	01.3783	01.2166
0.40	0.28247	0.10	0.26729	01.4336	0.01908	01.4140	01.2692
0.40	0.28247	0.20	0.25181	01.4921	0.00000	01.4518	01.3228
0.40	0.27767	0.00	0.27295	01.3783	0.01916	01.3783	01.2203
0.40	0.27767	0.10	0.26729	01.4336	0.00000	01.4138	01.2725
0.40	0.27295	0.00	0.27295	01.3783	0.00000	01.3783	01.2240

TABLE I.- FUNCTIONS FOR CALCULATING THE FLOW ABOUT FLAT-TOP CONFIGURATIONS - Continued

$M_{\infty} B_C$	$\frac{\lambda}{B_C}$	$\frac{a}{B_C}$	$(\frac{w_B}{B_C})_0$	$(\frac{p_C}{p_{\infty}})_{B_C}$	$(\frac{v}{x})_{x/2}$	$(\frac{p_C}{p_{\infty}})_{x/2}$	$(\frac{p}{p_{\infty}})_\lambda$
0.50	0.28166	0.00	0.22804	0.15412	0.06607	0.15432	0.12758
0.50	0.28166	0.10	0.22294	0.16217	0.06257	0.15905	0.13536
0.50	0.28166	0.20	0.21808	0.17073	0.05886	0.16424	0.14339
0.50	0.28166	0.30	0.21345	0.17981	0.05493	0.16988	0.15165
0.50	0.28166	0.40	0.20906	0.18942	0.05071	0.17598	0.16014
0.50	0.28166	0.50	0.20489	0.19958	0.04614	0.18254	0.16886
0.50	0.28166	0.60	0.20095	0.21029	0.04109	0.18956	0.17780
0.50	0.28166	0.70	0.19722	0.22158	0.03538	0.19706	0.18694
0.50	0.28166	0.80	0.19371	0.23346	0.02863	0.20500	0.19626
0.50	0.28166	0.90	0.19040	0.24592	0.01987	0.21335	0.20570
0.50	0.28166	1.00	0.18728	0.25900	0.00000	0.22161	0.21472
0.50	0.27605	0.00	0.22804	0.15412	0.06305	0.15428	0.12835
0.50	0.27605	0.10	0.22294	0.16217	0.05933	0.15902	0.13611
0.50	0.27605	0.20	0.21808	0.17073	0.05538	0.16421	0.14412
0.50	0.27605	0.30	0.21345	0.17981	0.05114	0.16985	0.15237
0.50	0.27605	0.40	0.20906	0.18942	0.04654	0.17594	0.16084
0.50	0.27605	0.50	0.20489	0.19958	0.04146	0.18249	0.16953
0.50	0.27605	0.60	0.20095	0.21029	0.03571	0.18949	0.17844
0.50	0.27605	0.70	0.19722	0.22158	0.02892	0.19694	0.18753
0.50	0.27605	0.80	0.19371	0.23346	0.02010	0.20480	0.19675
0.50	0.27605	0.90	0.19040	0.24592	0.00000	0.21262	0.20560
0.50	0.27049	0.00	0.22804	0.15412	0.05979	0.15425	0.12912
0.50	0.27049	0.10	0.22294	0.16217	0.05582	0.15899	0.13686
0.50	0.27049	0.20	0.21808	0.17073	0.05156	0.16418	0.14485
0.50	0.27049	0.30	0.21345	0.17981	0.04693	0.16982	0.15308
0.50	0.27049	0.40	0.20906	0.18942	0.04183	0.17591	0.16153
0.50	0.27049	0.50	0.20489	0.19958	0.03604	0.18244	0.17019
0.50	0.27049	0.60	0.20095	0.21029	0.02920	0.18942	0.17904
0.50	0.27049	0.70	0.19722	0.22158	0.02032	0.19679	0.18804
0.50	0.27049	0.80	0.19371	0.23346	0.00000	0.20419	0.19673
0.50	0.26497	0.00	0.22804	0.15412	0.05625	0.15422	0.12988
0.50	0.26497	0.10	0.22294	0.16217	0.05197	0.15897	0.13760
0.50	0.26497	0.20	0.21808	0.17073	0.04733	0.16416	0.14557
0.50	0.26497	0.30	0.21345	0.17981	0.04219	0.16980	0.15377
0.50	0.26497	0.40	0.20906	0.18942	0.03638	0.17588	0.16219
0.50	0.26497	0.50	0.20489	0.19958	0.02949	0.18239	0.17081
0.50	0.26497	0.60	0.20095	0.21029	0.02056	0.18930	0.17958
0.50	0.26497	0.70	0.19722	0.22158	0.00000	0.19630	0.18811
0.50	0.25950	0.00	0.22804	0.15412	0.05237	0.15419	0.13063
0.50	0.25950	0.10	0.22294	0.16217	0.04771	0.15895	0.13833
0.50	0.25950	0.20	0.21808	0.17073	0.04255	0.16415	0.14628
0.50	0.25950	0.30	0.21345	0.17981	0.03670	0.16978	0.15445
0.50	0.25950	0.40	0.20906	0.18942	0.02978	0.17584	0.16283
0.50	0.25950	0.50	0.20489	0.19958	0.02079	0.18231	0.17138
0.50	0.25950	0.60	0.20095	0.21029	0.00000	0.18891	0.17975
0.50	0.25408	0.00	0.22804	0.15412	0.04806	0.15417	0.13138
0.50	0.25408	0.10	0.22294	0.16217	0.04289	0.15893	0.13906
0.50	0.25408	0.20	0.21808	0.17073	0.03702	0.16413	0.14698
0.50	0.25408	0.30	0.21345	0.17981	0.03007	0.15976	0.15511
0.50	0.25408	0.40	0.20906	0.18942	0.02102	0.17579	0.16343
0.50	0.25408	0.50	0.20489	0.19958	0.00000	0.18201	0.17163
0.50	0.24872	0.00	0.22804	0.15412	0.04321	0.15415	0.13213
0.50	0.24872	0.10	0.22294	0.16217	0.03732	0.15892	0.13977
0.50	0.24872	0.20	0.21808	0.17073	0.03034	0.16412	0.14766
0.50	0.24872	0.30	0.21345	0.17981	0.02126	0.16973	0.15573
0.50	0.24872	0.40	0.20906	0.18942	0.00000	0.17557	0.16376
0.50	0.24342	0.00	0.22804	0.15412	0.03760	0.15413	0.13286
0.50	0.24342	0.10	0.22294	0.16217	0.03060	0.15891	0.14048
0.50	0.24342	0.20	0.21808	0.17073	0.02148	0.16410	0.14831
0.50	0.24342	0.30	0.21345	0.17981	0.00000	0.16957	0.15616
0.50	0.23820	0.00	0.22804	0.15412	0.03083	0.15412	0.13359
0.50	0.23820	0.10	0.22294	0.16217	0.02169	0.15890	0.14116
0.50	0.23820	0.20	0.21808	0.17073	0.00000	0.16401	0.14882
0.50	0.23306	0.00	0.22804	0.15412	0.02188	0.15412	0.13430
0.50	0.23306	0.10	0.22294	0.16217	0.00000	0.15886	0.14176
0.50	0.22804	0.00	0.22804	0.15412	0.00000	0.15412	0.13500

TABLE I.- FUNCTIONS FOR CALCULATING THE FLOW ABOUT FLAT-TOP CONFIGURATIONS - Continued

$M_\infty \delta_c$	$\frac{\lambda}{\delta_c}$	$\frac{a}{\delta_c}$	$(\frac{w_b}{\delta_c})_0$	$(\frac{p_e}{p_\infty})_0$	$(\gamma)_{\pi/2}$	$(\frac{p_e}{p_\infty})_{\pi/2}$	$(\frac{p}{p_\infty})_\lambda$
0.60	02.5563	0.00	01.9444	01.7278	0.7218	0.17336	01.3797
0.60	02.5563	0.10	01.9489	01.8384	0.6817	0.17931	01.4882
0.60	02.5563	0.20	01.9062	01.9567	0.6400	0.18595	01.5992
0.60	02.5563	0.30	01.8661	02.0830	0.5960	0.19329	01.7129
0.60	02.5563	0.40	01.8287	02.2175	0.5493	0.20132	01.8297
0.60	02.5563	0.50	01.7938	02.3603	0.4990	0.21006	01.9494
0.60	02.5563	0.60	01.7613	02.5118	0.4437	0.21952	02.0721
0.60	02.5563	0.70	01.7311	02.6719	0.3814	0.22970	02.1977
0.60	02.5563	0.80	01.7030	02.8410	0.3079	0.24058	02.3258
0.60	02.5563	0.90	01.6770	03.0191	0.2128	0.25209	02.4555
0.60	02.5563	1.00	01.6529	03.2063	0.0000	0.26341	02.5779
0.60	02.4964	0.00	01.9444	01.7278	0.6889	0.17325	01.3932
0.60	02.4964	0.10	01.9489	01.8384	0.6467	0.17921	01.5006
0.60	02.4964	0.20	01.9062	01.9567	0.6023	0.18585	01.6107
0.60	02.4964	0.30	01.8661	02.0830	0.5551	0.19317	01.7237
0.60	02.4964	0.40	01.8287	02.2175	0.5043	0.20119	01.8397
0.60	02.4964	0.50	01.7938	02.3603	0.4485	0.20991	01.9586
0.60	02.4964	0.60	01.7613	02.5118	0.3857	0.21932	02.0804
0.60	02.4964	0.70	01.7311	02.6719	0.3116	0.22942	02.2048
0.60	02.4964	0.80	01.7030	02.8410	0.2157	0.24015	02.3310
0.60	02.4964	0.90	01.6770	03.0191	0.0000	0.25079	02.4509
0.60	02.4372	0.00	01.9444	01.7278	0.6533	0.17315	01.4065
0.60	02.4372	0.10	01.9489	01.8384	0.6085	0.17911	01.5129
0.60	02.4372	0.20	01.9062	01.9567	0.5609	0.18575	01.6221
0.60	02.4372	0.30	01.8661	02.0830	0.5096	0.19307	01.7343
0.60	02.4372	0.40	01.8287	02.2175	0.4534	0.20108	01.8494
0.60	02.4372	0.50	01.7938	02.3603	0.3900	0.20976	01.9674
0.60	02.4372	0.60	01.7613	02.5118	0.3153	0.21912	02.0881
0.60	02.4372	0.70	01.7311	02.6719	0.2186	0.22909	02.2107
0.60	02.4372	0.80	01.7030	02.8410	0.0000	0.23907	02.3280
0.60	02.3785	0.00	01.9444	01.7278	0.6145	0.17306	01.4196
0.60	02.3785	0.10	01.9489	01.8384	0.5666	0.17903	01.5249
0.60	02.3785	0.20	01.9062	01.9567	0.5149	0.18567	01.6332
0.60	02.3785	0.30	01.8661	02.0830	0.4582	0.19299	01.7445
0.60	02.3785	0.40	01.8287	02.2175	0.3943	0.20097	01.8587
0.60	02.3785	0.50	01.7938	02.3603	0.3190	0.20961	01.9757
0.60	02.3785	0.60	01.7613	02.5118	0.2216	0.21886	02.0947
0.60	02.3785	0.70	01.7311	02.6719	0.0000	0.22822	02.2094
0.60	02.3206	0.00	01.9444	01.7278	0.5719	0.17298	01.4325
0.60	02.3206	0.10	01.9489	01.8384	0.5200	0.17896	01.5367
0.60	02.3206	0.20	01.9062	01.9567	0.4629	0.18561	01.6441
0.60	02.3206	0.30	01.8661	02.0830	0.3986	0.19291	01.7544
0.60	02.3206	0.40	01.8287	02.2175	0.3227	0.20086	01.8676
0.60	02.3206	0.50	01.7938	02.3603	0.2246	0.20942	01.9829
0.60	02.3206	0.60	01.7613	02.5118	0.0000	0.21817	02.0951
0.60	02.2634	0.00	01.9444	01.7278	0.5247	0.17291	01.4451
0.60	02.2634	0.10	01.9489	01.8384	0.4674	0.17891	01.5483
0.60	02.2634	0.20	01.9062	01.9567	0.4027	0.18555	01.6547
0.60	02.2634	0.30	01.8661	02.0830	0.3263	0.19284	01.7639
0.60	02.2634	0.40	01.8287	02.2175	0.2275	0.20073	01.8756
0.60	02.2634	0.50	01.7938	02.3603	0.0000	0.20889	01.9851
0.60	02.2072	0.00	01.9444	01.7278	0.4714	0.17286	01.4575
0.60	02.2072	0.10	01.9489	01.8384	0.4065	0.17886	01.5596
0.60	02.2072	0.20	01.9062	01.9567	0.3298	0.18550	01.6649
0.60	02.2072	0.30	01.8661	02.0830	0.2304	0.19275	01.7728
0.60	02.2072	0.40	01.8287	02.2175	0.0000	0.20033	01.8794
0.60	02.1520	0.00	01.9444	01.7278	0.4098	0.17282	01.4696
0.60	02.1520	0.10	01.9489	01.8384	0.3329	0.17882	01.5706
0.60	02.1520	0.20	01.9062	01.9567	0.2331	0.18545	01.6745
0.60	02.1520	0.30	01.8661	02.0830	0.0000	0.19247	01.7784
0.60	02.0980	0.00	01.9444	01.7278	0.3356	0.17279	01.4814
0.60	02.0980	0.10	01.9489	01.8384	0.2357	0.17880	01.5812
0.60	02.0980	0.20	01.9062	01.9567	0.0000	0.18528	01.6819
0.60	02.0454	0.00	01.9444	01.7278	0.2378	0.17277	01.4929
0.60	02.0454	0.10	01.9489	01.8384	0.0000	0.17872	01.5904
0.60	01.9944	0.00	01.9444	01.7278	0.0000	0.17278	01.5040

TABLE I.- FUNCTIONS FOR CALCULATING THE FLOW ABOUT FLAT-TOP CONFIGURATIONS - Continued

$\frac{M_\infty S_c}{\delta_c}$	$\frac{\lambda}{\delta_c}$	$\frac{\alpha}{\delta_c}$	$\left(\frac{u_2}{S_c}\right)$	$\left(\frac{P_c}{P_{\infty 0}}\right)$	$(r)_{x/2}$	$\left(\frac{P_c}{P_{\infty}}\right)_{x/2}$	$\left(\frac{P}{P_{\infty}}\right)_\lambda$
0.70	023802	0.00	018002	019388	00.7711	019522	014990
0.70	023802	0.10	017598	020849	00.7265	020239	016431
0.70	023802	0.20	017225	022420	00.6807	021057	017894
0.70	023802	0.30	016880	024106	00.6330	021975	019388
0.70	023802	0.40	016563	025909	00.5825	022994	020918
0.70	023802	0.50	016273	027832	00.5284	024117	022488
0.70	023802	0.60	016006	029876	00.4692	025344	024098
0.70	023802	0.70	015761	032045	00.4027	026677	025747
0.70	023802	0.80	015538	034339	00.3244	028113	027429
0.70	023802	0.90	015333	036760	00.2234	029640	029130
0.70	023802	1.00	015147	039309	00.0000	031133	030720
0.70	023171	0.00	018002	019388	00.7357	019496	015204
0.70	023171	0.10	017598	020849	00.6891	020214	016618
0.70	023171	0.20	017225	022420	00.6407	021032	018059
0.70	023171	0.30	016880	024106	00.5897	021949	019535
0.70	023171	0.40	016563	025909	00.5350	022956	021049
0.70	023171	0.50	016273	027832	00.4752	024084	022603
0.70	023171	0.60	016006	029876	00.4080	025304	024196
0.70	023171	0.70	015761	032045	00.3290	026625	025823
0.70	023171	0.80	015538	034339	00.2269	028036	027473
0.70	023171	0.90	015333	036760	00.0000	029431	029027
0.70	022548	0.00	018002	019388	00.6973	019473	015412
0.70	022548	0.10	017598	020849	00.6483	020192	016800
0.70	022548	0.20	017225	022420	00.5967	021010	018220
0.70	022548	0.30	016880	024106	00.5414	021925	019677
0.70	022548	0.40	016563	025909	00.4810	022940	021174
0.70	022548	0.50	016273	027832	00.4132	024053	022710
0.70	022548	0.60	016006	029876	00.3535	025284	024283
0.70	022548	0.70	015761	032045	00.2805	026555	025880
0.70	022548	0.80	015538	034339	00.0000	027864	027397
0.70	021932	0.00	018002	019388	00.6555	019452	015614
0.70	021932	0.10	017598	020849	00.6034	020173	016977
0.70	021932	0.20	017225	022420	00.5476	020991	018376
0.70	021932	0.30	016880	024106	00.4867	021905	019815
0.70	021932	0.40	016563	025909	00.4183	022916	021293
0.70	021932	0.50	016273	027832	00.3379	024022	022809
0.70	021932	0.60	016006	029876	00.2340	025218	024352
0.70	021932	0.70	015761	032045	00.0000	026425	025831
0.70	021325	0.00	018002	019388	00.6095	019434	015811
0.70	021325	0.10	017598	020849	00.5534	020156	017149
0.70	021325	0.20	017225	022420	00.4921	020974	018527
0.70	021325	0.30	016880	024106	00.4232	021887	019946
0.70	021325	0.40	016563	025909	00.3422	022893	021404
0.70	021325	0.50	016273	027832	00.2375	023987	022892
0.70	021325	0.60	016006	029876	00.0000	025107	024331
0.70	020730	0.00	018002	019388	00.5585	019418	016002
0.70	020730	0.10	017598	020849	00.4969	020142	017316
0.70	020730	0.20	017225	022420	00.4277	020960	018673
0.70	020730	0.30	016880	024106	00.3462	021870	020071
0.70	020730	0.40	016563	025909	00.2408	022867	021502
0.70	020730	0.50	016273	027832	00.0000	023902	022899
0.70	020147	0.00	018002	019388	00.5009	019406	016187
0.70	020147	0.10	017598	020849	00.4316	020131	017478
0.70	020147	0.20	017225	022420	00.3498	020948	018812
0.70	020147	0.30	016880	024106	00.2439	021852	020185
0.70	020147	0.40	016563	025909	00.0000	022804	021538
0.70	019580	0.00	018002	019388	00.4346	019396	016366
0.70	019580	0.10	017598	020849	00.3529	020123	017633
0.70	019580	0.20	017225	022420	00.2468	020937	018943
0.70	019580	0.30	016880	024106	00.0000	021808	020250
0.70	019031	0.00	018002	019388	00.3550	019390	016538
0.70	019031	0.10	017598	020849	00.2491	020116	017781
0.70	019031	0.20	017225	022420	00.0000	020910	019039
0.70	018504	0.00	018002	019388	00.2507	019387	016703
0.70	018504	0.10	017598	020849	00.0000	020104	017907
0.70	018002	0.00	018002	019388	00.0000	019388	016860

TABLE I.- FUNCTIONS FOR CALCULATING THE FLOW ABOUT FLAT-TOP CONFIGURATIONS - Continued

$M_{\infty} \delta_c$	$\frac{\lambda}{\delta_c}$	$\frac{a}{\delta_c}$	$(\frac{w}{\delta_c})_o$	$(\frac{p_e}{p_\infty})_o$	$(\frac{v}{x})_{x/2}$	$(\frac{p_e}{p_\infty})_{x/2}$	$(\frac{x}{p_\infty})_\lambda$
0.80	022554	0.00	016621	021751	008110	022017	016354
0.80	022554	0.10	016264	023623	007622	022852	018204
0.80	022554	0.20	015939	025647	007130	023829	020066
0.80	022554	0.30	015643	027827	006621	024947	021961
0.80	022554	0.40	015376	030165	006086	026207	023901
0.80	022554	0.50	015133	032666	005514	027610	025891
0.80	022554	0.60	014914	035330	004891	029159	027933
0.80	022554	0.70	014716	038161	004191	030855	030026
0.80	022554	0.80	014538	041159	003371	032694	032162
0.80	022554	0.90	014376	044326	002313	034658	034320
0.80	022554	1.00	014230	047668	000000	036570	036316
0.80	021897	0.00	016621	021751	007733	021965	016667
0.80	021897	0.10	016264	023623	007230	022803	018463
0.80	021897	0.20	015939	025647	006713	023782	020285
0.80	021897	0.30	015643	027827	006170	024898	022148
0.80	021897	0.40	015376	030165	005592	026154	024060
0.80	021897	0.50	015133	032666	004961	027551	026024
0.80	021897	0.60	014914	035330	004254	029091	028039
0.80	021897	0.70	014716	038161	003424	030770	030099
0.80	021897	0.80	014538	041159	002355	032573	032186
0.80	021897	0.90	014376	044326	000000	034349	034135
0.80	021247	0.00	016621	021751	007325	021917	016967
0.80	021247	0.10	016264	023623	006800	022760	018714
0.80	021247	0.20	015939	025647	006251	023739	020497
0.80	021247	0.30	015643	027827	005666	024854	022328
0.80	021247	0.40	015376	030165	005029	026107	024211
0.80	021247	0.50	015133	032666	004315	027497	026146
0.80	021247	0.60	014914	035330	003477	029023	028129
0.80	021247	0.70	014716	038161	0028396	030674	030143
0.80	021247	0.80	014538	041159	000000	032319	032042
0.80	020607	0.00	016621	021751	006880	021875	017256
0.80	020607	0.10	016264	023623	006326	022721	018955
0.80	020607	0.20	015939	025647	005736	023702	020702
0.80	020607	0.30	015643	027827	005094	024816	022501
0.80	020607	0.40	015376	030165	004373	026054	024353
0.80	020607	0.50	015133	032666	003527	027444	026255
0.80	020607	0.60	014914	035330	002437	028949	028194
0.80	020607	0.70	014716	038161	000000	030468	030040
0.80	019977	0.00	016621	021751	006390	021839	017534
0.80	019977	0.10	016264	023623	005798	022688	019189
0.80	019977	0.20	015939	025647	005152	023669	020898
0.80	019977	0.30	015643	027827	004427	024781	022664
0.80	019977	0.40	015376	030165	003575	026023	024483
0.80	019977	0.50	015133	032666	002476	027387	026343
0.80	019977	0.60	014914	035330	000000	028785	028132
0.80	019362	0.00	016621	021751	005846	021808	017800
0.80	019362	0.10	016264	023623	005200	022661	019413
0.80	019362	0.20	015939	025647	004473	023642	021086
0.80	019362	0.30	015643	027827	003618	024751	022817
0.80	019362	0.40	015376	030165	002512	025981	024594
0.80	019362	0.50	015133	032666	000000	027260	026384
0.80	018763	0.00	016621	021751	005233	021783	018056
0.80	018763	0.10	016264	023623	004509	022639	019628
0.80	018763	0.20	015939	025647	003654	023620	021264
0.80	018763	0.30	015643	027827	002544	024720	022954
0.80	018763	0.40	015376	030165	000000	025887	024620
0.80	018185	0.00	016621	021751	004528	021765	018300
0.80	018185	0.10	016264	023623	003678	022623	019833
0.80	018185	0.20	015939	025647	002571	023600	021429
0.80	018185	0.30	015643	027827	000000	024655	023025
0.80	017632	0.00	016621	021751	003686	021754	018533
0.80	017632	0.10	016264	023623	002588	022611	020026
0.80	017632	0.20	015939	025647	000000	023560	021546
0.80	017109	0.00	016621	021751	002593	021749	018753
0.80	017109	0.10	016264	023623	000000	022594	020189
0.80	016621	0.00	016621	021751	000000	021751	018960

TABLE I.- FUNCTIONS FOR CALCULATING THE FLOW ABOUT FLAT-TOP CONFIGURATIONS - Continued

$\frac{M_\infty S_c}{\alpha}$	$\frac{\lambda}{S_c}$	$\frac{\alpha}{S_c}$	$\left(\frac{w_\infty}{S_c}\right)_0$	$\left(\frac{p_c}{p_\infty}\right)_0$	$(\Psi)_{x/2}$	$\left(\frac{p_c}{p_\infty}\right)_{x/2}$	$\left(\frac{p}{p_\infty}\right)_\lambda$
0.90	0.21638	0.00	0.15603	0.24374	0.08430	0.24847	0.17914
0.90	0.21638	0.10	0.15288	0.26719	0.07907	0.25790	0.20222
0.90	0.21638	0.20	0.15006	0.29261	0.07385	0.26931	0.22527
0.90	0.21638	0.30	0.14753	0.32007	0.06850	0.28263	0.24867
0.90	0.21638	0.40	0.14527	0.34959	0.06291	0.29786	0.27261
0.90	0.21638	0.50	0.14325	0.38121	0.05694	0.31502	0.29720
0.90	0.21638	0.60	0.14144	0.41495	0.05044	0.3414	0.32244
0.90	0.21638	0.70	0.13983	0.45082	0.04318	0.35522	0.34831
0.90	0.21638	0.80	0.13840	0.48883	0.03467	0.37821	0.37472
0.90	0.21638	0.90	0.13711	0.52900	0.02373	0.40286	0.40135
0.90	0.21638	1.00	0.13596	0.57133	0.00000	0.42673	0.42579
0.90	0.20959	0.00	0.15603	0.24374	0.08034	0.24751	0.18342
0.90	0.20959	0.10	0.15288	0.26719	0.07500	0.25705	0.20560
0.90	0.20959	0.20	0.15006	0.29261	0.06955	0.26850	0.22802
0.90	0.20959	0.30	0.14753	0.32007	0.06387	0.28182	0.25094
0.90	0.20959	0.40	0.14527	0.34959	0.05782	0.29701	0.27446
0.90	0.20959	0.50	0.14325	0.38121	0.05125	0.31410	0.29866
0.90	0.20959	0.60	0.14144	0.41495	0.04389	0.33309	0.32350
0.90	0.20959	0.70	0.13983	0.45082	0.03528	0.35395	0.34891
0.90	0.20959	0.80	0.13840	0.48883	0.02420	0.37647	0.37463
0.90	0.20959	0.90	0.13711	0.52900	0.00000	0.39856	0.39847
0.90	0.20288	0.00	0.15603	0.24374	0.07606	0.24665	0.18747
0.90	0.20288	0.10	0.15288	0.26719	0.07053	0.25689	0.20885
0.90	0.20288	0.20	0.15006	0.29261	0.06478	0.26777	0.23067
0.90	0.20288	0.30	0.14753	0.32007	0.05867	0.28109	0.25310
0.90	0.20288	0.40	0.14527	0.34959	0.05202	0.29625	0.27620
0.90	0.20288	0.50	0.14325	0.38121	0.04459	0.31325	0.29997
0.90	0.20288	0.60	0.14144	0.41495	0.03588	0.33208	0.32435
0.90	0.20288	0.70	0.13983	0.45082	0.02467	0.35256	0.34911
0.90	0.20288	0.80	0.13840	0.48883	0.00000	0.37293	0.37230
0.90	0.19627	0.00	0.15603	0.24374	0.07138	0.24589	0.19133
0.90	0.19627	0.10	0.15288	0.26719	0.06559	0.25562	0.21196
0.90	0.19627	0.20	0.15006	0.29261	0.05943	0.26714	0.23321
0.90	0.19627	0.30	0.14753	0.32007	0.05274	0.28045	0.25515
0.90	0.19627	0.40	0.14527	0.34959	0.04524	0.29556	0.27780
0.90	0.19627	0.50	0.14325	0.38121	0.03645	0.31245	0.30110
0.90	0.19627	0.60	0.14144	0.41495	0.02512	0.33097	0.32486
0.90	0.19627	0.70	0.13983	0.45082	0.00000	0.34968	0.34735
0.90	0.18978	0.00	0.15603	0.24374	0.06622	0.24524	0.19500
0.90	0.18978	0.10	0.15288	0.26719	0.06007	0.25504	0.21495
0.90	0.18978	0.20	0.15006	0.29261	0.05336	0.26659	0.23564
0.90	0.18978	0.30	0.14753	0.32007	0.04582	0.27989	0.25709
0.90	0.18978	0.40	0.14527	0.34959	0.03697	0.29493	0.27925
0.90	0.18978	0.50	0.14325	0.38121	0.02555	0.31159	0.30194
0.90	0.18978	0.60	0.14144	0.41495	0.00000	0.32869	0.32368
0.90	0.18345	0.00	0.15603	0.24374	0.06049	0.24470	0.19851
0.90	0.18345	0.10	0.15288	0.26719	0.05382	0.25456	0.21781
0.90	0.18345	0.20	0.15006	0.29261	0.04629	0.26613	0.23795
0.90	0.18345	0.30	0.14753	0.32007	0.03742	0.27940	0.25888
0.90	0.18345	0.40	0.14527	0.34959	0.02594	0.29428	0.28044
0.90	0.18345	0.50	0.14325	0.38121	0.00000	0.30982	0.30137
0.90	0.17733	0.00	0.15603	0.24374	0.05404	0.24427	0.20184
0.90	0.17733	0.10	0.15288	0.26719	0.04659	0.25419	0.22053
0.90	0.17733	0.20	0.15006	0.29261	0.03775	0.26576	0.24012
0.90	0.17733	0.30	0.14753	0.32007	0.02627	0.27893	0.26046
0.90	0.17733	0.40	0.14527	0.34959	0.00000	0.29297	0.28050
0.90	0.17147	0.00	0.15603	0.24374	0.04664	0.24397	0.20500
0.90	0.17147	0.10	0.15288	0.26719	0.03791	0.25392	0.22311
0.90	0.17147	0.20	0.15006	0.29261	0.02650	0.26545	0.24212
0.90	0.17147	0.30	0.14753	0.32007	0.00000	0.27802	0.26117
0.90	0.16592	0.00	0.15603	0.24374	0.03784	0.24378	0.20799
0.90	0.16592	0.10	0.15288	0.26719	0.02659	0.25373	0.22552
0.90	0.16592	0.20	0.15006	0.29261	0.00000	0.26490	0.24349
0.90	0.16075	0.00	0.15603	0.24374	0.02649	0.24371	0.21079
0.90	0.16075	0.10	0.15288	0.26719	0.00000	0.25350	0.22754
0.90	0.15603	0.00	0.15603	0.24374	0.00000	0.24374	0.21340

TABLE I.- FUNCTIONS FOR CALCULATING THE FLOW ABOUT FLAT-TOP CONFIGURATIONS - Continued

$M_{\infty} \delta_c$	$\frac{\lambda}{\delta_c}$	$\frac{a}{\delta_c}$	$(\frac{w_a}{\delta_c})_o$	$(\frac{p_c}{p_{\infty}})_o$	$(\tau)_{\pi/2}$	$(\frac{p_o}{p_{\infty}})_{\pi/2}$	$(\frac{p}{p_{\infty}})_{\pi/2}$
1.00	02.0945	0.00	01.4832	02.7266	0.08685	02.8033	01.9691
1.00	02.0945	0.10	01.4555	03.0143	0.08132	02.9071	02.2502
1.00	02.0945	0.20	01.4310	03.3271	0.07587	03.0376	02.5290
1.00	02.0945	0.30	01.4093	03.6656	0.07031	03.1934	02.8118
1.00	02.0945	0.40	01.3902	04.0300	0.06451	03.3742	03.1013
1.00	02.0945	0.50	01.3733	04.4207	0.05834	03.5804	03.3986
1.00	02.0945	0.60	01.3584	04.8379	0.05164	03.8120	03.7040
1.00	02.0945	0.70	01.3452	05.2816	0.04415	04.0691	04.0178
1.00	02.0945	0.80	01.3335	05.7520	0.03540	04.3508	04.3367
1.00	02.0945	0.90	01.3232	06.2491	0.02417	04.6538	04.6585
1.00	02.0945	1.00	01.3140	06.7728	0.00000	04.9458	04.9517
1.00	02.0249	0.00	01.4832	02.7266	0.08274	02.7872	02.0244
1.00	02.0249	0.10	01.4555	03.0143	0.07714	02.8934	02.2922
1.00	02.0249	0.20	01.4310	03.3271	0.07147	03.0249	02.5622
1.00	02.0249	0.30	01.4093	03.6656	0.06558	03.1810	02.8382
1.00	02.0249	0.40	01.3902	04.0300	0.05932	03.3617	03.1219
1.00	02.0249	0.50	01.3733	04.4207	0.05253	03.5671	03.4139
1.00	02.0249	0.60	01.3584	04.8379	0.04495	03.7972	03.7140
1.00	02.0249	0.70	01.3452	05.2816	0.03608	04.0515	04.0210
1.00	02.0249	0.80	01.3335	05.7520	0.02469	04.3270	04.3314
1.00	02.0249	0.90	01.3232	06.2491	0.00000	04.5964	04.6171
1.00	01.9561	0.00	01.4832	02.7266	0.07829	02.7730	02.0763
1.00	01.9561	0.10	01.4555	03.0143	0.07254	02.8811	02.3324
1.00	01.9561	0.20	01.4310	03.3271	0.06558	03.0136	02.5940
1.00	01.9561	0.30	01.4093	03.6656	0.06026	03.1701	02.8633
1.00	01.9561	0.40	01.3902	04.0300	0.05339	03.3505	03.1411
1.00	01.9561	0.50	01.3733	04.4207	0.04572	03.5549	03.4274
1.00	01.9561	0.60	01.3584	04.8379	0.03674	03.7830	03.7212
1.00	01.9561	0.70	01.3452	05.2816	0.02521	04.0323	04.0195
1.00	01.9561	0.80	01.3335	05.7520	0.00000	04.2798	04.2972
1.00	01.8882	0.00	01.4832	02.7266	0.07343	02.7605	02.1253
1.00	01.8882	0.10	01.4555	03.0143	0.06744	02.8704	02.3708
1.00	01.8882	0.20	01.4310	03.3271	0.06109	03.0037	02.6243
1.00	01.8882	0.30	01.4093	03.6656	0.05417	03.1604	02.8869
1.00	01.8882	0.40	01.3902	04.0300	0.04644	03.3404	03.1585
1.00	01.8882	0.50	01.3733	04.4207	0.03737	03.5435	03.4384
1.00	01.8882	0.60	01.3584	04.8379	0.02571	03.7677	03.7239
1.00	01.8882	0.70	01.3452	05.2816	0.00000	03.9941	03.9928
1.00	01.8217	0.00	01.4832	02.7266	0.06807	02.7499	02.1716
1.00	01.8217	0.10	01.4555	03.0143	0.06174	02.8613	02.4074
1.00	01.8217	0.20	01.4310	03.3271	0.05483	02.9953	02.6532
1.00	01.8217	0.30	01.4093	03.6656	0.04706	03.1521	02.9090
1.00	01.8217	0.40	01.3902	04.0300	0.03794	03.3312	03.1739
1.00	01.8217	0.50	01.3733	04.4207	0.02618	03.5315	03.4456
1.00	01.8217	0.60	01.3584	04.8379	0.00000	03.7373	03.7049
1.00	01.7570	0.00	01.4832	02.7266	0.06210	02.7412	02.2156
1.00	01.7570	0.10	01.4555	03.0143	0.05526	02.8538	02.4424
1.00	01.7570	0.20	01.4310	03.3271	0.04753	02.9883	02.6806
1.00	01.7570	0.30	01.4093	03.6656	0.03841	03.1448	02.9292
1.00	01.7570	0.40	01.3902	04.0300	0.02659	03.3221	03.1861
1.00	01.7570	0.50	01.3733	04.4207	0.00000	03.5080	03.4348
1.00	01.6947	0.00	01.4832	02.7266	0.05538	02.7344	02.2572
1.00	01.6947	0.10	01.4555	03.0143	0.04777	02.8479	02.4756
1.00	01.6947	0.20	01.4310	03.3271	0.03872	02.9827	02.7062
1.00	01.6947	0.30	01.4093	03.6656	0.02692	03.1380	02.9468
1.00	01.6947	0.40	01.3902	04.0300	0.00000	03.3046	03.1838
1.00	01.6354	0.00	01.4832	02.7266	0.04767	02.7296	02.2966
1.00	01.6354	0.10	01.4555	03.0143	0.03879	02.8438	02.5070
1.00	01.6354	0.20	01.4310	03.3271	0.02711	02.9781	02.7296
1.00	01.6354	0.30	01.4093	03.6656	0.00000	03.1260	02.9534
1.00	01.5798	0.00	01.4832	02.7266	0.03854	02.7268	02.3336
1.00	01.5798	0.10	01.4555	03.0143	0.02712	02.8411	02.5362
1.00	01.5798	0.20	01.4310	03.3271	0.00000	02.9709	02.7452
1.00	01.5289	0.00	01.4832	02.7266	0.02687	02.7258	02.3682
1.00	01.5289	0.10	01.4555	03.0143	0.00000	02.8382	02.5604
1.00	01.4832	0.00	01.4832	02.7266	0.00000	02.7266	02.4000

TABLE I.- FUNCTIONS FOR CALCULATING THE FLOW ABOUT FLAT-TOP CONFIGURATIONS - Continued

$X_c S_c$	$\frac{\lambda}{S_c}$	$\frac{a}{S_c}$	$(\frac{w_s}{S_c})_0$	$(\frac{p_c}{p_{\infty}})_0$	$(\Psi)_{\pi/2}$	$(\frac{p_c}{p_{\infty}})_{\pi/2}$	$(\frac{p}{p_{\infty}})_{\lambda}$
1.20	01.9985	0.00	01.3764	03.3873	00.9046	03.5537	02.3959
1.20	01.9985	0.10	01.3549	03.8001	00.8451	03.6700	02.7884
1.20	01.9985	0.20	01.3364	04.2503	00.7873	03.8324	03.1757
1.20	01.9985	0.30	01.3204	04.7384	00.7286	04.0366	03.5686
1.20	01.9985	0.40	01.3066	05.2647	00.6676	04.2812	03.9712
1.20	01.9985	0.50	01.2947	05.8293	00.6030	04.5660	04.3853
1.20	01.9985	0.60	01.2843	06.4324	00.5330	04.8911	04.8111
1.20	01.9985	0.70	01.2753	07.0740	00.4549	05.2560	05.2478
1.20	01.9985	0.80	01.2675	07.7541	00.3639	05.6591	05.6931
1.20	01.9985	0.90	01.2607	08.4726	00.2474	06.0945	06.1408
1.20	01.9985	1.00	01.2548	09.2296	00.0000	06.5107	06.5432
1.20	01.9264	0.00	01.3764	03.3873	00.8616	03.5171	02.4775
1.20	01.9264	0.10	01.3549	03.8001	00.8020	03.6408	02.8471
1.20	01.9264	0.20	01.3364	04.2503	00.7421	03.8069	03.2198
1.20	01.9264	0.30	01.3204	04.7384	00.6802	04.0129	03.6016
1.20	01.9264	0.40	01.3066	05.2647	00.6145	04.2581	03.9950
1.20	01.9264	0.50	01.2947	05.8293	00.5435	04.5425	04.4005
1.20	01.9264	0.60	01.2843	06.4324	00.4642	04.8657	04.8177
1.20	01.9264	0.70	01.2753	07.0740	00.3718	05.2264	05.2446
1.20	01.9264	0.80	01.2675	07.7541	00.2535	05.6199	05.6755
1.20	01.9264	0.90	01.2607	08.4726	00.0000	06.0023	06.0675
1.20	01.8549	0.00	01.3764	03.3873	00.8149	03.4853	02.5531
1.20	01.8549	0.10	01.3549	03.8001	00.7543	03.6150	02.9029
1.20	01.8549	0.20	01.3364	04.2503	00.6917	03.7843	03.2618
1.20	01.8549	0.30	01.3204	04.7384	00.6254	03.9920	03.6327
1.20	01.8549	0.40	01.3066	05.2647	00.5535	04.2377	04.0164
1.20	01.8549	0.50	01.2947	05.8293	00.4732	04.5212	04.4128
1.20	01.8549	0.60	01.2843	06.4324	00.3796	04.8415	04.8199
1.20	01.8549	0.70	01.2753	07.0740	00.2595	05.1948	05.2330
1.20	01.8549	0.80	01.2675	07.7541	00.0000	05.5443	05.6135
1.20	01.7844	0.00	01.3764	03.3873	00.7638	03.4579	02.6237
1.20	01.7844	0.10	01.3549	03.8001	00.7013	03.5925	02.9560
1.20	01.7844	0.20	01.3364	04.2503	00.6348	03.7647	03.3016
1.20	01.7844	0.30	01.3204	04.7384	00.5625	03.9737	03.6615
1.20	01.7844	0.40	01.3066	05.2647	00.4815	04.2195	04.0353
1.20	01.7844	0.50	01.2947	05.8293	00.3869	04.5014	04.4212
1.20	01.7844	0.60	01.2843	06.4324	00.2653	04.8162	04.8150
1.20	01.7844	0.70	01.2753	07.0740	00.0000	05.1336	05.1828
1.20	01.7154	0.00	01.3764	03.3873	00.7072	03.4348	02.6901
1.20	01.7154	0.10	01.3549	03.8001	00.6416	03.5736	03.0065
1.20	01.7154	0.20	01.3364	04.2503	00.5696	03.7481	03.3394
1.20	01.7154	0.30	01.3204	04.7384	00.4885	03.9581	03.6881
1.20	01.7154	0.40	01.3066	05.2647	00.3933	04.2032	04.0509
1.20	01.7154	0.50	01.2947	05.8293	00.2707	04.4812	04.4237
1.20	01.7154	0.60	01.2843	06.4324	00.0000	04.7674	04.7771
1.20	01.6485	0.00	01.3764	03.3873	00.6441	03.4161	02.7529
1.20	01.6485	0.10	01.3549	03.8001	00.5736	03.5582	03.0546
1.20	01.6485	0.20	01.3364	04.2503	00.4933	03.7345	03.3750
1.20	01.6485	0.30	01.3204	04.7384	00.3983	03.9448	03.7120
1.20	01.6485	0.40	01.3066	05.2647	00.2752	04.1874	04.0617
1.20	01.6485	0.50	01.2947	05.8293	00.0000	04.4434	04.3990
1.20	01.5845	0.00	01.3764	03.3873	00.5727	03.4018	02.8124
1.20	01.5845	0.10	01.3549	03.8001	00.4947	03.5465	03.1004
1.20	01.5845	0.20	01.3364	04.2503	00.4010	03.7238	03.4083
1.20	01.5845	0.30	01.3204	04.7384	00.2785	03.9328	03.7328
1.20	01.5845	0.40	01.3066	05.2647	00.0000	04.1593	04.0510
1.20	01.5242	0.00	01.3764	03.3873	00.4909	03.3920	02.8688
1.20	01.5242	0.10	01.3549	03.8001	00.4002	03.5384	03.1436
1.20	01.5242	0.20	01.3364	04.2503	00.2798	03.7155	03.4385
1.20	01.5242	0.30	01.3204	04.7384	00.0000	03.9135	03.7561
1.20	01.4687	0.00	01.3764	03.3873	00.3946	03.3865	02.9218
1.20	01.4687	0.10	01.3549	03.8001	00.2783	03.5336	03.1839
1.20	01.4687	0.20	01.3364	04.2503	00.0000	03.7042	03.4574
1.20	01.4192	0.00	01.3764	03.3873	00.2731	03.3852	02.9710
1.20	01.4192	0.10	01.3549	03.8001	00.0000	03.5295	03.2171
1.20	01.3764	0.00	01.3764	03.3873	00.0000	03.3873	03.0160

TABLE I.- FUNCTIONS FOR CALCULATING THE FLOW ABOUT FLAT-TOP CONFIGURATIONS - Continued

$M_\infty S_c$	$\frac{\lambda}{S_c}$	$\frac{a}{S_c}$	$(\frac{u_x}{S_c})_0$	$(\frac{p_x}{p_\infty})_0$	$(\frac{x}{\lambda})_{\pi/2}$	$(\frac{p_x}{p_\infty})_{\pi/2}$	$(\frac{p}{p_\infty})_\lambda$
1.40	019366	0.00	013077	041604	009271	044615	029220
1.40	019366	0.10	012911	047230	008653	045793	034386
1.40	019366	0.20	012770	053374	008054	047710	039494
1.40	019366	0.30	012651	060041	007448	050271	044687
1.40	019366	0.40	012551	067231	006820	053440	050021
1.40	019366	0.50	012465	074945	006154	057806	055514
1.40	019366	0.60	012392	083184	005434	061561	061168
1.40	019366	0.70	012330	091946	004632	066497	066968
1.40	019366	0.80	012277	101231	003700	071982	072880
1.40	019366	0.90	012232	111038	002508	077923	078811
1.40	019366	1.00	012193	121366	000000	083566	084091
1.40	018628	0.00	013077	041604	008832	043932	030296
1.40	018628	0.10	012911	047230	008216	045274	035137
1.40	018628	0.20	012770	053374	007598	047275	040038
1.40	018628	0.30	012651	060041	006958	049882	045075
1.40	018628	0.40	012551	067231	006282	053075	050276
1.40	018628	0.50	012465	074945	005550	056843	055647
1.40	018628	0.60	012392	083184	004736	061179	061176
1.40	018628	0.70	012330	091946	003787	066058	066833
1.40	018628	0.80	012277	101231	002574	071405	072537
1.40	018628	0.90	012232	111038	000000	076576	077679
1.40	017896	0.00	013077	041604	008355	043345	031289
1.40	017896	0.10	012911	047230	007731	044818	035850
1.40	017896	0.20	012770	053374	007086	046893	040554
1.40	017896	0.30	012651	060041	006402	049542	045435
1.40	017896	0.40	012551	067231	005661	052753	050498
1.40	017896	0.50	012465	074945	004835	056518	055736
1.40	017896	0.60	012392	083184	003873	060819	061120
1.40	017896	0.70	012330	091946	002640	065594	066577
1.40	017896	0.80	012277	101231	000000	070303	071555
1.40	017173	0.00	013077	041604	007830	042844	032215
1.40	017173	0.10	012911	047230	007189	044425	036526
1.40	017173	0.20	012770	053374	006505	046564	041042
1.40	017173	0.30	012651	060041	005760	049248	045765
1.40	017173	0.40	012551	067231	004927	052471	050682
1.40	017173	0.50	012465	074945	003954	056220	055769
1.40	017173	0.60	012392	083184	002704	060445	060959
1.40	017173	0.70	012330	091946	000000	064702	065772
1.40	016466	0.00	013077	041604	007247	042426	033087
1.40	016466	0.10	012911	047230	006576	044095	037172
1.40	016466	0.20	012770	053374	005837	046287	041504
1.40	016466	0.30	012651	060041	005003	048998	046053
1.40	016466	0.40	012551	067231	004024	052221	050881
1.40	016466	0.50	012465	074945	002763	055919	055717
1.40	016466	0.60	012392	083184	000000	059735	060331
1.40	015781	0.00	013077	041604	006593	042090	033914
1.40	015781	0.10	012911	047230	005874	043830	037788
1.40	015781	0.20	012770	053374	005053	046062	041938
1.40	015781	0.30	012651	060041	004077	048787	046326
1.40	015781	0.40	012551	067231	002813	051982	050892
1.40	015781	0.50	012465	074945	000000	055367	055280
1.40	015128	0.00	013077	041604	005851	041836	034703
1.40	015128	0.10	012911	047230	005058	043629	038378
1.40	015128	0.20	012770	053374	004101	045886	042344
1.40	015128	0.30	012651	060041	002846	048603	046538
1.40	015128	0.40	012551	067231	000000	051570	050663
1.40	014518	0.00	013077	041604	004999	041665	035455
1.40	014518	0.10	012911	047230	004081	043494	038939
1.40	014518	0.20	012770	053374	002853	045758	042712
1.40	014518	0.30	012651	060041	000000	048320	046530
1.40	013966	0.00	013077	041604	004000	041575	036168
1.40	013966	0.10	012911	047230	002825	043420	039466
1.40	013966	0.20	012770	053374	000000	045595	042931
1.40	013483	0.00	013077	041604	002751	041559	036834
1.40	013483	0.10	012911	047230	000000	043369	039900
1.40	013077	0.00	013077	041604	000000	041604	037440

TABLE I. - FUNCTIONS FOR CALCULATING THE FLOW ABOUT FLAT-TOP CONFIGURATIONS - Continued

$\frac{M_\infty \delta_c}{c}$	$\frac{\lambda}{\delta_c}$	$\frac{\alpha}{\delta_c}$	$\left(\frac{w_\infty}{\delta_c}\right)$	$\left(\frac{p_\infty}{\delta_{\infty}^2}\right)$	$(\gamma)_{x/2}$	$\left(\frac{p_\infty}{p_{\infty}}\right)_{x/2}$	$\left(\frac{p}{p_{\infty}}\right)_\lambda$
1.60	01.8944	0.00	01.2612	05.0478	00.9414	05.5312	03.5468
1.60	01.8944	0.10	01.2482	05.7847	00.8785	05.6374	04.2003
1.60	01.8944	0.20	01.2375	06.5900	00.8174	05.8547	04.8497
1.60	01.8944	0.30	01.2286	07.4638	00.7555	06.1657	05.5123
1.60	01.8944	0.40	01.2212	08.4061	00.6914	06.5634	06.1941
1.60	01.8944	0.50	01.2151	09.4169	00.6235	07.0450	06.8974
1.60	01.8944	0.60	01.2099	10.4961	00.5502	07.6085	07.6218
1.60	01.8944	0.70	01.2056	11.6435	00.4686	08.2518	08.3651
1.60	01.8944	0.80	01.2020	12.8590	00.3738	08.9701	09.1224
1.60	01.8944	0.90	01.1989	14.1424	00.2528	09.7498	09.8812
1.60	01.8944	1.00	01.1964	15.4937	00.0000	10.4862	10.5515
1.60	01.8194	0.00	01.2612	05.0478	00.8973	05.4196	03.6799
1.60	01.8194	0.10	01.2482	05.7847	00.8345	05.5555	04.2917
1.60	01.8194	0.20	01.2375	06.5900	00.7715	05.7883	04.9142
1.60	01.8194	0.30	01.2286	07.4638	00.7062	06.1081	05.5561
1.60	01.8194	0.40	01.2212	08.4061	00.6372	06.5107	06.2204
1.60	01.8194	0.50	01.2151	09.4169	00.5626	06.9938	06.9071
1.60	01.8194	0.60	01.2099	10.4961	00.4797	07.5555	07.6147
1.60	01.8194	0.70	01.2056	11.6435	00.3831	08.1917	08.3385
1.60	01.8194	0.80	01.2020	12.8590	00.2598	08.8913	09.0675
1.60	01.8194	0.90	01.1989	14.1424	00.0000	09.5650	09.7202
1.60	01.7450	0.00	01.2612	05.0478	00.8491	05.3242	03.8028
1.60	01.7450	0.10	01.2482	05.7847	00.7857	05.4839	04.3783
1.60	01.7450	0.20	01.2375	06.5900	00.7199	05.7302	04.9751
1.60	01.7450	0.30	01.2286	07.4638	00.6501	06.0580	05.5952
1.60	01.7450	0.40	01.2212	08.4061	00.5745	06.4648	06.2420
1.60	01.7450	0.50	01.2151	09.4169	00.4904	06.9485	06.9108
1.60	01.7450	0.60	01.2099	10.4961	00.3983	07.5061	07.5985
1.60	01.7450	0.70	01.2056	11.6435	00.2669	08.1283	08.2952
1.60	01.7450	0.80	01.2020	12.8590	00.0000	08.7405	08.9279
1.60	01.5715	0.00	01.2612	05.0478	00.7959	05.2433	03.9177
1.60	01.5715	0.10	01.2482	05.7847	00.7308	05.4224	04.4607
1.60	01.5715	0.20	01.2375	06.5900	00.6611	05.6804	05.0325
1.60	01.5715	0.30	01.2286	07.4638	00.5851	06.0151	05.6324
1.60	01.5715	0.40	01.2212	08.4061	00.5002	06.4249	06.2585
1.60	01.5715	0.50	01.2151	09.4169	00.4010	06.9072	06.9067
1.60	01.5715	0.60	01.2099	10.4961	00.2738	07.4550	07.5681
1.60	01.5715	0.70	01.2056	11.6435	00.0000	08.0066	08.1780
1.60	01.5995	0.00	01.2612	05.0478	00.7366	05.1760	04.0263
1.60	01.5995	0.10	01.2482	05.7847	00.6585	05.3710	04.5394
1.60	01.5995	0.20	01.2375	06.5900	00.5932	05.6388	05.0866
1.60	01.5995	0.30	01.2286	07.4638	00.5083	05.9788	05.6645
1.60	01.5995	0.40	01.2212	08.4061	00.4085	06.3897	06.2688
1.60	01.5995	0.50	01.2151	09.4169	00.2801	06.8659	06.8909
1.60	01.5995	0.60	01.2099	10.4961	00.0000	07.3581	07.4747
1.60	01.5299	0.00	01.2612	05.0478	00.6697	05.1222	04.1301
1.60	01.5299	0.10	01.2482	05.7847	00.5969	05.3298	04.6150
1.60	01.5299	0.20	01.2375	06.5900	00.5134	05.6053	05.1375
1.60	01.5299	0.30	01.2286	07.4638	00.4141	05.9486	05.6919
1.60	01.5299	0.40	01.2212	08.4061	00.2853	06.3564	06.2699
1.60	01.5299	0.50	01.2151	09.4169	00.0000	06.7905	06.8235
1.60	01.4636	0.00	01.2612	05.0478	00.5935	05.0818	04.2299
1.60	01.4636	0.10	01.2482	05.7847	00.5134	05.2990	04.6879
1.60	01.4636	0.20	01.2375	06.5900	00.4162	05.5796	05.1852
1.60	01.4636	0.30	01.2286	07.4638	00.2886	05.9225	05.7129
1.60	01.4636	0.40	01.2212	08.4061	00.0000	06.3000	06.2310
1.60	01.4021	0.00	01.2612	05.0478	00.5059	05.0550	04.3261
1.60	01.4021	0.10	01.2482	05.7847	00.4133	05.2786	04.7580
1.60	01.4021	0.20	01.2375	06.5900	00.2889	05.5609	05.2285
1.60	01.4021	0.30	01.2286	07.4638	00.0000	05.8837	05.7051
1.60	01.3471	0.00	01.2612	05.0478	00.4033	05.0414	04.4183
1.60	01.3471	0.10	01.2482	05.7847	00.2851	05.2681	04.8244
1.60	01.3471	0.20	01.2375	06.5900	00.0000	05.5390	05.2530
1.60	01.2998	0.00	01.2612	05.0478	00.2759	05.0398	04.5049
1.60	01.2998	0.10	01.2482	05.7847	00.0000	05.2622	04.8795
1.60	01.2612	0.00	01.2612	05.0478	00.0000	05.0478	04.5840

TABLE I. - FUNCTIONS FOR CALCULATING THE FLOW ABOUT FLAT-TOP CONFIGURATIONS - Continued

$M_\infty \delta_c$	$\frac{\lambda}{\delta_c}$	$\frac{c}{\delta_c}$	$(\frac{w_\infty}{\delta_{c0}})$	$(\frac{p_c}{p_{\infty 0}})$	$(\frac{v}{\delta})_{x/2}$	$(\frac{p_c}{p_\infty})_{x/2}$	$(\frac{p}{p_\infty})_{x/2}$
1.80	01.8643	0.00	01.2283	06.0504	00.9509	06.7661	04.2679
1.80	01.8643	0.10	01.2182	06.9862	00.8874	06.8456	05.0718
1.80	01.8643	0.20	01.2100	08.0087	00.8255	07.0838	05.8758
1.80	01.8643	0.30	01.2033	09.1181	00.7629	07.4525	06.6986
1.80	01.8643	0.40	01.1979	10.3141	00.6978	07.9397	07.5471
1.80	01.8643	0.50	01.1935	11.5967	00.6291	08.5397	08.4232
1.80	01.8643	0.60	01.1898	12.9656	00.5548	09.2488	09.3263
1.80	01.8643	0.70	01.1869	14.4206	00.4782	10.0634	10.2532
1.80	01.8643	0.80	01.1844	15.9615	00.3763	10.9761	11.1973
1.80	01.8643	0.90	01.1824	17.5881	00.2540	11.9683	12.1421
1.80	01.8643	1.00	01.1808	19.3002	00.0000	12.9010	12.9718
1.80	01.7886	0.00	01.2283	06.0504	00.9068	06.5989	04.4264
1.80	01.7886	0.10	01.2182	06.9862	00.8434	06.7261	05.1798
1.80	01.7886	0.20	01.2100	08.0087	00.7796	06.9895	05.9503
1.80	01.7886	0.30	01.2033	09.1181	00.7134	07.3728	06.7471
1.80	01.7886	0.40	01.1979	10.3141	00.6435	07.8683	07.5732
1.80	01.7886	0.50	01.1935	11.5967	00.5678	08.4718	08.4281
1.80	01.7886	0.60	01.1898	12.9656	00.4838	09.1794	09.3094
1.80	01.7886	0.70	01.1869	14.4206	00.3861	09.9852	10.2109
1.80	01.7886	0.80	01.1844	15.9615	00.2614	10.8736	11.1181
1.80	01.7886	0.90	01.1824	17.5881	00.0000	11.7262	11.9259
1.80	01.7133	0.00	01.2283	06.0504	00.8585	06.4566	04.5732
1.80	01.7133	0.10	01.2182	06.9862	00.7943	06.6221	05.2820
1.80	01.7133	0.20	01.2100	08.0087	00.7277	06.9075	06.0203
1.80	01.7133	0.30	01.2033	09.1181	00.6570	07.3039	06.7908
1.80	01.7133	0.40	01.1979	10.3141	00.5804	07.8067	07.5931
1.80	01.7133	0.50	01.1935	11.5967	00.4951	08.4121	08.4249
1.80	01.7133	0.60	01.1898	12.9656	00.3957	09.1152	09.2804
1.80	01.7133	0.70	01.1869	14.4206	00.2688	09.9031	10.1466
1.80	01.7133	0.80	01.1844	15.9615	00.0000	10.6765	10.9293
1.80	01.6389	0.00	01.2283	06.0504	00.8050	06.3364	04.7111
1.80	01.6389	0.10	01.2182	06.9862	00.7391	06.5332	05.3795
1.80	01.6389	0.20	01.2100	08.0087	00.6685	06.8375	06.0861
1.80	01.6389	0.30	01.2033	09.1181	00.5915	07.2453	06.8295
1.80	01.6389	0.40	01.1979	10.3141	00.5054	07.7536	07.6063
1.80	01.6389	0.50	01.1935	11.5967	00.4048	08.3582	08.4113
1.80	01.6389	0.60	01.1898	12.9656	00.2760	09.0490	09.2324
1.80	01.6389	0.70	01.1869	14.4206	00.0000	09.7443	09.9865
1.80	01.5660	0.00	01.2283	06.0504	00.7450	06.2369	04.8422
1.80	01.5660	0.10	01.2182	06.9862	00.6761	06.4591	05.4729
1.80	01.5660	0.20	01.2100	08.0087	00.6000	05.7793	06.1480
1.80	01.5660	0.30	01.2033	09.1181	00.5139	07.1962	06.8629
1.80	01.5660	0.40	01.1979	10.3141	00.4128	07.7072	07.6114
1.80	01.5660	0.50	01.1935	11.5967	00.2826	08.3045	08.3822
1.80	01.5660	0.60	01.1898	12.9656	00.0000	08.9227	09.1030
1.80	01.4954	0.00	01.2283	06.0504	00.6771	06.1574	04.9683
1.80	01.4954	0.10	01.2182	06.9862	00.6036	06.4000	05.5631
1.80	01.4954	0.20	01.2100	08.0087	00.5191	06.7327	06.2063
1.80	01.4954	0.30	01.2033	09.1181	00.4185	07.1555	06.8905
1.80	01.4954	0.40	01.1979	10.3141	00.2880	07.6633	07.6045
1.80	01.4954	0.50	01.1935	11.5967	00.0000	08.2060	08.2865
1.80	01.4284	0.00	01.2283	06.0504	00.5995	06.0979	05.0908
1.80	01.4284	0.10	01.2182	06.9862	00.5187	06.3560	05.6507
1.80	01.4284	0.20	01.2100	08.0087	00.4205	06.6973	06.2609
1.80	01.4284	0.30	01.2033	09.1181	00.2913	07.1206	06.9099
1.80	01.4284	0.40	01.1979	10.3141	00.0000	07.5895	07.5461
1.80	01.3666	0.00	01.2283	06.0504	00.5100	06.0587	05.2103
1.80	01.3666	0.10	01.2182	06.9862	00.4168	06.3873	05.7359
1.80	01.3666	0.20	01.2100	08.0087	00.2913	06.6719	06.3106
1.80	01.3666	0.30	01.2033	09.1181	00.0000	07.0697	06.8930
1.80	01.3117	0.00	01.2283	06.0504	00.4054	06.0395	05.3260
1.80	01.3117	0.10	01.2182	06.9862	00.2866	06.3131	05.8175
1.80	01.3117	0.20	01.2100	08.0087	00.0000	06.6436	06.3374
1.80	01.2654	0.00	01.2283	06.0504	00.2762	06.0380	05.4357
1.80	01.2654	0.10	01.2182	06.9862	00.0000	06.3066	05.8857
1.80	01.2283	0.00	01.2283	06.0504	00.0000	06.0504	05.5360

TABLE I.- FUNCTIONS FOR CALCULATING THE FLOW ABOUT FLAT-TOP CONFIGURATIONS - Continued

$\frac{M_\infty \delta_c}{\delta_c}$	$\frac{\lambda}{\delta_c}$	$\frac{\alpha}{\delta_c}$	$\left(\frac{u_a}{V_\infty}\right)_0$	$\left(\frac{p_e}{p_\infty}\right)_0$	$(\bar{x})_{x/2}$	$\left(\frac{p_2}{p_\infty}\right)_{x/2}$	$\left(\frac{p}{p_\infty}\right)_\lambda$
2.00	01.8422	0.00	01.2042	071690	00.9573	081681	05.0824
2.00	01.8422	0.10	01.1963	083278	00.8936	082043	06.0517
2.00	01.8422	0.20	01.1901	095939	00.8313	084584	07.0266
2.00	01.8422	0.30	01.1851	10.9671	00.7680	088875	08.0272
2.00	01.8422	0.40	01.1812	12.4471	00.7024	094730	09.0606
2.00	01.8422	0.50	01.1780	14.0337	00.6330	102051	101289
2.00	01.8422	0.60	01.1755	15.7266	00.5580	110776	112306
2.00	01.8422	0.70	01.1735	17.5256	00.4748	120851	123616
2.00	01.8422	0.80	01.1719	19.4302	00.3781	132169	135132
2.00	01.8422	0.90	01.1706	21.4404	00.2548	144484	146648
2.00	01.8422	1.00	01.1697	23.5559	00.0000	156018	156713
2.00	01.7659	0.00	01.2042	071690	00.9134	079329	052671
2.00	01.7659	0.10	01.1963	083278	00.8497	080398	061768
2.00	01.7659	0.20	01.1901	095939	00.7853	083314	071114
2.00	01.7659	0.30	01.1851	10.9671	00.7185	087825	08.0801
2.00	01.7659	0.40	01.1812	12.4471	00.6479	093806	09.0858
2.00	01.7659	0.50	01.1780	14.0337	00.5716	101185	101277
2.00	01.7659	0.60	01.1755	15.7266	00.4867	109903	112020
2.00	01.7659	0.70	01.1735	17.5256	00.3882	119872	123011
2.00	01.7659	0.80	01.1719	19.4302	00.2625	130883	134062
2.00	01.7659	0.90	01.1706	21.4404	00.0000	141421	143860
2.00	01.6900	0.00	01.2042	071690	00.8652	07.7334	054389
2.00	01.6900	0.10	01.1963	083278	00.8006	078972	062954
2.00	01.6900	0.20	01.1901	095939	00.7333	082215	071907
2.00	01.6900	0.30	01.1851	10.9671	00.6619	086922	081270
2.00	01.6900	0.40	01.1812	12.4471	00.5845	093014	091033
2.00	01.6900	0.50	01.1780	14.0337	00.4984	100432	101160
2.00	01.6900	0.60	01.1755	15.7266	00.3982	109100	111580
2.00	01.6900	0.70	01.1735	17.5256	00.2701	118845	122124
2.00	01.6900	0.80	01.1719	19.4302	00.0000	128395	131616
2.00	01.6149	0.00	01.2042	071690	00.8115	075653	056009
2.00	01.6149	0.10	01.1963	083278	00.7451	077756	064085
2.00	01.6149	0.20	01.1901	095939	00.6738	081280	072650
2.00	01.6149	0.30	01.1851	10.9671	00.5961	085158	081676
2.00	01.6149	0.40	01.1812	12.4471	00.5091	092338	091120
2.00	01.6149	0.50	01.1780	14.0337	00.4076	099757	100911
2.00	01.6149	0.60	01.1755	15.7266	00.2776	108275	110897
2.00	01.6149	0.70	01.1735	17.5256	00.0000	116844	120035
2.00	01.5413	0.00	01.2042	071690	00.7511	074263	057557
2.00	01.5413	0.10	01.1963	083278	00.6817	075746	065172
2.00	01.5413	0.20	01.1901	095939	00.6048	080507	073347
2.00	01.5413	0.30	01.1851	10.9671	00.5179	085523	082017
2.00	01.5413	0.40	01.1812	12.4471	00.4158	091751	091103
2.00	01.5413	0.50	01.1780	14.0337	00.2844	099085	100463
2.00	01.5413	0.60	01.1755	15.7266	00.0000	106685	109189
2.00	01.4700	0.00	01.2042	071690	00.6825	073155	059057
2.00	01.4700	0.10	01.1963	083278	00.6085	075941	066227
2.00	01.4700	0.20	01.1901	095939	00.5232	079891	074002
2.00	01.4700	0.30	01.1851	10.9671	00.4217	084999	082284
2.00	01.4700	0.40	01.1812	12.4471	00.2899	091198	090933
2.00	01.4700	0.50	01.1780	14.0337	00.0000	097843	099176
2.00	01.4025	0.00	01.2042	071690	00.6038	072328	060527
2.00	01.4025	0.10	01.1963	083278	00.5225	075345	067261
2.00	01.4025	0.20	01.1901	095939	00.4235	079426	074617
2.00	01.4025	0.30	01.1851	10.9671	00.2933	084553	082451
2.00	01.4025	0.40	01.1812	12.4471	00.0000	090265	090121
2.00	01.3403	0.00	01.2042	071690	00.5130	071786	061978
2.00	01.3403	0.10	01.1963	083278	00.4193	074960	068276
2.00	01.3403	0.20	01.1901	095939	00.2930	079097	075177
2.00	01.3403	0.30	01.1851	10.9671	00.0000	083909	082169
2.00	01.2856	0.00	01.2042	071690	00.4066	071524	063399
2.00	01.2856	0.10	01.1963	083278	00.2876	074776	069259
2.00	01.2856	0.20	01.1901	095939	00.0000	078742	075465
2.00	01.2400	0.00	01.2042	071690	00.2761	071513	064757
2.00	01.2400	0.10	01.1963	083278	00.0000	074706	070088
2.00	01.2042	0.00	01.2042	071690	00.0000	071690	066000

TABLE I.- FUNCTIONS FOR CALCULATING THE FLOW ABOUT FLAT-TOP CONFIGURATIONS - Continued

$M_\infty \delta_c$	$\frac{\lambda}{\delta_c}$	$\frac{a}{\delta_c}$	$(\frac{w_\infty}{\delta_c})_0$	$(\frac{p_\infty}{p_\infty})_0$	$(\gamma)_{\pi/2}$	$(\frac{p_\infty}{p_\infty})_{\pi/2}$	$(\frac{p}{p_\infty})_\lambda$
2.50	01.8072	0.00	011662	10.4755	00.9667	12.4136	07.5173
2.50	01.8072	0.10	011621	12.2973	00.9028	12.2613	08.9691
2.50	01.8072	0.20	011592	14.2863	00.8399	12.5308	10.4449
2.50	01.8072	0.30	011570	16.4420	00.7758	13.1238	11.9677
2.50	01.8072	0.40	011554	18.7639	00.7093	13.9943	13.5453
2.50	01.8072	0.50	011543	21.2515	00.6389	15.1175	15.1790
2.50	01.8072	0.60	011535	23.9042	00.5629	16.4778	16.8655
2.50	01.8072	0.70	011530	26.7217	00.4785	18.0614	18.5974
2.50	01.8072	0.80	011528	29.7036	00.3806	19.8487	20.3603
2.50	01.8072	0.90	011527	32.8495	00.2559	21.7957	22.1205
2.50	01.8072	1.00	011527	36.1591	00.0000	23.6068	23.6466
2.50	01.7299	0.00	011662	10.4755	00.9232	11.9517	07.7739
2.50	01.7299	0.10	011621	12.2973	00.8591	11.9516	09.1415
2.50	01.7299	0.20	011592	14.2863	00.7939	12.3018	10.5575
2.50	01.7299	0.30	011570	16.4420	00.7262	12.9417	12.0318
2.50	01.7299	0.40	011554	18.7639	00.6546	13.8397	13.5661
2.50	01.7299	0.50	011543	21.2515	00.5771	14.9768	15.1581
2.50	01.7299	0.60	011535	23.9042	00.4911	16.3384	16.8008
2.50	01.7299	0.70	011530	26.7217	00.3912	17.9058	18.4813
2.50	01.7299	0.80	011528	29.7036	00.2640	19.6443	20.1691
2.50	01.7299	0.90	011527	32.8495	00.0000	21.2984	21.6545
2.50	01.6530	0.00	011662	10.4755	00.8753	11.5622	08.0145
2.50	01.6530	0.10	011621	12.2973	00.8100	11.6851	09.3049
2.50	01.6530	0.20	011592	14.2863	00.7418	12.1053	10.6619
2.50	01.6530	0.30	011570	16.4420	00.6694	12.7871	12.0859
2.50	01.6530	0.40	011554	18.7639	00.5909	13.7093	13.5740
2.50	01.6530	0.50	011543	21.2515	00.5034	14.8566	15.1195
2.50	01.6530	0.60	011535	23.9042	00.4018	16.2126	16.7102
2.50	01.6530	0.70	011530	26.7217	00.2720	17.7455	18.3186
2.50	01.6530	0.80	011528	29.7036	00.0000	19.2424	19.7568
2.50	01.5768	0.00	011662	10.4755	00.8215	11.2357	08.2433
2.50	01.5768	0.10	011621	12.2973	00.7543	11.4593	09.4610
2.50	01.5768	0.20	011592	14.2863	00.6820	11.9398	10.7586
2.50	01.5768	0.30	011570	16.4420	00.6031	12.6581	12.1299
2.50	01.5768	0.40	011554	18.7639	00.5148	13.5999	13.5673
2.50	01.5768	0.50	011543	21.2515	00.4117	14.7507	15.0586
2.50	01.5768	0.60	011535	23.9042	00.2799	16.0838	16.5790
2.50	01.5768	0.70	011530	26.7217	00.0000	17.4237	17.9623
2.50	01.5020	0.00	011662	10.4755	00.7607	10.9667	08.4642
2.50	01.5020	0.10	011621	12.2973	00.6904	11.2726	09.6119
2.50	01.5020	0.20	011592	14.2863	00.6123	11.8040	10.8485
2.50	01.5020	0.30	011570	16.4420	00.5241	12.5522	12.1631
2.50	01.5020	0.40	011554	18.7639	00.4204	13.5064	13.5428
2.50	01.5020	0.50	011543	21.2515	00.2871	14.6455	14.9642
2.50	01.5020	0.60	011535	23.9042	00.0000	15.8286	16.2827
2.50	01.4295	0.00	011662	10.4755	00.5910	10.7525	08.6815
2.50	01.4295	0.10	011621	12.2973	00.5160	11.1244	09.7597
2.50	01.4295	0.20	011592	14.2863	00.5295	11.6967	10.9325
2.50	01.4295	0.30	011570	16.4420	00.4265	12.4660	12.1843
2.50	01.4295	0.40	011554	18.7639	00.8928	13.4185	13.4927
2.50	01.4295	0.50	011543	21.2515	00.0000	14.4460	14.7345
2.50	01.3610	0.00	011662	10.4755	00.6106	10.5930	08.8989
2.50	01.3610	0.10	011621	12.2973	00.5284	11.0154	09.9070
2.50	01.3610	0.20	011592	14.2863	00.4281	11.6167	11.0114
2.50	01.3610	0.30	011570	16.4420	00.2961	12.3930	12.1894
2.50	01.3610	0.40	011554	18.7639	00.0000	13.2675	13.3394
2.50	01.2983	0.00	011662	10.4755	00.5173	10.4891	09.1186
2.50	01.2983	0.10	011621	12.2973	00.4288	10.9460	10.0550
2.50	01.2983	0.20	011592	14.2863	00.8953	11.5612	11.0836
2.50	01.2983	0.30	011570	16.4420	00.0000	12.2883	12.1243
2.50	01.2439	0.00	011662	10.4755	00.4080	10.4403	09.3392
2.50	01.2439	0.10	011621	12.2973	00.2886	10.9149	10.2018
2.50	01.2439	0.20	011592	14.2863	00.0000	11.5046	11.1158
2.50	01.1997	0.00	011662	10.4755	00.8751	10.4404	09.5535
2.50	01.1997	0.10	011621	12.2973	00.0000	10.9074	10.3281
2.50	01.1662	0.00	011662	10.4755	00.0000	10.4755	09.7500

TABLE I.- FUNCTIONS FOR CALCULATING THE FLOW ABOUT FLAT-TOP CONFIGURATIONS - Concluded

$M_\infty b_c$	$\frac{\lambda}{b_c}$	$\frac{a}{b_c}$	$(\frac{w}{b_c})_0$	$(\frac{p_c}{b_c})_0$	$(\bar{v})_{x/2}$	$(\frac{p_a}{b_c})_{x/2}$	$(\frac{p}{b_c})_\lambda$
3.00	01.7874	0.00	011450	14.5128	00.9714	17.7219	10.5103
3.00	01.7874	0.10	011433	171469	00.9076	17.2605	12.5474
3.00	01.7874	0.20	011422	20.0211	00.8444	17.5115	14.6318
3.00	01.7874	0.30	011416	231345	00.7799	18.2681	16.7897
3.00	01.7874	0.40	011414	26.4863	00.7129	19.5014	19.0295
3.00	01.7874	0.50	011414	30.0756	00.6420	21.1033	21.3515
3.00	01.7874	0.60	011416	33.9019	00.5654	23.0639	23.7501
3.00	01.7874	0.70	011420	37.9646	00.4805	25.3582	26.2139
3.00	01.7874	0.80	011425	42.2632	00.3819	27.9537	28.7211
3.00	01.7874	0.90	011430	46.7972	00.2564	30.7823	31.2222
3.00	01.7874	1.00	011436	51.5663	00.0000	33.4018	33.3801
3.00	01.7097	0.00	011450	14.5128	00.9284	16.9512	10.8510
3.00	01.7097	0.10	011433	171469	00.8641	16.7597	12.7750
3.00	01.7097	0.20	011422	20.0211	00.7985	17.1520	14.7765
3.00	01.7097	0.30	011416	231345	00.7303	18.0099	16.8657
3.00	01.7097	0.40	011414	26.4863	00.6581	19.2708	19.0435
3.00	01.7097	0.50	011414	30.0756	00.5801	20.8976	21.3051
3.00	01.7097	0.60	011416	33.9019	00.4934	22.8629	23.6399
3.00	01.7097	0.70	011420	37.9646	00.3928	25.1362	26.0283
3.00	01.7097	0.80	011425	42.2632	00.2647	27.6587	28.4253
3.00	01.7097	0.90	011430	46.7972	00.0000	30.0514	30.5255
3.00	01.6322	0.00	011450	14.5128	00.8806	16.3041	11.1720
3.00	01.6322	0.10	011433	171469	00.8151	16.3310	12.9905
3.00	01.6322	0.20	011422	20.0211	00.7464	16.8457	14.9093
3.00	01.6322	0.30	011416	231345	00.6734	17.7760	16.9270
3.00	01.6322	0.40	011414	26.4863	00.5942	19.0790	19.0381
3.00	01.6322	0.50	011414	30.0756	00.5061	20.7247	21.2321
3.00	01.6322	0.60	011416	33.9019	00.4036	22.6839	23.4906
3.00	01.6322	0.70	011420	37.9646	00.2730	24.9056	25.7733
3.00	01.6322	0.80	011425	42.2632	00.0000	27.0702	27.8061
3.00	01.5554	0.00	011450	14.5128	00.8270	15.7639	11.4787
3.00	01.5554	0.10	011433	171469	00.7593	15.9695	13.1965
3.00	01.5554	0.20	011422	20.0211	00.6864	16.5895	15.0311
3.00	01.5554	0.30	011416	231345	00.6069	17.5830	16.9730
3.00	01.5554	0.40	011414	26.4863	00.5178	18.9203	19.0104
3.00	01.5554	0.50	011414	30.0756	00.4139	20.5742	21.1252
3.00	01.5554	0.60	011416	33.9019	00.2810	22.5010	23.2806
3.00	01.5554	0.70	011420	37.9646	00.0000	24.4361	25.2344
3.00	01.4798	0.00	011450	14.5128	00.7660	15.3201	11.7773
3.00	01.4798	0.10	011433	171469	00.6951	15.6717	13.3961
3.00	01.4798	0.20	011422	20.0211	00.6164	16.3807	15.1432
3.00	01.4798	0.30	011416	231345	00.5274	17.4263	17.0028
3.00	01.4798	0.40	011414	26.4863	00.4229	18.7862	18.9556
3.00	01.4798	0.50	011414	30.0756	00.2884	20.4251	20.9674
3.00	01.4798	0.60	011416	33.9019	00.0000	22.1296	22.8279
3.00	01.4067	0.00	011450	14.5128	00.6958	14.9670	12.0740
3.00	01.4067	0.10	011433	171469	00.6202	15.4360	13.5931
3.00	01.4067	0.20	011422	20.0211	00.5329	16.2169	15.2473
3.00	01.4067	0.30	011416	231345	00.4291	17.2999	17.0145
3.00	01.4067	0.40	011414	26.4863	00.2944	18.6603	18.8619
3.00	01.4067	0.50	011414	30.0756	00.0000	20.1343	20.6107
3.00	01.3375	0.00	011450	14.5128	00.6144	14.7039	12.3754
3.00	01.3375	0.10	011433	171469	00.5315	15.2630	13.7918
3.00	01.3375	0.20	011422	20.0211	00.4305	16.0956	15.3447
3.00	01.3375	0.30	011416	231345	00.2976	17.1930	17.0019
3.00	01.3375	0.40	011414	26.4863	00.0000	18.4392	18.6164
3.00	01.2745	0.00	011450	14.5128	00.5194	14.5328	12.6857
3.00	01.2745	0.10	011433	171469	00.4245	15.1538	13.9949
3.00	01.2745	0.20	011422	20.0211	00.2963	16.0122	15.4338
3.00	01.2745	0.30	011416	231345	00.0000	17.0388	16.8877
3.00	01.2203	0.00	011450	14.5128	00.4083	14.4535	13.0029
3.00	01.2203	0.10	011433	171469	00.2887	15.1067	14.2003
3.00	01.2203	0.20	011422	20.0211	00.0000	15.9296	15.4680
3.00	01.1770	0.00	011450	14.5128	00.2740	14.4552	13.3144
3.00	01.1770	0.10	011433	171469	00.0000	15.0993	14.3792
3.00	011450	0.00	011450	14.5128	00.0000	14.5128	13.6000



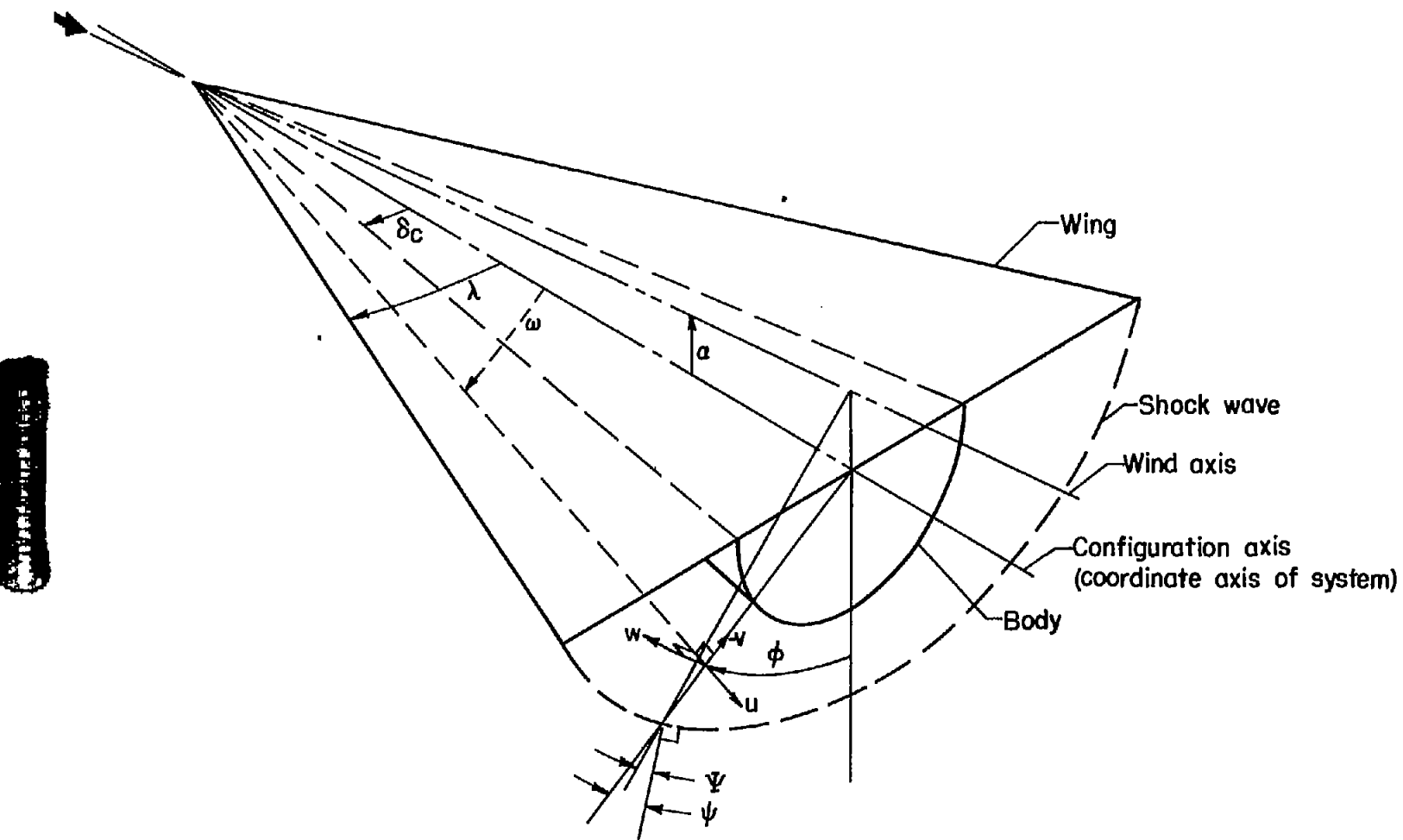


Figure 1.- Schematic diagram of polar coordinate system.

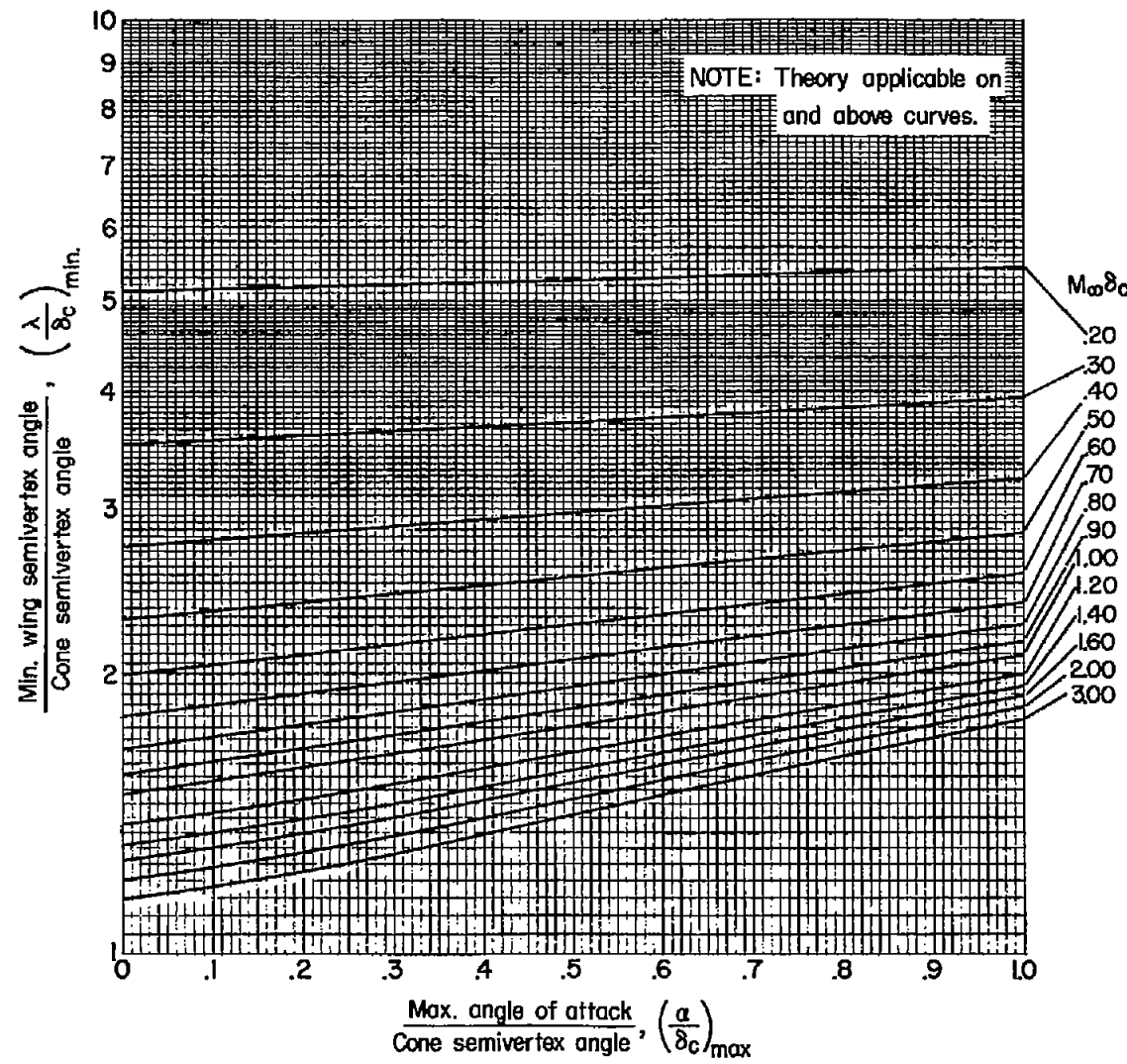
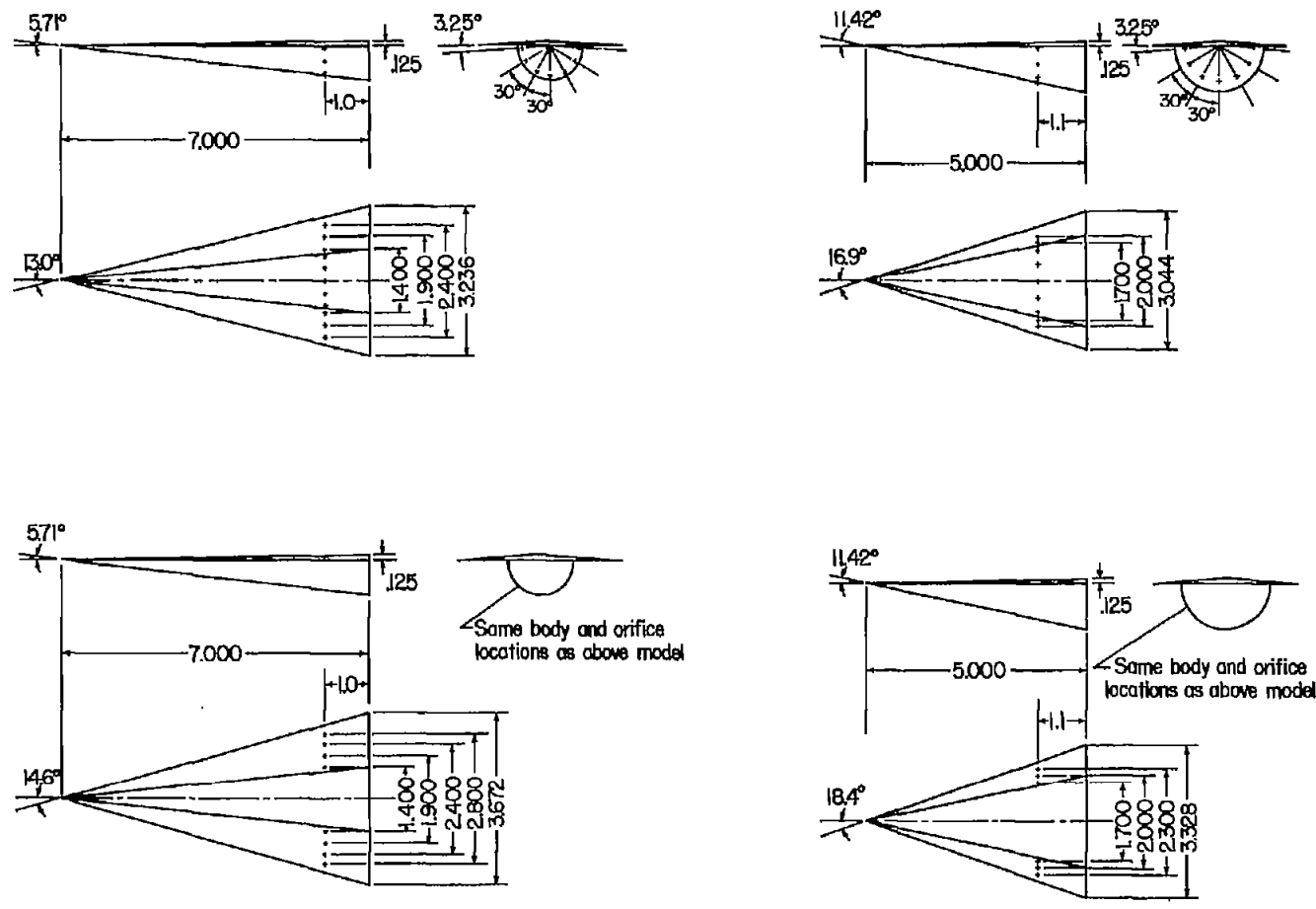


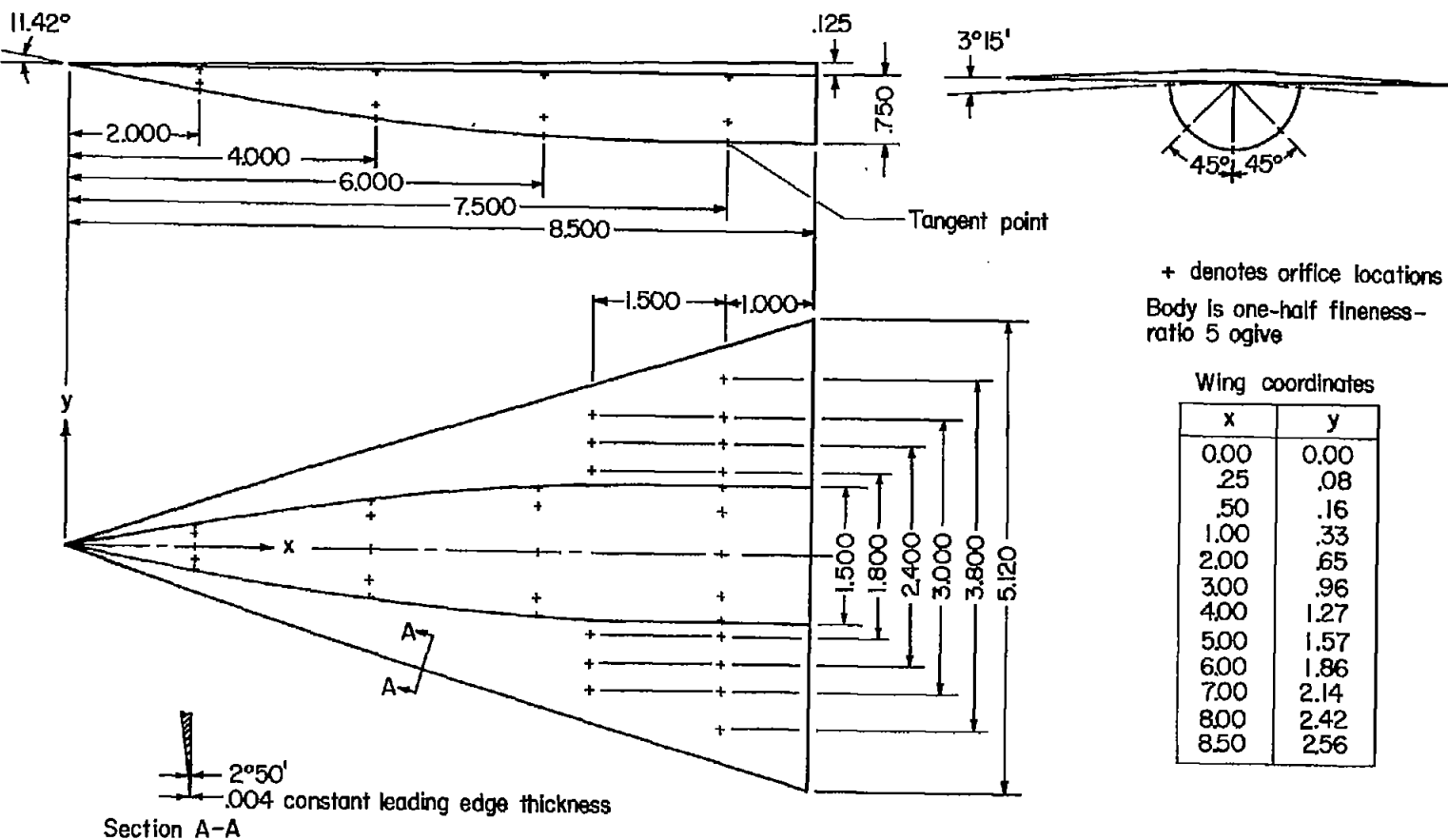
Figure 2. - Variation of wing semivertex angle with maximum angle of attack for applicability of theory;  $(\Psi)_{\pi/2} = 0$ .



+ denotes orifice locations  
.004 constant leading edge thickness for all wings

**(a) Conical models.**

Figure 3.- Dimensions of pressure-distribution test models showing location of pressure orifices.



(b) Ogive model.

Figure 3.- Concluded.

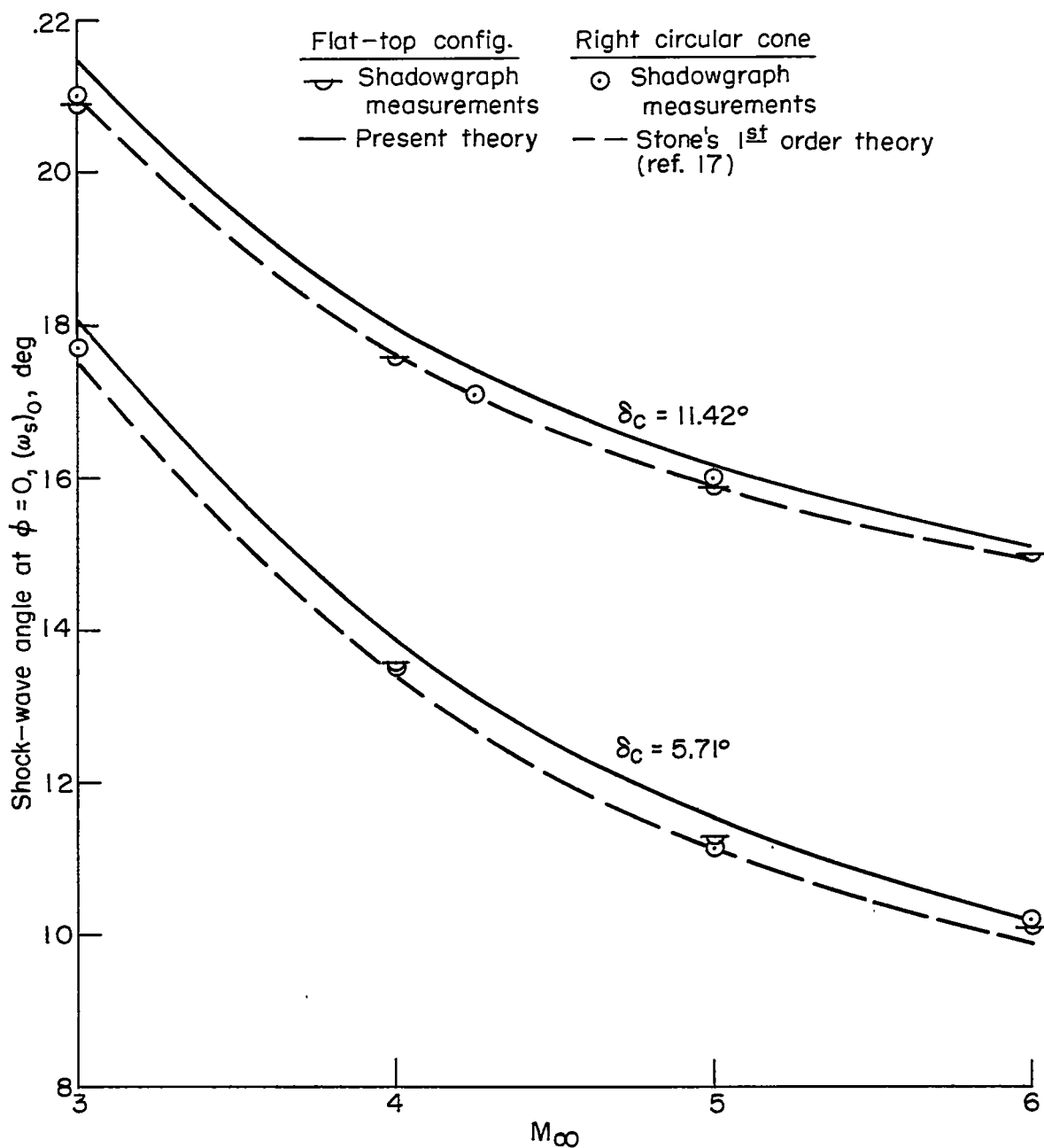


Figure 4.- Variation of shock-wave angle at  $\varphi = 0$  with Mach number for  $\alpha = 3^\circ$ .

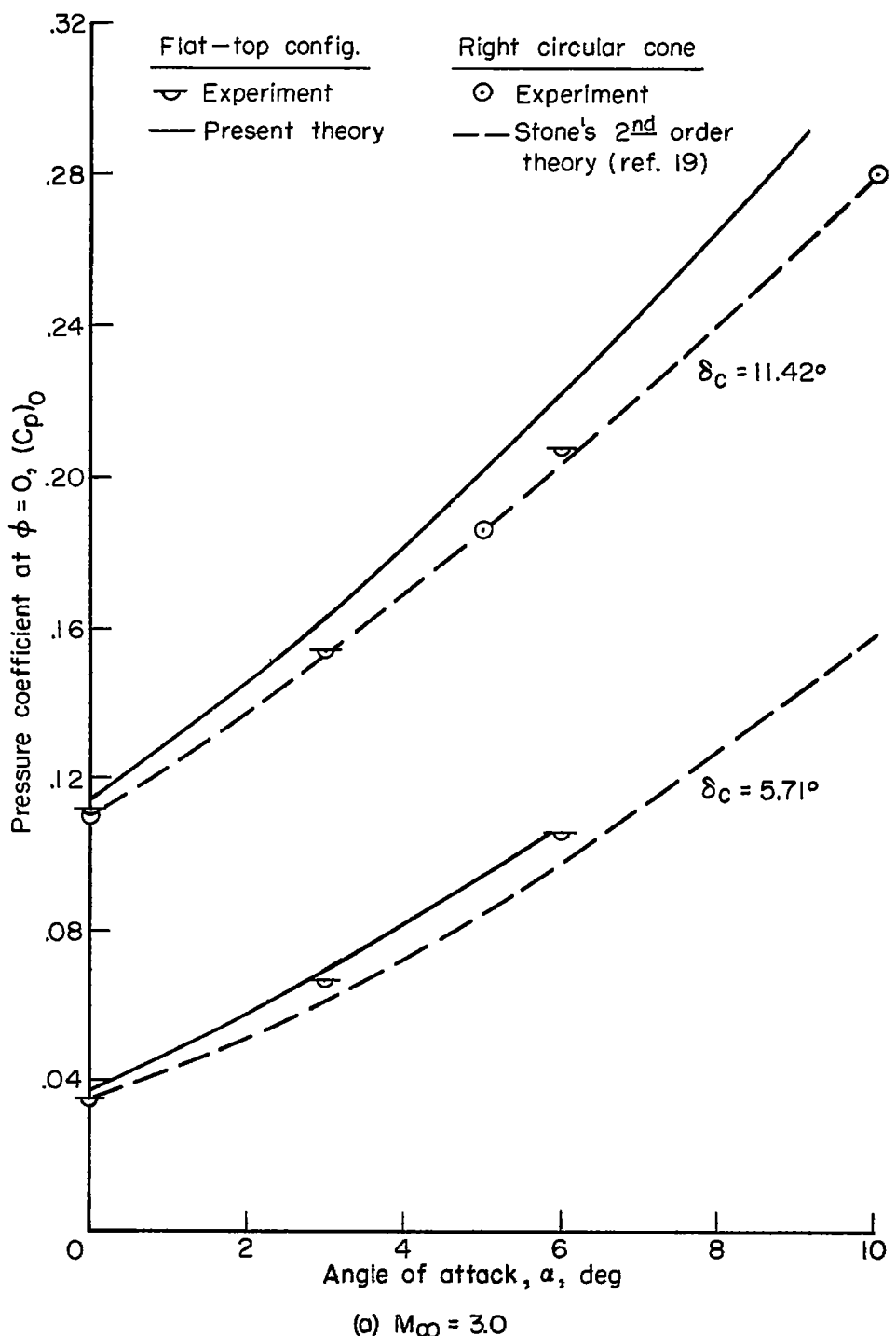


Figure 5.- Variation of pressure coefficient at  $\phi = 0$  with angle of attack for Mach numbers 3.0 and 5.0.

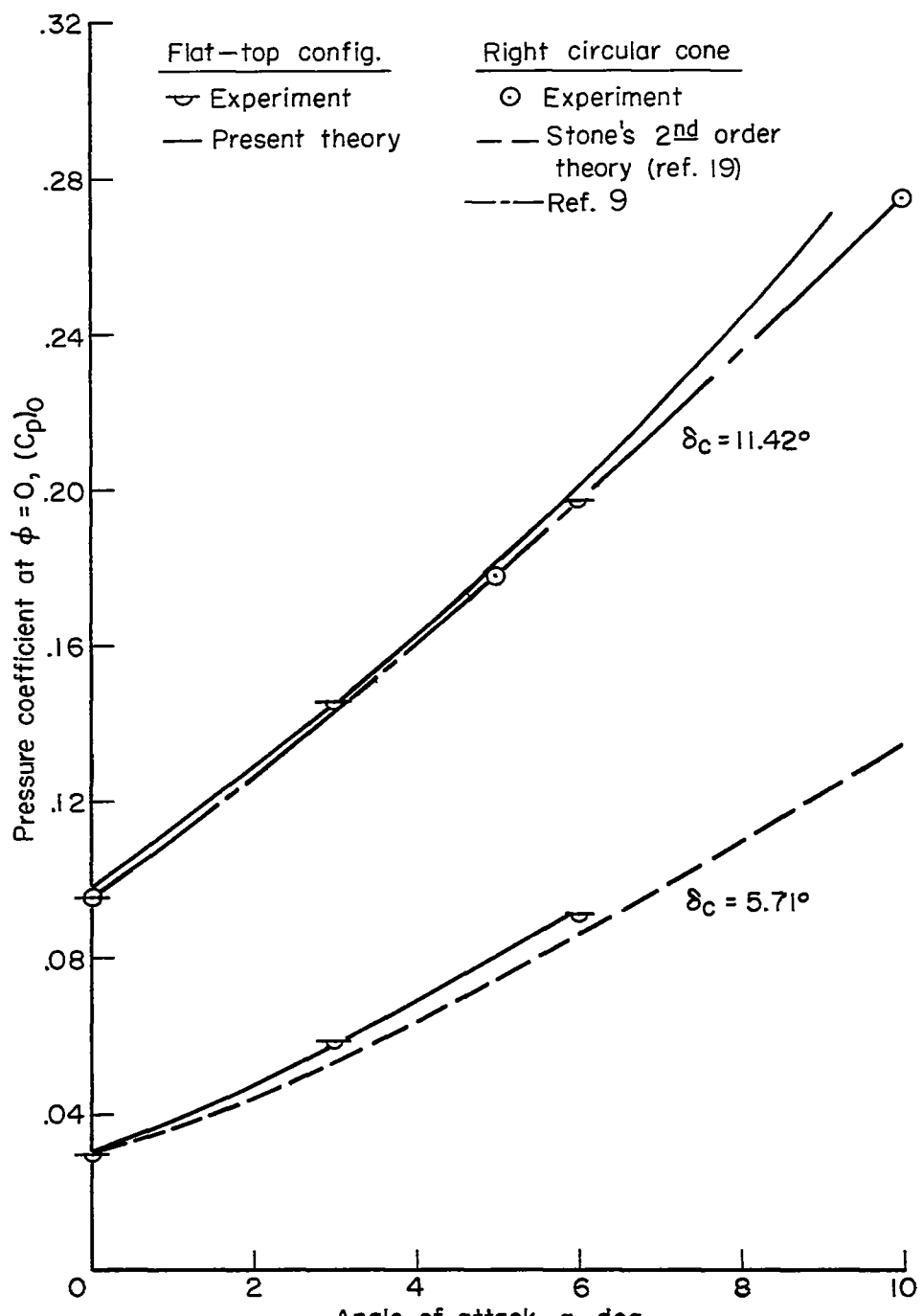
(b)  $M_\infty = 5.0$ 

Figure 5.- Concluded.

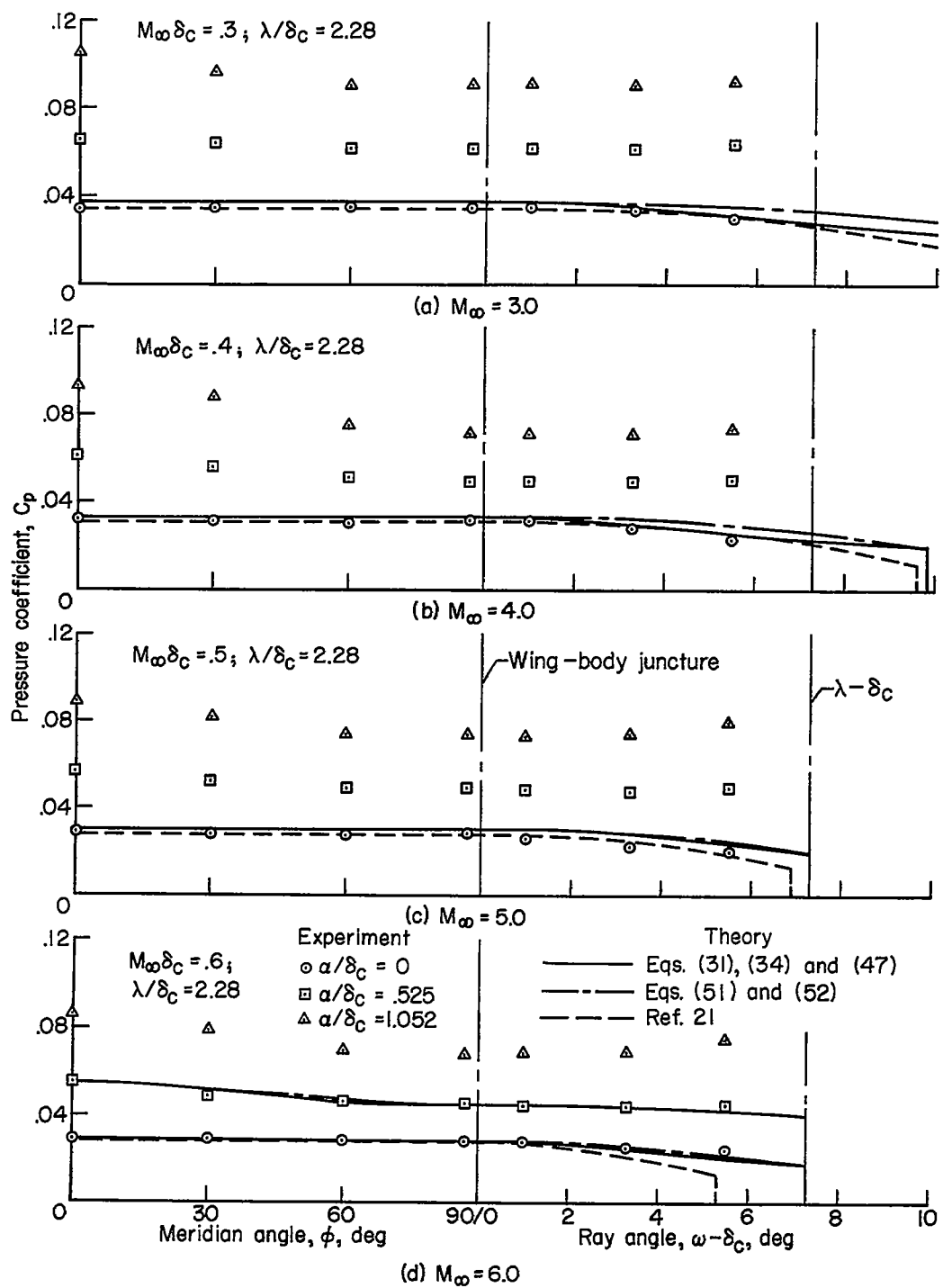


Figure 6.- Surface pressure coefficients for configuration with  $\delta_C = 5.71^\circ$  and  $\lambda = 13^\circ$  at angles of attack of  $0^\circ$ ,  $3^\circ$ , and  $6^\circ$ .

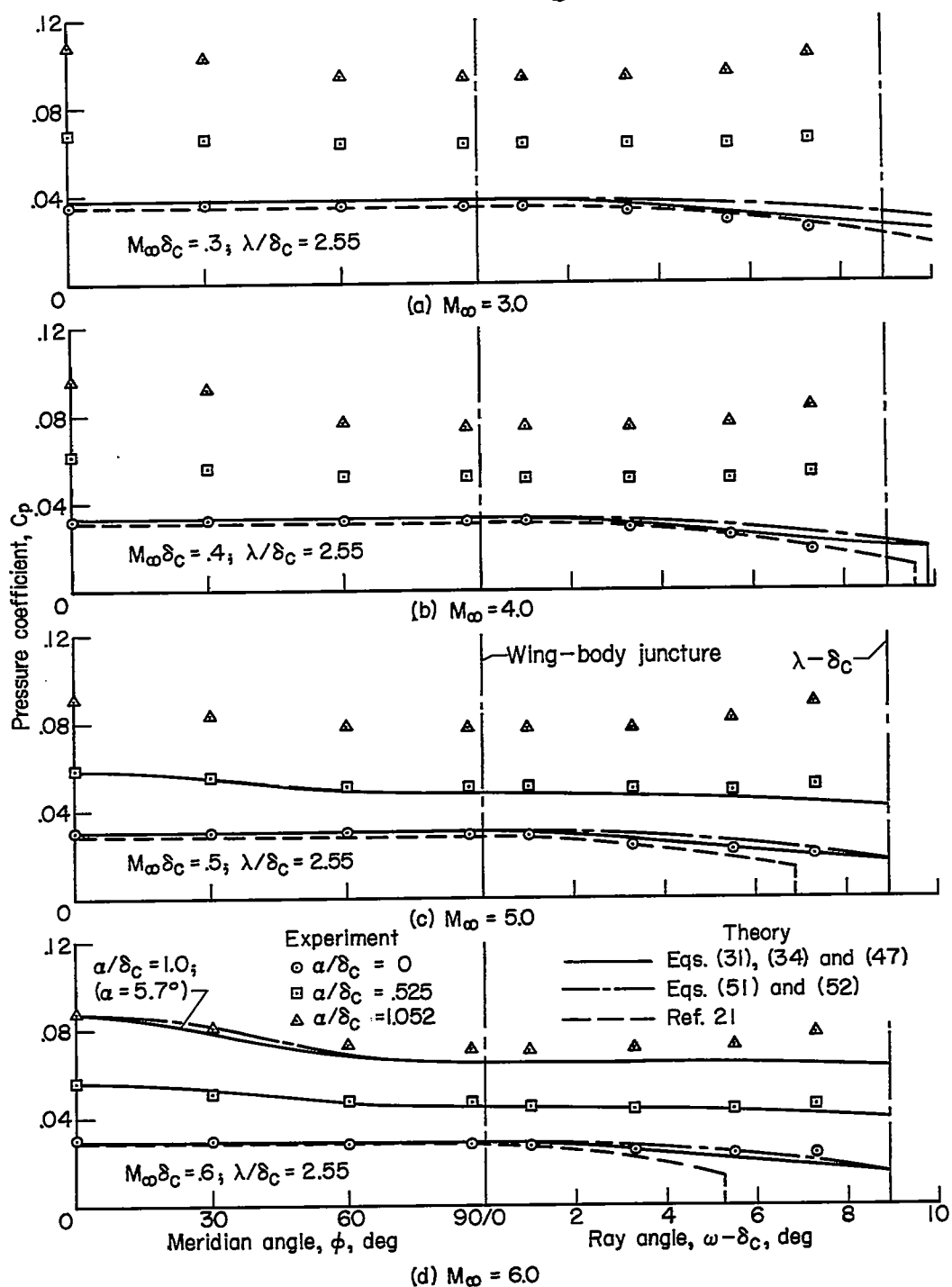


Figure 7.- Surface pressure coefficients for configuration with  $\delta_c = 5.71^\circ$  and  $\lambda = 14.6^\circ$  at angles of attack of  $0^\circ$ ,  $3^\circ$ , and  $6^\circ$ .

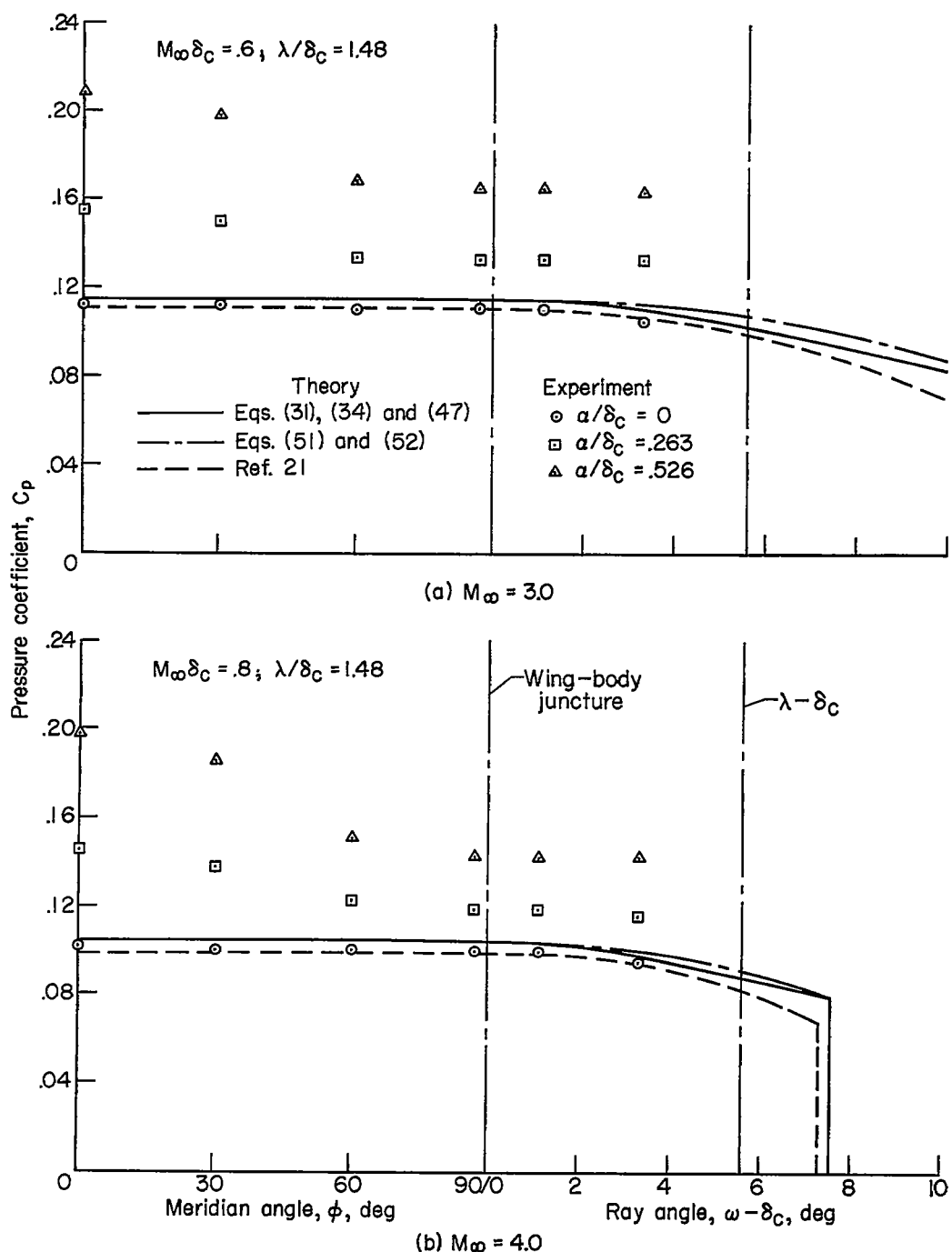


Figure 8.- Surface pressure coefficients for configuration with  $\delta_c = 11.42^\circ$  and  $\lambda = 16.9^\circ$  at angles of attack of  $0^\circ$ ,  $3^\circ$ , and  $6^\circ$ .

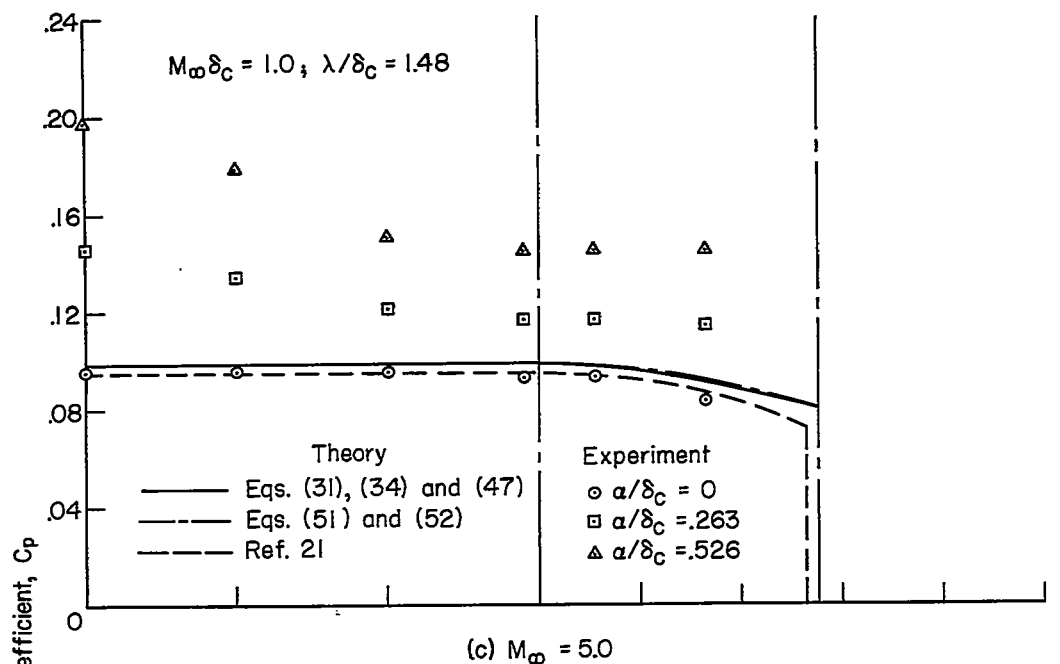
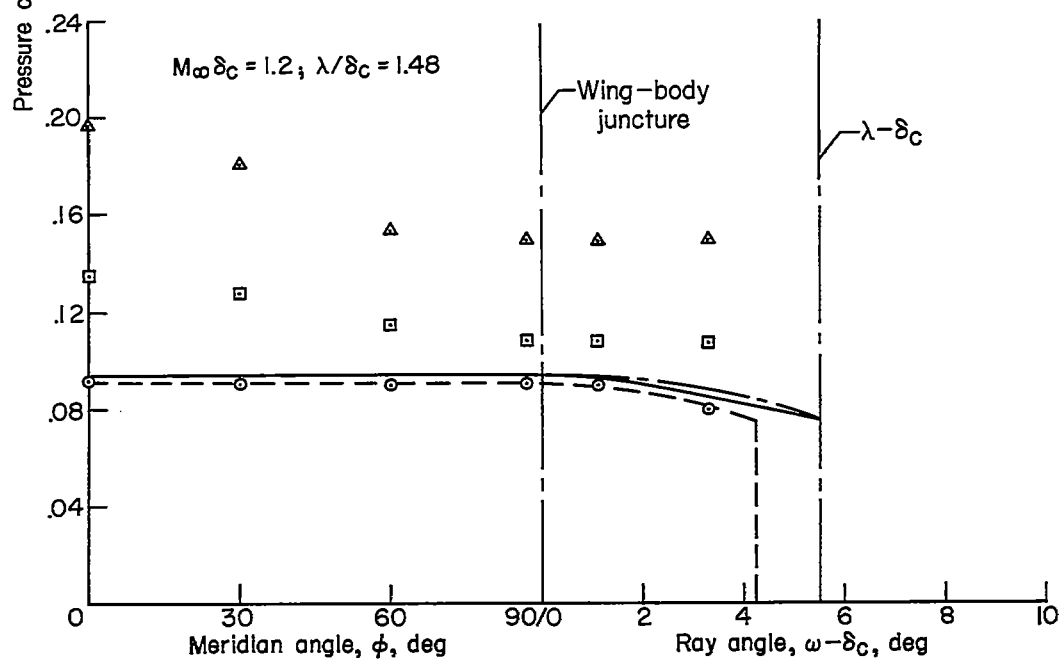
(c)  $M_\infty = 5.0$ (d)  $M_\infty = 6.0$ 

Figure 8.- Concluded.

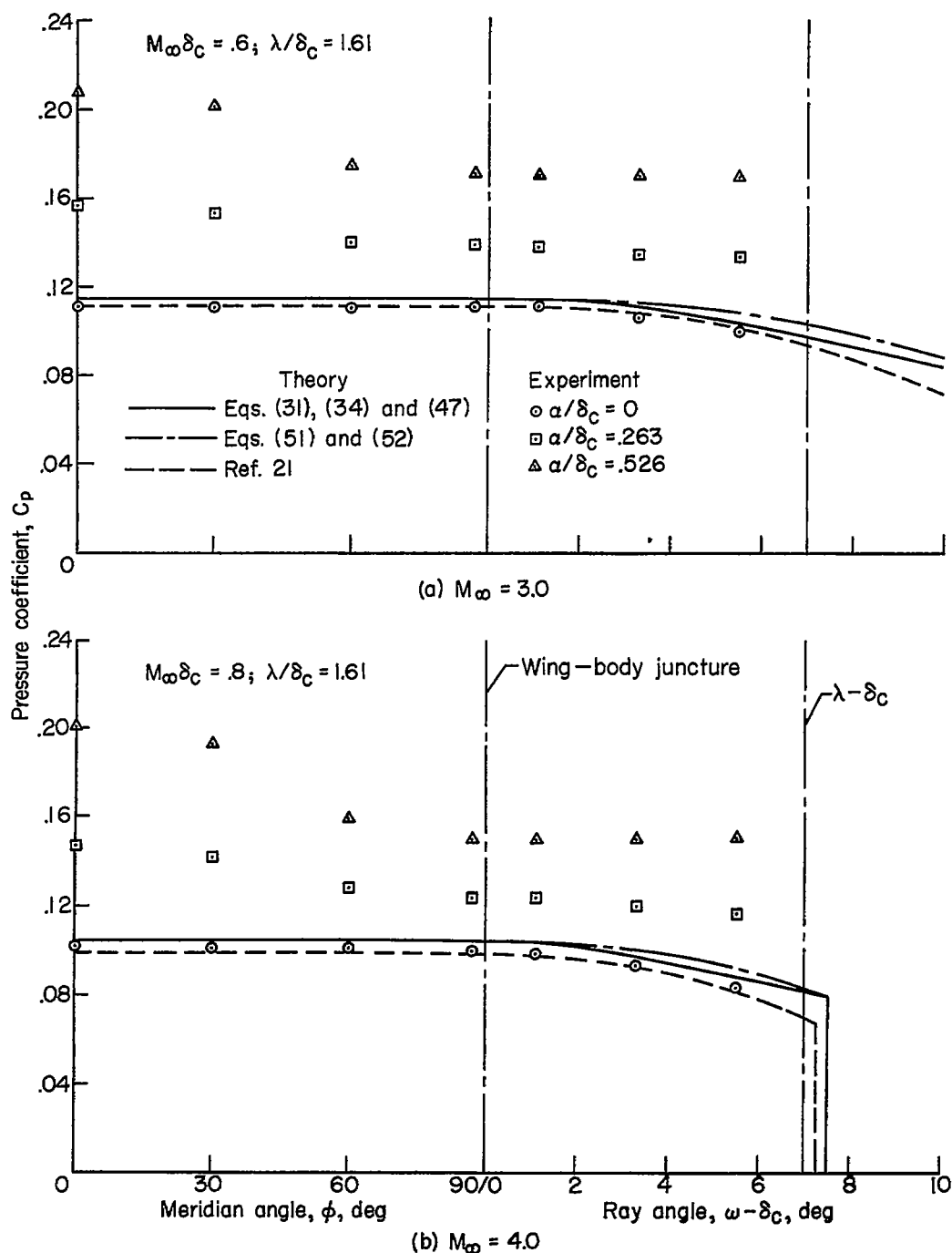


Figure 9.- Surface pressure coefficients for configuration with  $\delta_c = 11.42^\circ$  and  $\lambda = 18.4^\circ$  at angles of attack of  $0^\circ$ ,  $3^\circ$ , and  $6^\circ$ .

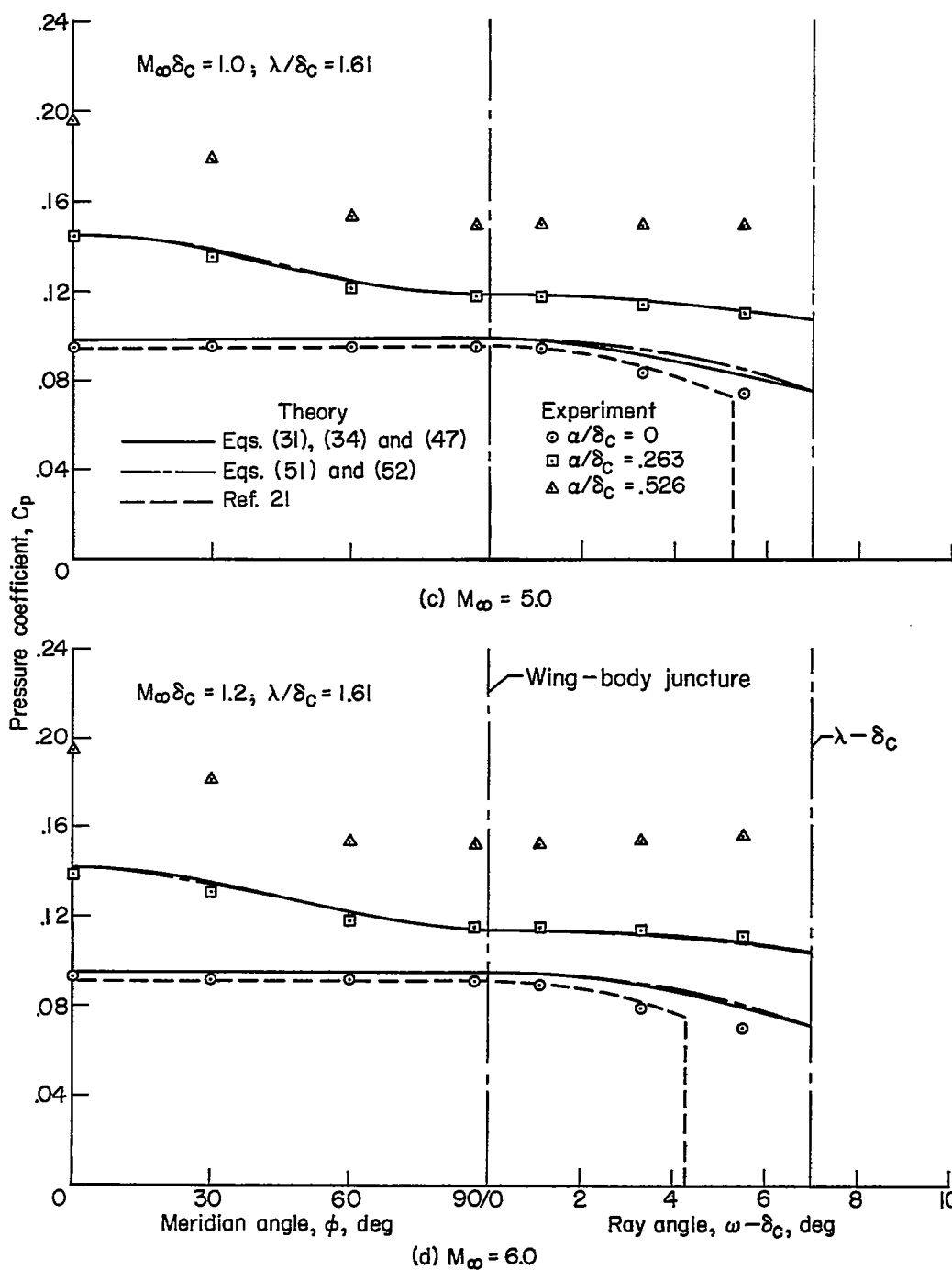


Figure 9.- Concluded.

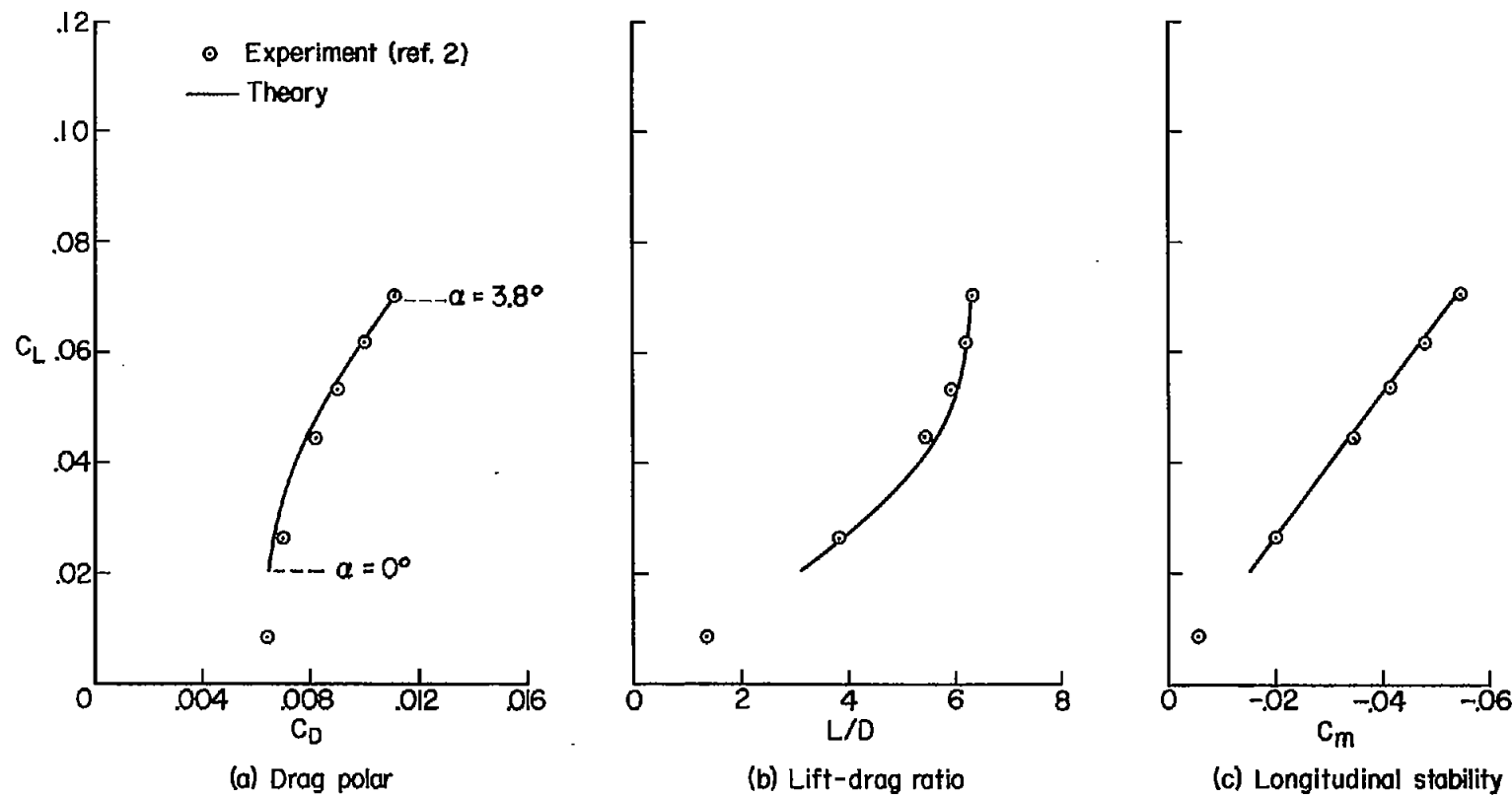


Figure 10. - Aerodynamic characteristics of a conical flat-top wing-body configuration at  $M_\infty = 5.0$ ;  $\delta_C = 5.71^\circ$ ;  $\lambda = 15^\circ$ .

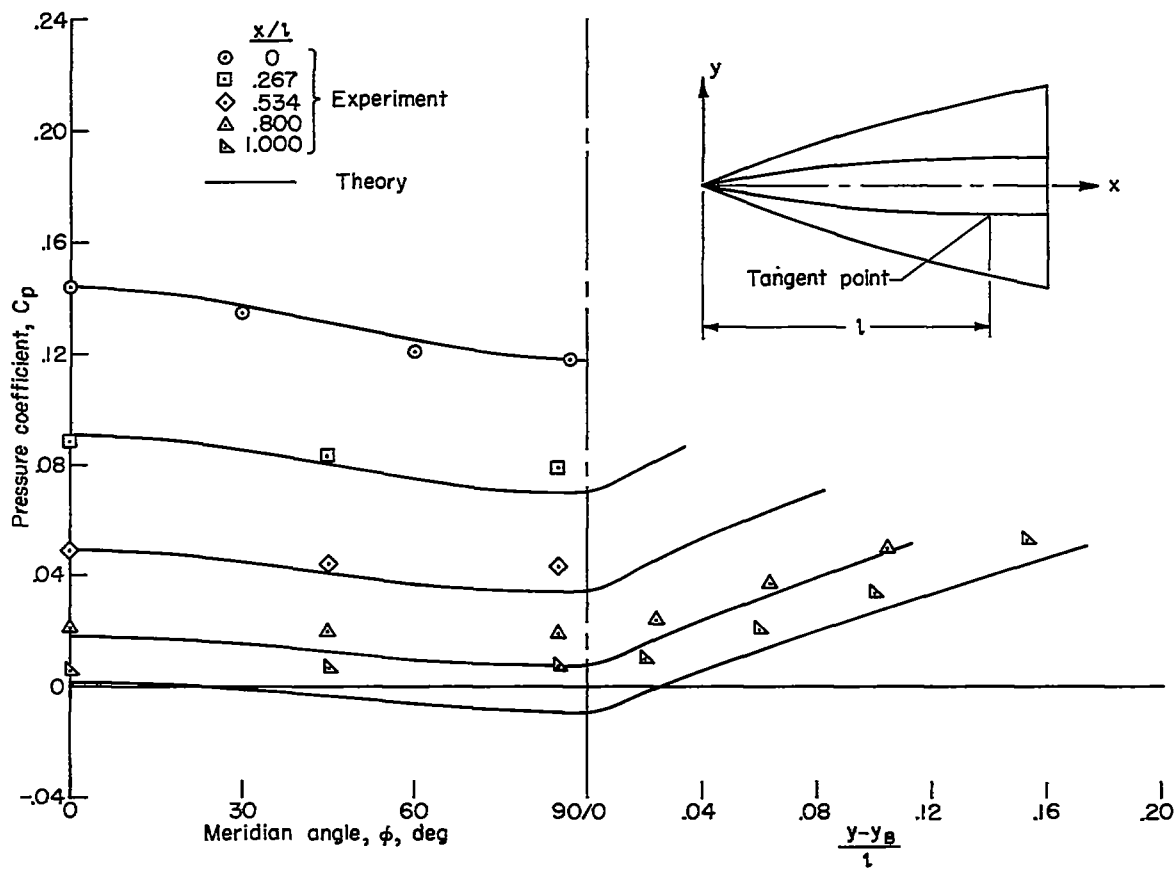


Figure 11.- Variation of surface pressure coefficient on ogive configuration at  $M_\infty = 5.0$  and  $\alpha = 3^\circ$ .